USGS
science for a changing world

Prepared in cooperation with the U.S. Fish and Wildlife Service

Hydrogeology of, Simulation of Groundwater Flow in, and Potential Effects of Sea-Level Rise on the Kirkwood-Cohansey Aquifer System in the Vicinity of Edwin B. Forsythe National Wildlife Refuge, New Jersey

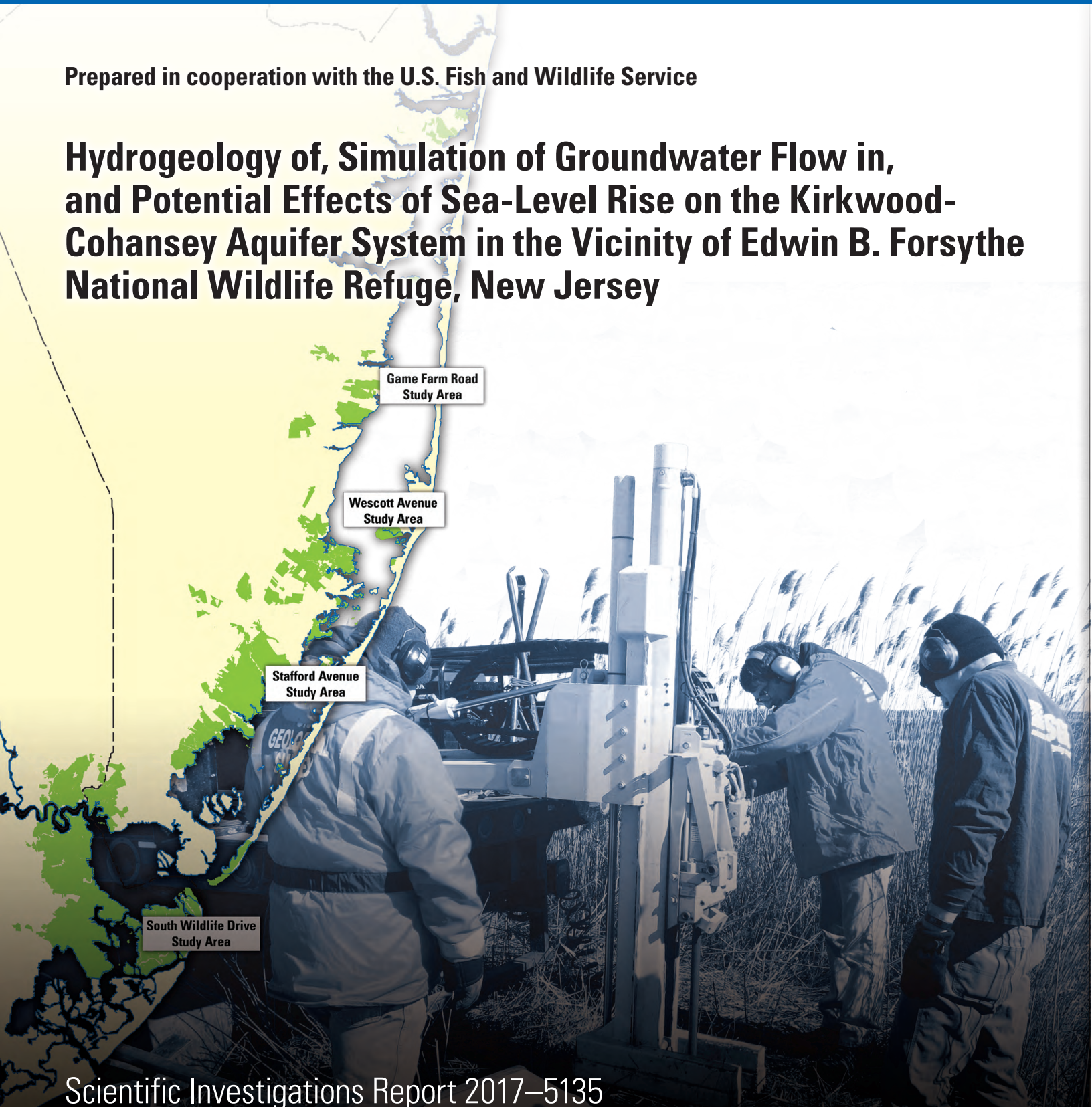

Scientific Investigations Report 2017–5135

U.S. Department of the Interior
U.S. Geological Survey

Front cover. Locations of study areas at Edwin B. Forsythe National Wildlife Refuge (in green), New Jersey. Photograph shows U.S. Geological Survey (USGS) hydrologists installing a drive-point test hole, Stafford Township, Ocean County, New Jersey. Photo by Christine Wieben, USGS.

Back cover. Photographs of (left) sunrise over Barnegat Bay, Edwin B, Forsythe National Wildlife Refuge, New Jersey, and (right) USGS hydrologists installing a drive-point test hole near Forked River, Ocean County, New Jersey. Photos by Christine Wieben, USGS.

Hydrogeology of, Simulation of Groundwater Flow in, and Potential Effects of Sea-Level Rise on the Kirkwood-Cohansey Aquifer System in the Vicinity of Edwin B. Forsythe National Wildlife Refuge, New Jersey

By Alex R. Fiore, Lois M. Voronin, and Christine M. Wieben

Prepared in cooperation with the U.S. Fish and Wildlife Service

Scientific Investigations Report 2017–5135

U.S. Department of the Interior
U.S. Geological Survey

U.S. Department of the Interior
RYAN K. ZINKE, Secretary

U.S. Geological Survey
William H. Werkheiser, Deputy Director
exercising the authority of the Director

U.S. Geological Survey, Reston, Virginia: 2018

Suggested citation:
Fiore, A.R., Voronin, L.M., and Wieben, C.M., 2018, Hydrogeology of, simulation of groundwater flow in, and potential effects of sea-level rise on the Kirkwood-Cohansey aquifer system in the vicinity of Edwin B. Forsythe National Wildlife Refuge, New Jersey: U.S. Geological Survey Scientific Investigations Report 2017–5135, 59 p., https://doi.org/10.3133/sir20175135.

ISSN 2328-0328 (online)

Contents

Figures

Tables

Conversion Factors

U.S. customary units to International System of Units

Multiply	By	To obtain
	Length	
inch (in.)	2.54	centimeter (cm)
foot (ft)	0.3048	meter (m)
mile (mi)	1.609	kilometer (km)
	Area	
acre	0.4047	hectare (ha)
acre	0.004047	square kilometer (km^2)
square mile (mi^2)	259.0	hectare (ha)
square mile (mi^2)	2.590	square kilometer (km^2)
	Volume	
gallon (gal)	3.785	liter (L)
gallon (gal)	0.003785	cubic meter (m^3)
million gallons (Mgal)	3,785	cubic meter (m^3)
	Flow rate	
cubic foot per second (ft^3/s)	0.02832	cubic meter per second (m^3/s)
gallon per day (gal/d)	0.003785	cubic meter per day (m^3/d)

Temperature in degrees Celsius (°C) may be converted to degrees Fahrenheit (°F) as follows:

$$°F = (1.8 \times °C) + 32.$$

Temperature in degrees Fahrenheit (°F) may be converted to degrees Celsius (°C) as follows:

$$°C = (°F - 32) / 1.8.$$

Datum

Vertical coordinate information is referenced to the North American Vertical Datum of 1988 (NAVD 88).

Horizontal coordinate information is referenced to the North American Datum of 1983 (NAD 83).

Altitude, as used in this report, refers to distance above the vertical datum. Negative altitude refers to distance below the vertical datum.

Supplemental Information

Specific conductance is given in microsiemens per centimeter at 25 degrees Celsius (µS/cm at 25 °C).

Abbreviations

CSS	composite scaled sensitivities
FHB1	Flow and Head Boundary module
NJDEP	New Jersey Department of Environmental Protection
NJGWS	New Jersey Geological and Water Survey
RASA	Regional Aquifer System Analysis
SC	specific conductance
USGS	U.S. Geological Survey

Hydrogeology of, Simulation of Groundwater Flow in, and Potential Effects of Sea-Level Rise on the Kirkwood-Cohansey Aquifer System in the Vicinity of Edwin B. Forsythe National Wildlife Refuge, New Jersey

By Alex R. Fiore, Lois M. Voronin, and Christine M. Wieben

Abstract

The Edwin B. Forsythe National Wildlife Refuge encompasses more than 47,000 acres of New Jersey coastal habitats, including salt marshes, freshwater wetlands, tidal wetlands, barrier beaches, woodlands, and swamps. The refuge is along the Atlantic Flyway and provides breeding habitat for fish, migratory birds, and other wildlife species. The refuge area may be threatened by global climate change, including sea-level rise (SLR).

The Kirkwood-Cohansey aquifer system underlies the Edwin B. Forsythe National Wildlife Refuge. Groundwater is an important source of freshwater flow into the refuge, but information about the interaction of surface water and groundwater in the refuge area and the potential effects of SLR on the underlying aquifer system is limited. The U.S. Geological Survey (USGS), in cooperation with the U.S. Fish and Wildlife Service (USFWS), conducted a hydrologic assessment of the refuge in New Jersey and developed a groundwater flow model to improve understanding of the geohydrology of the refuge area and to serve as a tool to evaluate changes in groundwater-level altitudes that may result from a rise in sea level.

Groundwater flow simulations completed for this study include a calibrated baseline simulation that represents 2005–15 hydraulic conditions and three SLR scenarios—20, 40, and 60 centimeters (cm) (0.656, 1.312, and 1.968 feet, respectively). Results of the three SLR simulations indicate that the water table in the unconfined Kirkwood-Cohansey aquifer system in the refuge area will rise, resulting in increased discharge of fresh groundwater to freshwater wetlands and streams. As sea level rises, simulated groundwater discharge to the salt marsh, bay, and ocean is projected to decrease. Flow from the salt marsh, bay, and ocean to the overlying surface water is projected to increase as sea level rises.

The simulated movement of the freshwater-seawater interface as sea level rises depends on the hydraulic-head gradient. In the center of the Forsythe model area, topographic relief is 23 feet (ft) and the hydraulic-head gradient is 0.0033. In the center of the Forsythe model area, the simulated interface moved inland about 600 ft and downward about 15 ft from the baseline simulation to scenario 3 as a result of a SLR of 60 cm. In the southern part of the Forsythe model area, the topography is flatter (relief of 8 ft) and the hydraulic-head gradient is smaller (0.001). In the southern part of the Forsythe model study area, the simulated interface in this area is projected to move inland about 200 ft from the baseline simulation to scenario 3 and does not move downward.

Introduction

The Edwin B. Forsythe National Wildlife Refuge (NWR) occupies 47,000 acres along the Atlantic Flyway (U.S. Fish and Wildlife Service, 2009). The refuge provides breeding habitat for fish, migratory birds, and other wildlife species. About 82 percent of the refuge is wetlands, of which 78 percent is salt marsh (U.S. Fish and Wildlife Service, 2009). Salt marshes flourish in areas where there is a delicate balance of fresh groundwater discharge and intermittent flooding with saltwater. The vertical development of salt marshes depends on the rate of supply of fine-grained sediments and plant organic matter (Kirwan and others, 2016; Kemp and others, 2013). The unconfined Kirkwood-Cohansey aquifer system is an important source of fresh groundwater flow to the refuge in New Jersey. There is a need for refuge managers to understand the interaction of surface-water and groundwater flow and the effect of sea-level rise on the refuge. However, few published data or analyses of the interaction of surface-water and groundwater flow into the refuge are available.

In 2014, the U.S. Geological Survey (USGS), in cooperation with the U.S. Fish and Wildlife Service (USFWS), began a hydrologic assessment of the Edwin B. Forsythe NWR in New Jersey. The results of data collection and analysis conducted as part of the hydrologic assessment will be used by USFWS personnel to make decisions about habitat restoration projects. The hydrologic assessment included the development of a groundwater flow model designed to improve understanding of the hydrogeology of the refuge area and serve as a tool that can also be used by USFWS personnel to inform management decisions regarding habitat restoration.

Purpose and Scope

This report describes the hydrogeology and documents the development and application of a groundwater flow model and the results of the simulation of groundwater flow in the aquifers underlying the Edwin B. Forsythe NWR, New Jersey.

The model focuses on the unconfined Kirkwood-Cohansey aquifer system in the Atlantic Coastal Plain of New Jersey in the vicinity of the refuge. The report describes the results of investigative work, including conducting surface geophysical surveys, collecting water-level and water-quality data from drive-point wells, and incorporating additional existing lithologic and geophysical data from available boreholes in the area. The field investigation was performed to refine details of the hydrogeology in the heterogeneous aquifer system and guide decisions for choosing input parameters for an accurate representation of the aquifer system in the model. Additionally, installation of 44 temporary piezometers and a synoptic water-level study that included measuring water levels in the 44 piezometers and 28 existing wells provided additional information regarding groundwater conditions in the study area.

Previous Investigations

Many published reports that describe the hydrology and geologic framework of New Jersey Coastal Plain sediments are available. A hydrogeologic framework study of these sediments that includes mapping the subsurface extent and stratigraphic relations of all the aquifers and confining units in the New Jersey Coastal Plain was published by Zapecza (1989). Isphording (1970) initially described the stratigraphy of the Kirkwood Formation. Sugarman (2001) describes the geology and stratigraphic relations of the Kirkwood and Cohansey Formations. Newell and others (2000) published descriptions and results of mapping of the surficial sedimentary deposits of central and southern New Jersey.

The geology and groundwater resources of Ocean County are presented in a report by Anderson and Appel (1969). Watt and others (1994) describe the hydrology of the unconfined Kirkwood-Cohansey aquifer system in the Toms River Basin in Ocean County. The hydrology of the Atlantic Coastal Basins and the Mullica River Basin in the southern part of Ocean County is described by Gordon (2004) and Johnson and Watt (1996), respectively. The geology and hydrology of the Mullica River Basin are documented by Rhodehamel (1973).

Several groundwater flow models of the Coastal Plain aquifers in New Jersey that extend into the Forsythe model area were developed. The Regional Aquifer System Analysis (RASA) model simulated flow in the aquifers and confining units of the New Jersey Coastal Plain, which includes the Forsythe model area (Martin, 1998; Voronin, 2004). Nicholson and Watt (1997) developed a groundwater flow model of the Kirkwood-Cohansey aquifer system in the Metedeconk and Toms River Basins in the northern half of Ocean County and southern Monmouth County. Pope and others (2012) developed a groundwater flow model of the Kirkwood-Cohansey aquifer system in the Great Egg Harbor and Mullica River Basins in Burlington and Atlantic Counties. Cauller and others (2016) developed a groundwater flow model of the Kirkwood-Cohansey aquifer system in Ocean County and parts of Monmouth and Burlington Counties.

Well-Numbering System

The well-numbering system used in this report has been used by the USGS in New Jersey since 1978. The well number consists of a county code number and a sequence number assigned to the well in the county. The county codes used in this report are 1, Atlantic County; 5, Burlington County; and 29, Ocean County. For example, well 29-100 is the 100th well inventoried in Ocean County.

Location and Description of Study Area

The Edwin B. Forsythe NWR (fig. 1) encompasses more than 47,000 acres of New Jersey coastal habitats, including salt marshes, freshwater wetlands, tidal wetlands, barrier beaches, woodlands, and swamps. In order to understand the interaction of surface-water and groundwater discharge into the Edwin B. Forsythe NWR, the study area includes areas upland from the refuge. The extent of the study area (fig. 1) is referred to in this report as the "Forsythe model area." The Forsythe model area includes Barnegat Bay, Little Egg Harbor, Great Bay, and the tidal portion of the Mullica River (fig. 1). The eastern boundary extends approximately 30 miles (mi) east of the barrier islands into the Atlantic Ocean, the northeastern boundary extends into the southern part of Monmouth County, the southwestern boundary extends into the eastern part of Atlantic County, and the northwestern boundary extends into Ocean and Burlington Counties (fig. 1).

Description of Hydrologic System

For a detailed description of the surficial hydrologic flow system in the Edwin B. Forsythe NWR, the reader is referred to Wieben and Chepiga (2018). Groundwater levels in the refuge area range from altitudes of 0 to 65 feet (ft) relative to the North American Vertical Datum of 1988 (NAVD 88), with most water-table altitudes within 3 ft above sea level. Groundwater generally flows eastward from upland areas toward the coast, where hydraulic-head gradients are less steep because topographic relief is lower, the water table is less than 2 ft below land surface, and groundwater discharge to wetlands and streams is increased. Base flow accounts for the majority (68–94 percent) of streamflow to the refuge, and recharge to the water table occurs primarily in the uplands where 30 to 40 percent of precipitation enters the subsurface, compared to nearly 0 in the wetlands. The discharge of groundwater to wetlands and streams and the lack of groundwater recharge

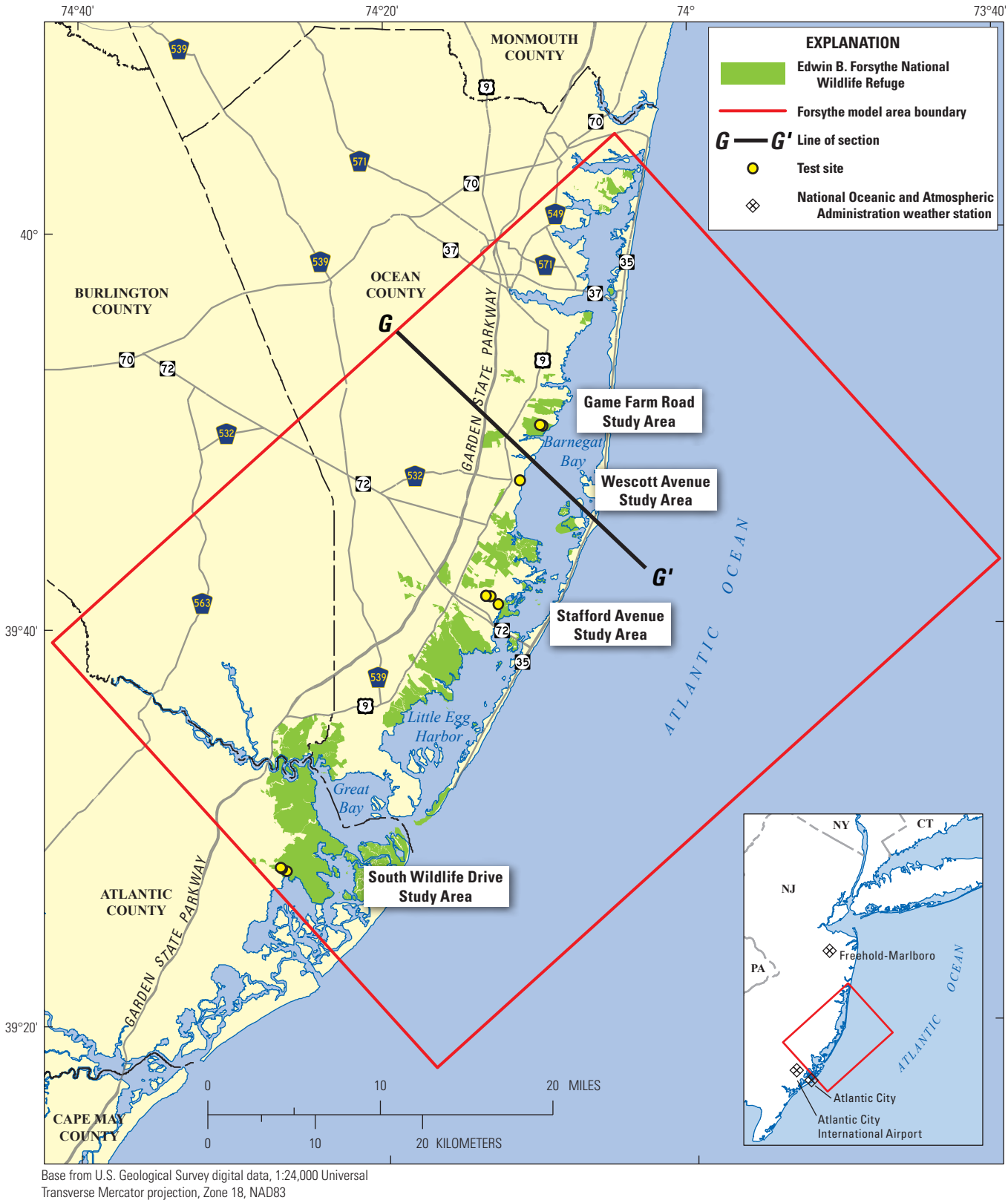

Base from U.S. Geological Survey digital data, 1:24,000 Universal Transverse Mercator projection, Zone 18, NAD83

Figure 1. Locations of model area, test sites, and line of section, Forsythe model area, New Jersey.

to the underlying aquifer system in these areas highlight the importance of groundwater as a prominent source of freshwater to the refuge.

Use of the general term "wetlands" in this report applies to both freshwater wetlands and salt marshes, as both are hydrologically areas of groundwater discharge. Whether a wetland is freshwater or salt marsh is determined by the intertidal range in that particular location. High tides transport saline water to the wetlands from the surface. Because wetlands within the tidal range are still areas of groundwater discharge, the high hydraulic head of the freshwater flowing upward from the subsurface prevents the saline surface water from infiltrating deeper into the subsurface, creating a shallow perched lens of saline water that forms the salt marsh at land surface (fig. 2). The water in this saline lens recirculates back to the low-tide mark and forces a portion of the underlying freshwater to discharge seaward (Michael and others, 2005; Bratton, 2010), likely to a zone within Barnegat Bay. This process creates a distinction between this saline lens of perched water in the marsh and the separate, deeper freshwater-saltwater interface formed in Barnegat Bay seaward of the zone of freshwater discharge (fig. 2).

Hydrogeologic Framework

The Edwin B. Forsythe NWR overlies the Kirkwood-Cohansey aquifer system, which consists of Coastal Plain formations including the namesake Kirkwood (Tkw) and Cohansey (Tch) Formations, Beacon Hill Gravel, Bridgeton Formation, Cape May Formation (Qcm), and various other surficial deposits such as marsh deposits (Qm) and alluvium (Qal) (Zapecza, 1989; Sugarman, 2001). A distinction is made in this report between time-stratigraphic units, which are geologic units correlated on the basis of age and depositional environment, and hydrostratigraphic units, which are aquifer units correlated on the basis of permeability and hydrolithology. The time stratigraphy and hydrostratigraphy are not necessarily correlated, but both are used in this report for reference purposes.

Although regionally regarded as an unconfined aquifer system, the Kirkwood-Cohansey aquifer system contains several low-permeability units that create local confined or semi-confined conditions (Zapecza, 1989). Both the Kirkwood and Cohansey Formations are predominantly sands, but regional silt and clay beds of low permeability have been identified in

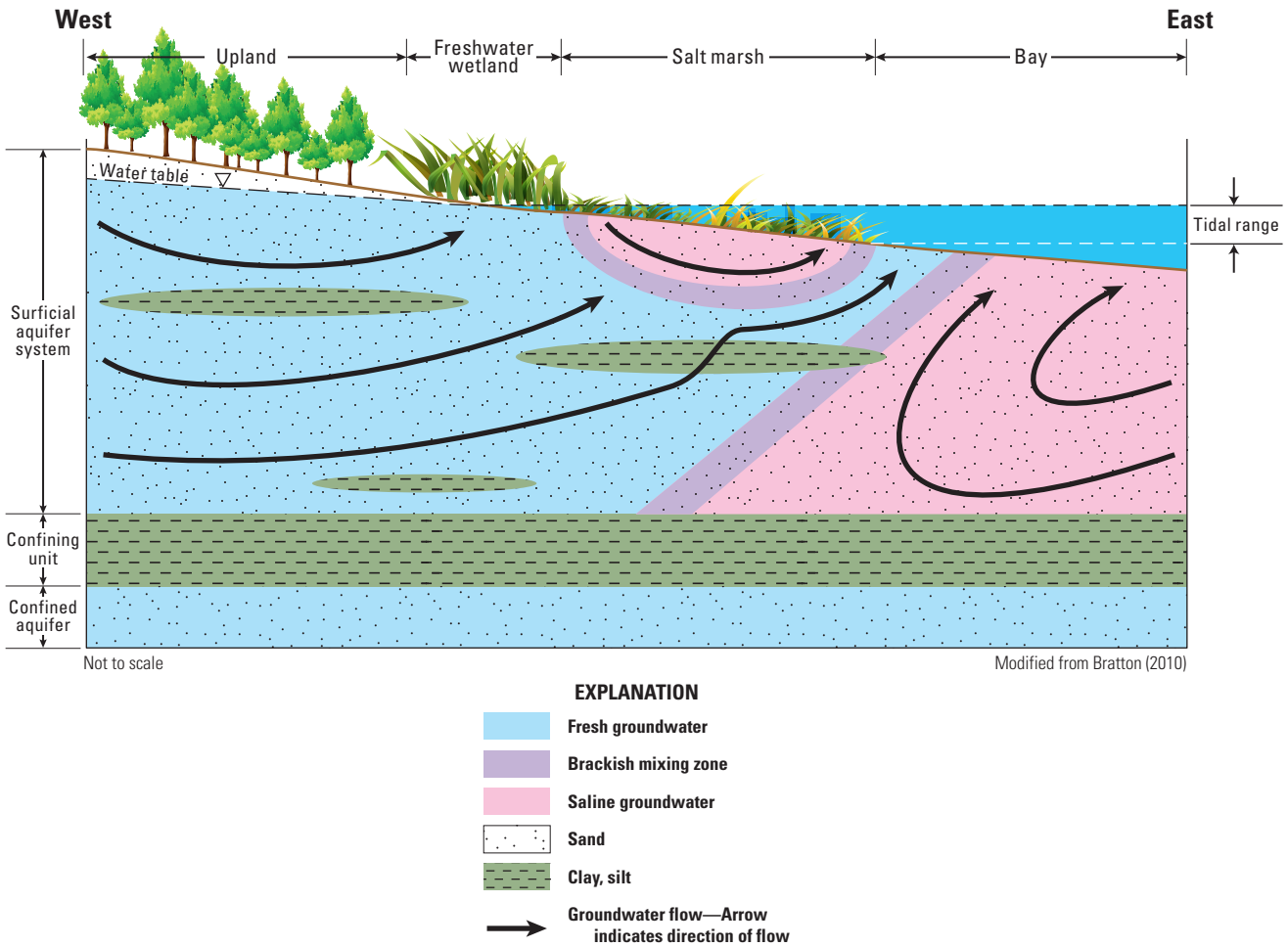

Figure 2. Conceptual groundwater flow and discharge, Forsythe model area, New Jersey.

both formations within the study area (Stanford, 2010; Stanford, 2011; Stanford, 2012; Stanford, 2013a; Stanford, 2013b; Stanford, 2014; Sugarman, 2001). These low-permeability beds directly affect the hydrology of the refuge even in more distant areas. For example, an interbedded clay-sand subunit of the Cohansey Formation, mapped by Stanford (2013a) as Tchc, underlies sands and gravels of the Beacon Hill Gravel and other surficial units in the topographically high uplands northwest of the refuge. Groundwater seeps above the Tch form the headwaters of streams that eventually discharge into the marsh (Stanford, 2010; Stanford, 2011; Stanford, 2014). The Kirkwood and Cohansey Formations are prevalent throughout the study area and continue offshore (Uptegrove and others, 2012).

The Cape May Formation also is hydrogeologically important in the Forsythe NWR area because uplands at the boundary with salt marshes are typically within the Cape May Formation (Newell and others, 2000; Stanford, 2013a). Most of the Cape May Formation is hydrogeologically similar to the Kirkwood and Cohansey Formations overall. A clay and silt bay facies of the Cape May Formation mapped by Stanford (2013a) as Qcm2f may create local confined conditions similar to those caused by Tchc. The Qcm2f is entirely subsurficial, and extends from the upland as far eastward as the barrier islands (Stanford, 2013a). Above the Qcm2f and underlying the marsh deposits is a marine platform facies unit of the Cape May Formation mapped by Stanford (2013a) as Qcm2p. This unit is mostly sand and can extend beyond the barrier island in the subsurface to the inner continental shelf (Uptegrove and others, 2012; Stanford 2013a).

The Bridgeton Formation is primarily coarse sand and gravel (Zapecza, 1989; Newell and others, 2000; Stanford, 2015), and is present in the uplands of Atlantic County near the refuge area, where it forms a terrace that caps topographic highs and does not extend below the marshes (Newell and others, 2000). Low-permeability clay lenses and iron oxide-cemented sand and gravel beds present in the Bridgeton Formation can create heterogeneity, but this formation as a whole has higher permeability and adds thickness to the unconfined aquifer system (Zapecza, 1989). Marsh sediments tend to vary in size from clay to gravel (Stanford, 2014; Stanford, 2013a; Newell and others, 2000), which indicates heterogeneous hydraulic properties. However, these deposits are thinner than other units in the overall hydrogeologic framework (Stanford, 2014; Stanford, 2013a; Newell and others, 2000), and marshes act as areas of groundwater discharge, so in this study the marsh deposits are considered to be one hydrogeologic feature and there is no differentiation among the hydraulic properties present. This simplification is assumed to have a negligible effect on the groundwater flow regime.

Methods of Field Evaluation

The hydrolithologic heterogeneity of the Kirkwood-Cohansey aquifer system creates high levels of variability in groundwater flow and discharge processes. This is especially true for the Forsythe NWR owing to its large area, where processes at one location may differ from processes at another location. The aquifer characteristics of the Kirkwood-Cohansey aquifer system should be evaluated locally rather than regionally, as comparing higher resolution hydrogeologic data collected at specific locations is more informative than considering broader views across swaths of the refuge for which no data are available. Qualitative hydrogeologic properties at four areas within the refuge were evaluated in the field using ground-penetrating radar (GPR) and (or) drive-point test holes. From north to south, these areas are Game Farm Road (Forked River, N.J.), Wescott Avenue (Waretown, N.J.), Stafford Avenue (Stafford, N.J.), and South Wildlife Drive (Galloway, N.J.) (fig. 1).

The primary function of the GPR in this study was to assist in the detection of low-permeability units within the subsurface that would otherwise go undetected by other methods of investigation. Detecting such units is essential given the discontinuity of clay units and overall hydrolithologic heterogeneity within the Kirkwood-Cohansey aquifer system. The GPR data also served as a location reconnaissance for drive-point test holes to further inform aquifer characteristics. The GPR data collected are available in Fiore (2018).

GPR is a common surface geophysical imaging survey tool that emits a radiofrequency electromagnetic (EM) pulse into the subsurface from a transmitter antenna. When the pulse encounters an interface of subsurface materials with contrasting dielectric permittivity and EM conductivity, part of the signal is reflected back to a receiver antenna, and the remainder continues to travel deeper into the subsurface. Interfaces with high contrast, such as a contact between sand and clay or between unsaturated and saturated conditions, will produce large reflections in the GPR image (Beres and Haeni, 1991). The raw data of a GPR survey consist of times that the EM pulse has traveled to the reflector and back to the receiver antenna. The conversion of travel time to depth below land surface is given by the equation

$$d = tV/2 \quad (1)$$

where

- d is the reflector depth below land surface,
- t is the two-way travel time to the reflector and back to land surface, and
- V is the mean velocity of the radar wave to the reflector.

The value of *V* depends on the particular subsurface lithotypes and groundwater conditions present, and is associated with typical ranges of values for which many resources are available for reference (Beres and Haeni, 1991). When the type of subsurface material is known, an appropriate value of *V* is assumed for estimating depth below land surface. Alternatively, *V* can be determined when depth to a particular interface is known. Materials such as clay and saltwater attenuate much of the radar wave, so delineating such zones with GPR results is useful when evaluating the hydrogeology of an area. GPR surveys for this study were conducted with a 100-megahertz (MHz) shielded antenna at Wescott Avenue, Stafford Avenue, and South Wildlife Drive, and an 80-MHz shielded antenna at Game Farm Road. GPR data reported in this study were post-processed first with a direct current (DC) removal filter, then with a time-varying gain to increase later time amplitudes. The gain was applied starting at reflection times just below the water table, which creates the strongest reflection on these GPR lines other than the initial reflection from the antenna-ground surface interface.

A Geoprobe® SP-15 drive-point sampler was used at three sites (table 1): Game Farm Road, Stafford Avenue, and South Wildlife Drive. Drive-point sites were selected on the basis of location in the marsh-upland regime: marsh, upland (defined here as simply nonmarsh areas upgradient from the bay) and the transitional area between the marsh and upland. The drive point consists of a 1.25-inch- (in.) diameter screen inside a 1.5-in.-diameter sheath pipe that was driven into the subsurface by a truck-mounted rig to a depth of up to 60 ft below land surface (BLS). The maximum depth is tested first, and upon reaching that depth, a plug at the bottom of the sheath is pushed out and the rod string is raised, exposing the screen to the aquifer at the depth. Site SW-T2 on South Wildlife Drive was tested with a mill slot screen instead of a SP-15. The mill slot screen is driven into the subsurface and intervals are tested from the shallow intervals downward, with the deepest interval tested last. Only one site was installed with a mill slot because the drive-point rods were clogged with about 4 ft of sediment after testing, making the data from that site suspect. When the desired depth was reached, groundwater was pumped out of each interval to flush sediment from the well screen, and specific conductance (SC) was monitored during pumping as a rough indication of the relative freshness/salinity of the groundwater, as the SC of freshwater is lower than that of brackish and saline water. Although many factors must be considered to relate SC to salinity, freshwater roughly has a SC less than 2,000 microsiemens per centimeter (µS/cm) at 25 degrees Celsius (°C) (Miller and others, 1988). Mean SC of Barnegat Bay surface water ranges from approximately 24,000 to 47,000 µS/cm, with values in the north generally lower than values in the south (F.J. Spitz, U.S. Geological Survey, written commun., 2016). SC values measured in this study are temperature corrected to 25 °C. After water-quality parameters had stabilized, pumping ceased, and depth to water was measured in that interval until levels stabilized. Two to four intervals were tested in each test hole (table 1; U.S. Geological Survey, 2016).

Natural gamma geophysical logs for 10 wells in the National Water Information System database (table 2; U.S. Geological Survey, 2016) were then evaluated for continuity of aquifer units indicated by drive-point tests. The 10 natural gamma logs are accessible in the USGS GeoLog Locator database (U.S. Geological Survey, 2017). Finer grained, lower permeability sediments generally have larger quantities of gamma-emitting radioisotopes such as potassium-40, which correspond to inflections to the right on a natural gamma log (Keys, 1990).

Game Farm Road Area

Two drive-point test holes were installed on Game Farm Road (fig. 3; table 1). One site was located in the upland (GF-U3), and the other was in a transitional area to the marsh (GF-T2). No site in the marsh was tested because of poor access with the truck-mounted rig.

The two shallowest intervals in the upland drive-point GF-U3 (A, B) had similar water levels (1.43 and 1.42 ft, respectively) and maintained constant and relatively high pumping rates of 600 milliliters per minute (mL/min) (228.25 gallons per day [gal/d]) (table 1), which indicates hydraulic connection between intervals A and B and permeable sediments, respectively (fig. 4). Interval D also maintained this pumping rate and is likely in similarly permeable material (table 1; fig. 4). Water-level altitudes are higher in A and B than in D (table 1), which indicates groundwater flow from the upland to the marsh. The three deepest intervals (C, E, F) had lower pumping rates, with a maximum of 455 mL/min (173.09 gal/d), and water levels did not recover after pumping (with interval C having no recovery at all) (table 1), indicating lower permeability sediments than at the shallower intervals (fig. 4). The GF-U3 and GF-T2 test holes are in the Cape May Formation (Stanford, 2013a), and permeability decreases between intervals B and E at about -20 ft relative to NAVD 88 (fig. 4); this is approximately the same altitude at which Stanford (2013a) estimates the contact of sandy platform facies (Qcm2p) and fine-grained bay facies (Qcm2f) of the Cape May Formation. Therefore, the drive-point results confirm Qcm2f is less permeable than Qcm2p, which is to be expected from the lithologic descriptions of Stanford (2013a). Intervals C and F may be open to clayey units within the Cohansey Formation (Tch) or the overlying Cape May Formation (Qcm), depending on the exact altitude of the contact between the two formations near GF-U3 and GF-T2.

Brackish groundwater was present in interval D, where the SC was 2,490 µS/cm; all other intervals at GF-U3 and GT-T2 contained freshwater with SC values ranging from 240 to 1,350 µS/cm (table 1). The fresh groundwater in intervals open to deeper, less permeable Qcm2f sediments indicate that any saline water from the marsh that enters the subsurface

Table 1. Drive-point test hole information, water levels, specific conductance, and pumping rate during well development, Edwin B. Forsythe National Wildlife Refuge, 2015.

[NWIS, National Water Information System; NAVD 88, North American Vertical Datum of 1988; NAD 83, North American Datum of 1983; ft, feet; DDMMSS, degrees, minutes, seconds; BLS, below land surface; SC, specific conductance; µS/cm, microsiemens per centimeter at 25 degrees Celsius; mL/min, milliliters per minute; NM, not measured; NA, not applicable or not available]

NWIS site number	Site name	Interval name	Land-surface altitude (ft, NAVD 88)	Latitude (DDMMSS, NAD 83)	Longitude (DDMMSS, NAD 83)	Top of interval (ft BLS)	Bottom of interval (ft BLS)	Water level (ft BLS)	Water level (ft, NAVD 88)	SC (µS/cm)	Pump rate (mL/min)	Test date
395014074094802	29-2286 Game Farm U-3 (GF-U3)	A	3.4	39°50'13.92"	-074°09'48.12"	6.7	10.2	1.97	1.43	348	600	2/18/2015
395014074094802	29-2286 Game Farm U-3 (GF-U3)	B	3.4	39°50'13.92"	-074°09'48.12"	19.05	22.55	1.98	1.42	1,350	600	2/18/2015
395014074094802	29-2286 Game Farm U-3 (GF-U3)	C	3.4	39°50'13.92"	-074°09'48.12"	39.4	41.9	Dry[1]	Dry[1]	651	NA	2/18/2015
395012074093801	29-2285 Game Farm T-2 (GF-T2)	D	1.6	39°50'11.76"	-074°09'38.1"	8.45	11.95	1.87	-0.27	2,490	600	2/18/2015
395012074093801	29-2285 Game Farm T-2 (GF-T2)	E	1.6	39°50'11.76"	-074°09'38.1"	22.65	26.15	NA[2]	NA[2]	240	455	2/18/2015
395012074093801	29-2285 Game Farm T-2 (GF-T2)	F	1.6	39°50'11.76"	-074°09'38.1"	47.75	49.75	NA[2]	NA[2]	293	250	2/18/2015
394137074132702	29-2283 Stafford U-3 (ST-U3-a)	G	7.7	39°41'37.26"	-074°13'27.3"	10.45	13.95	2.82	4.88	138	600	2/12/2015
394137074132702	29-2283 Stafford U-3 (ST-U3-a)	H	7.7	39°41'37.26"	-074°13'27.3"	16.7	20.2	2.91	4.79	126	600	2/12/2015
394137074132703	29-2284 Stafford U-3b (ST-U3-b)	I	7.7	39°41'37.38"	-074°13'27.18"	35	38.5	[3]-2.80	[3]10.5	104	600	3/12/2015
394137074132703	29-2284 Stafford U-3b (ST-U3-b)	J	7.7	39°41'37.38"	-074°13'27.18"	57	59	NA[2]	NA[2]	63	500	3/12/2015
394136074131001	29-2282 Stafford T-2 (ST-T2)	K	3.6	39°41'36.24"	-074°13'09.96"	6.9	10.4	2.26	1.34	1,630	600	2/12/2015
394136074131001	29-2282 Stafford T-2 (ST-T2)	L	3.6	39°41'36.24"	-074°13'09.96"	17.55	21.05	NA[2]	NA[2]	126	NM	2/12/2015
394136074131001	29-2282 Stafford T-2 (ST-T2)	M	3.6	39°41'36.24"	-074°13'09.96"	30	33.5	Dry[1]	Dry[1]	94	NA	2/12/2015
394136074131001	29-2282 Stafford T-2 (ST-T2)	N	3.6	39°41'36.24"	-074°13'09.96"	50.55	54.05	[3]-3.53	[3]7.13	54	600	2/12/2015
394112074123901	29-2281 Stafford M-1 (ST-M1)	O	2.5	39°41'12.36"	-074°12'38.88"	7.3	11.3	NA[2]	NA[2]	8,680	500	3/12/2015
394112074123901	29-2281 Stafford M-1 (ST-M1)	P	2.5	39°41'12.36"	-074°12'38.88"	29.3	33.3	NM	NM	147	600	3/12/2015
394112074123901	29-2281 Stafford M-1 (ST-M1)	Q	2.5	39°41'12.36"	-074°12'38.88"	54	58	[3]-1.10	[3]3.6	92	600	3/12/2015
392757074265802	1-2269 South Wildlife U-3 (SW-U3)	R	6.9	39°27'57.36"	-074°26'58.38"	9.5	13	4.3	2.6	141	500	2/11/2015
392757074265802	1-2269 South Wildlife U-3 (SW-U3)	S	6.9	39°27'57.36"	-074°26'58.38"	29.5	33	4.37	2.53	857	500	2/11/2015
392757074265802	1-2269 South Wildlife U-3 (SW-U3)	T	6.9	39°27'57.36"	-074°26'58.38"	60	62	4.62	2.28	81	500	2/11/2015
392754074265201	1-2268 South Wildlife T-2 (SW-T2)	U	5.8	39°27'54.54"	-074°26'52.56"	7.65	9.65	NM	NM	1,190	500	2/6/2015
392754074265201	1-2268 South Wildlife T-2 (SW-T2)	V	5.8	39°27'54.54"	-074°26'52.56"	29.65	31.65	NM	NM	1,350	500	2/6/2015
392754074265201	1-2268 South Wildlife T-2 (SW-T2)	W	5.8	39°27'54.54"	-074°26'52.56"	59.1	61.1	NA[2]	NA[2]	264	100	2/6/2015
392746074263501	1-2267 South Wildlife M-1 (SW-M1)	X	6.5	39°27'46.2"	-074°26'34.9"	15.5	19	Dry[1]	Dry[1]	6,500	NA	2/10/2015
392746074263501	1-2267 South Wildlife M-1 (SW-M1)	Y	6.5	39°27'46.2"	-074°26'34.9"	30.1	34.1	4.93	1.57	3,090	600	2/10/2015
392746074263501	1-2267 South Wildlife M-1 (SW-M1)	Z	6.5	39°27'46.2"	-074°26'34.9"	50.7	52.7	NA[2]	NA[2]	2,880	300	2/10/2015

[1]Interval was pumped dry and did not recover; no water-level measurement possible.

[2]Water level too slow to recover to static condition following pumping.

[3]Water level above land surface.

Table 2. Wells in National Water Information System database used in hydrogeologic cross sections.

[NWIS, National Water Information System; ft, feet; NAVD 88, North American Vertical Datum of 1988; DDMMSS, degrees, minutes, seconds; NAD 83, North American Datum of 1983]

NWIS site number	Site name	Altitude (ft, NAVD 88)	Latitude (DDMMSS, NAD 83)	Longitude (DDMMSS, NAD 83)
395028074104401	29-585 DOE-Forked River Obs	12	39°50’27.6”	-074°10’42.5”
395024074102501	29-723 Game Farm 1912 Test Well	8.8	39°50’24”	-074°10’23”
394733074125401	29-1622 PW6/Obs1	43	39°47’32.6”	-074°12’54.2”
394655074111001	29-2289 Birdsall Well 1891	4	39°46’55.2”	-074°11’09.6”
394146074145301	29-1774 Stafford Township 7	21	39°41’33.9”	-074°14’54.2”
394042074141102	29-774 Stafford Township 4	7.8	39°40’42.2”	-074°14’09.5”
394201074121201	29-598 Test 1960	2.9	39°42’02.2”	-074°12’07.8”
393845074105301	29-547 Test 1973	4.3	39°38’45”	-074°10’51”
392754074270101	1-180 Oceanville 1 Obs	22	39°27’54”	-074°26’59”
392324074231401	1-39 Brigantine 4	6.2	39°23’29.6”	-074°23’45.5”

does not infiltrate to altitudes deeper than the top of Qcm2f, as the SC in interval E was only 240 µS/cm (table 1). This lack of infiltration is also evident from the SC of 1,350 µS/cm (the highest freshwater SC value at Game Farm Road) in interval B above the contact (table 1, fig. 4). Interval B also had the highest SC of upland groundwater measured in this study, indicating that this groundwater may be a remnant of storm-surge overwash that introduced higher SC water to the upland from the marsh or bay. This saline front may have moved through interval A and been diluted and dispersed by fresh groundwater flow from the uplands before the downward density-driven flow of the overwash saline slug reached interval B.

Gamma logs of nearby wells indicate the fine-grained unit of the Cape May Formation (Qcm2f) pinches out between wells 29-723 and 29-585 (Stanford, 2013a) (fig. 4). The top of Qcm2f is about 21 ft BLS at 29-723 and is not present at 29-585. A strong, continuous reflection that causes substantial signal attenuation on GPR line 1 (fig. 5) is likely caused by the top of the fine-grained Qcm2f. On the western side of GPR line 1, this reflection is seen at about 160 nanoseconds (ns). If reflection depth is assumed to be about 21 ft BLS, the signal ground velocity would be about 0.262 feet per nanosecond (ft/ns). This value is appropriate for radar velocity through saturated sand (Beres and Haeni, 1991), which is applicable given the shallow water table in this area (Wieben and Chepiga, 2018). The reflection is not evident on GPR line 2 (fig. 6), which has less penetration depth likely as a result of faster attenuation by the higher SC values measured during drive-point testing. The strong attenuation on the eastern side of line 2 (fig. 6) is caused by the substantially higher SC on the outer edge of the salt marsh (fig. 3).

Wescott Avenue Area

No drive points were installed at Westcott Avenue (fig. 7), so the hydrogeologic section was based on gamma logs of nearby wells (fig. 8), results of previous investigations, and a GPR line (figs. 8 and 9). The GPR line at Wescott Avenue includes a large reflection that first appears at about 160 ns at the northwest end of the line (fig. 9). The GPR signal is quickly attenuated by this reflection, which indicates an interface with finer grained material likely equivalent to Qcm2f at Game Farm Road (fig. 8). The gamma log of well 29–2289 southeast of the GPR line indicates a clayey unit about 10 ft deep (fig. 8), and Woolman (1893) identified clay in this well at a depth of 20 ft. Using a 0.262-ft/ns velocity as at Game Farm Road, the 160-ns reflection at the western end would occur approximately 22 ft BLS, and given that Wescott Avenue and Game Farm Road are both in the Forked River topographic quadrangle, the geologic descriptions by Stanford (2013a) likely apply, and the Qcm2f is hydraulically consistent geographically. Well 29–2289 is also described as being artesian at a depth of 70 ft, with a water level about 6 to 8 ft above land surface (Woolman, 1893), which indicates the deeper groundwater at this location has a high hydraulic head and the upward freshwater flow toward the marsh is strong.

Observed changes in vegetation along Wescott Avenue coincide with changes in GPR penetration at approximately 900 and 1,200 ft (figs. 7 and 9). At 900 ft, the fine-grained bedding reflection disappears as most of the emitted GPR signal is attenuated soon after reflection from the water table, which occurs slightly later in time because radar velocity is slower (fig. 9). This distance also marks the approximate first appearance of *Phragmites,* a grass common in marsh to upland transitional areas, along Wescott Avenue. At 1,200 ft, the GPR signal attenuates immediately at the surface, and no reflections are present below the ground-surface reflection (fig. 9), which coincides with the easternmost upland-type trees present along the survey line and the western extent of the marsh deposits (Qm) (fig. 8). These changes indicate the GPR signal is attenuated by increasingly higher SC groundwater in the marsh.

Aerial imagery from New Jersey Office of Information Technology, Office of Geographic Information Systems, 2008

Surficial geology modified from Stanford, 2013a

EXPLANATION

- Cape May Formation
- Marsh or wetland deposits
- Alluvium
- Other surficial deposits
- A — A' Line of section
- 1 Ground-penetrating radar line and identifier
- GF-U3 Drive-point site and identifier
- 29-585 Well and identifier

Figure 3. Surficial geology and locations of wells, drive-point sites, line of section, and ground-penetrating radar lines, Game Farm Road study area, Ocean County, New Jersey.

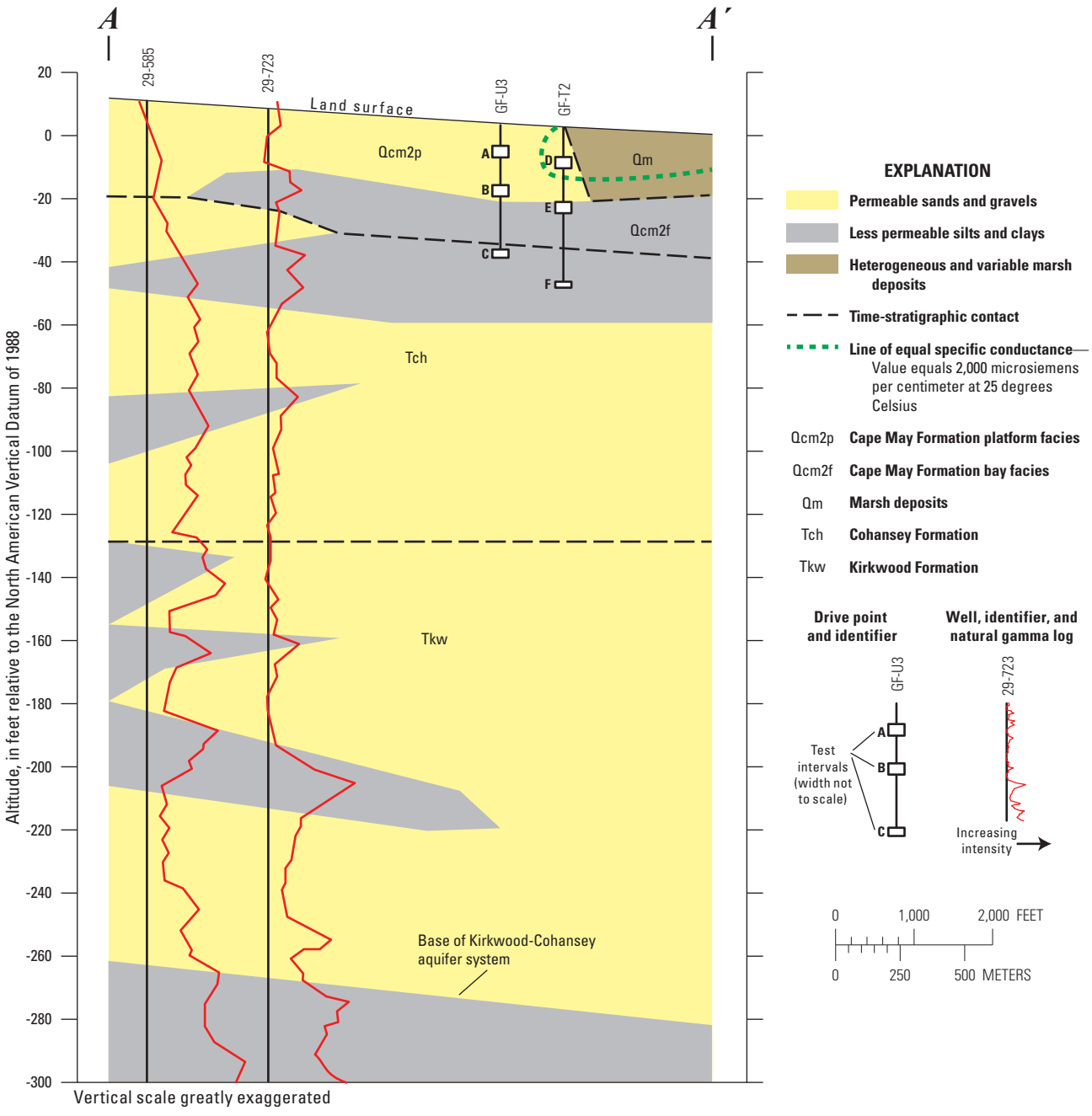

Figure 4. Hydrogeologic cross section *A-A′* at Game Farm Road study area, Ocean County, New Jersey. Line of section shown in figure 3.

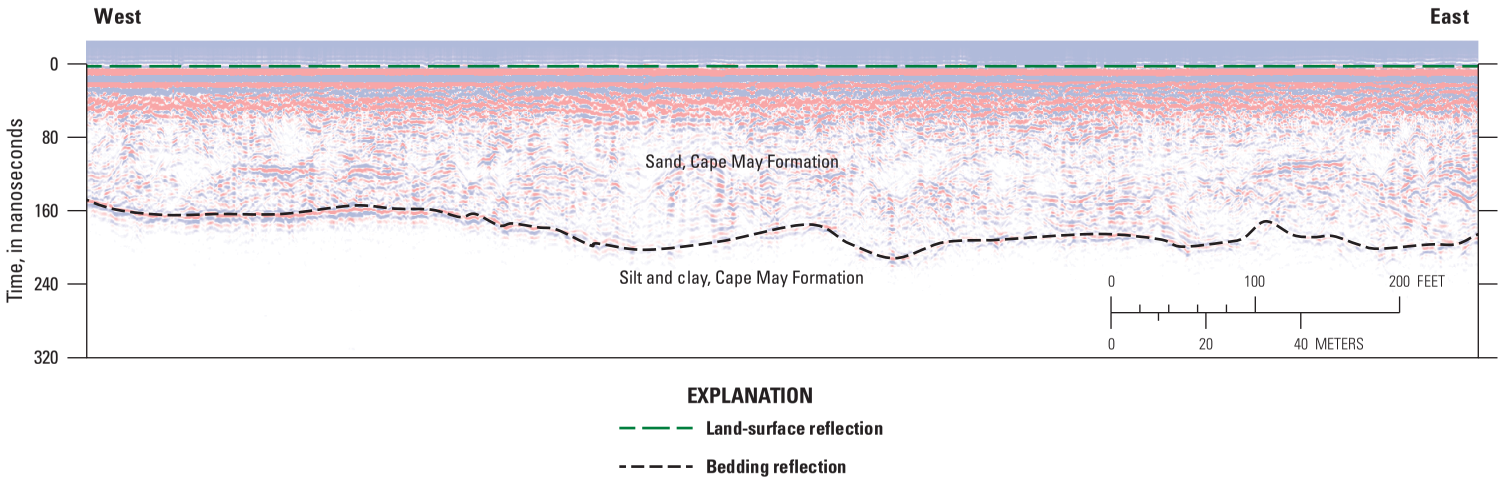

Figure 5. Ground-penetrating radar (GPR) line 1 from Game Farm Road study area, Ocean County, New Jersey, and reflection interpretations. Line includes direct current removal and time-varying gain filters. GPR line shown in figure 3.

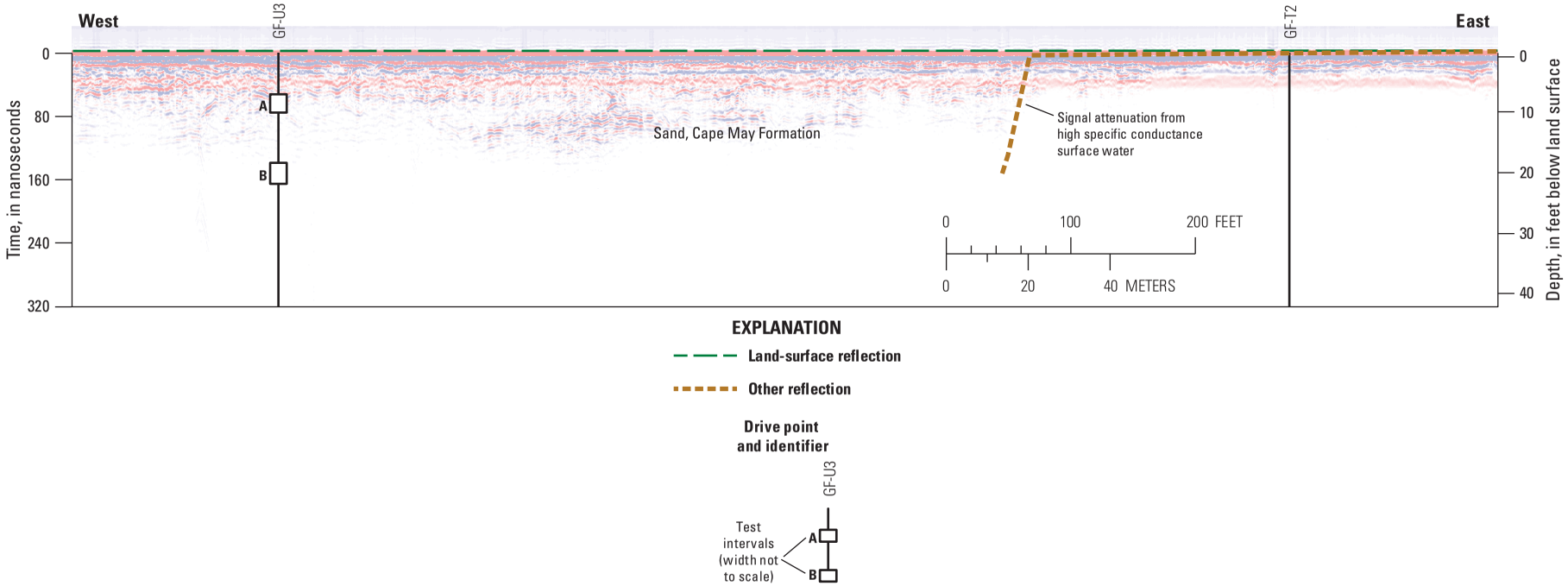

Figure 6. Ground-penetrating radar (GPR) line 2 from Game Farm Road study area, Ocean County, New Jersey, and reflection interpretations. Line includes direct current removal and time-varying gain filters. Depth scale is variable and not applicable to entire profile. GPR line shown in figure 3.

Figure 7. Surficial geology and locations of wells, line of section, and ground-penetrating radar line, Wescott Avenue study area, Ocean County, New Jersey.

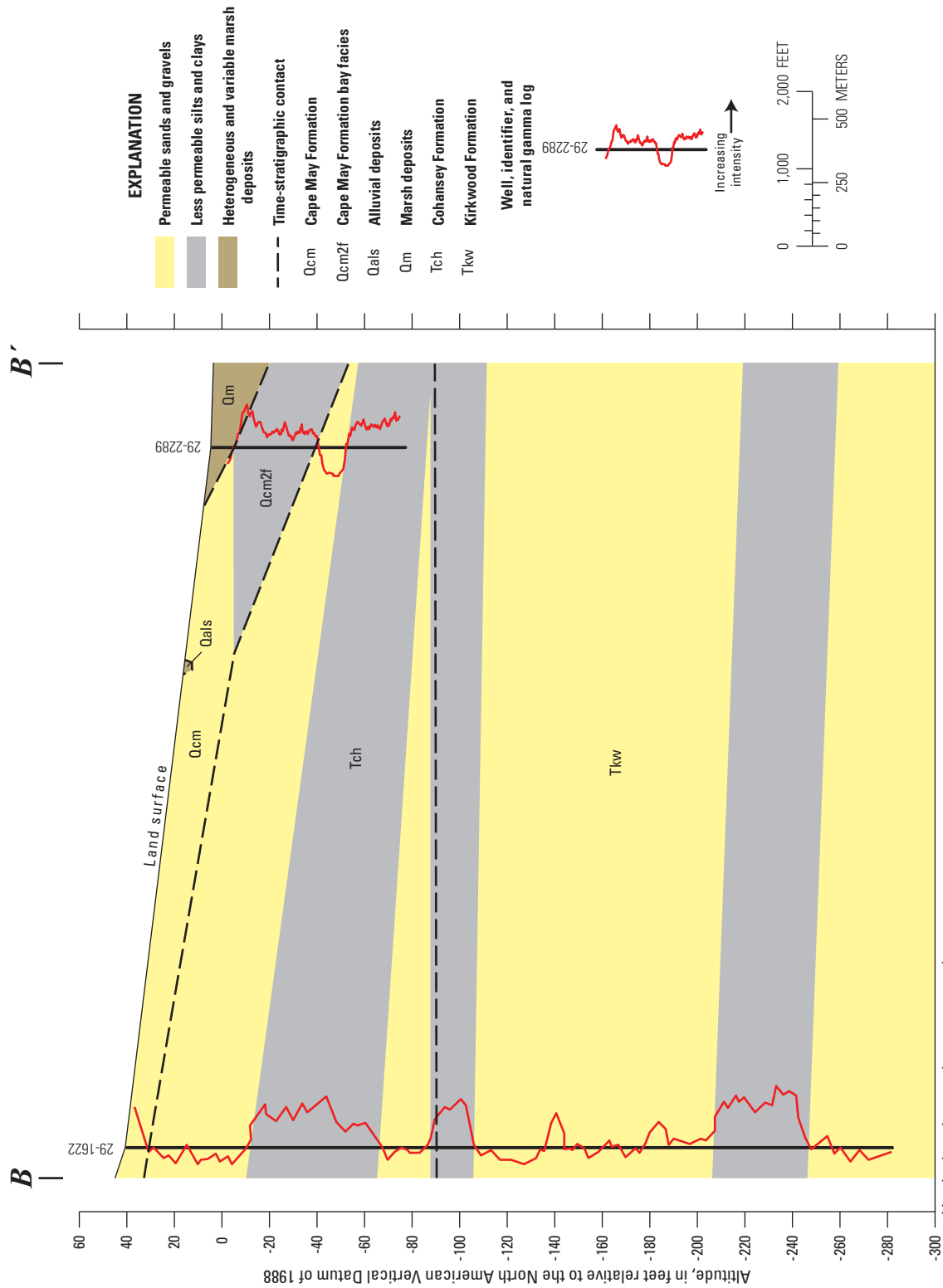

Figure 8. Hydrogeologic cross section *B-B′* at Wescott Avenue study area, Ocean County, New Jersey. Line of section shown in figure 7.

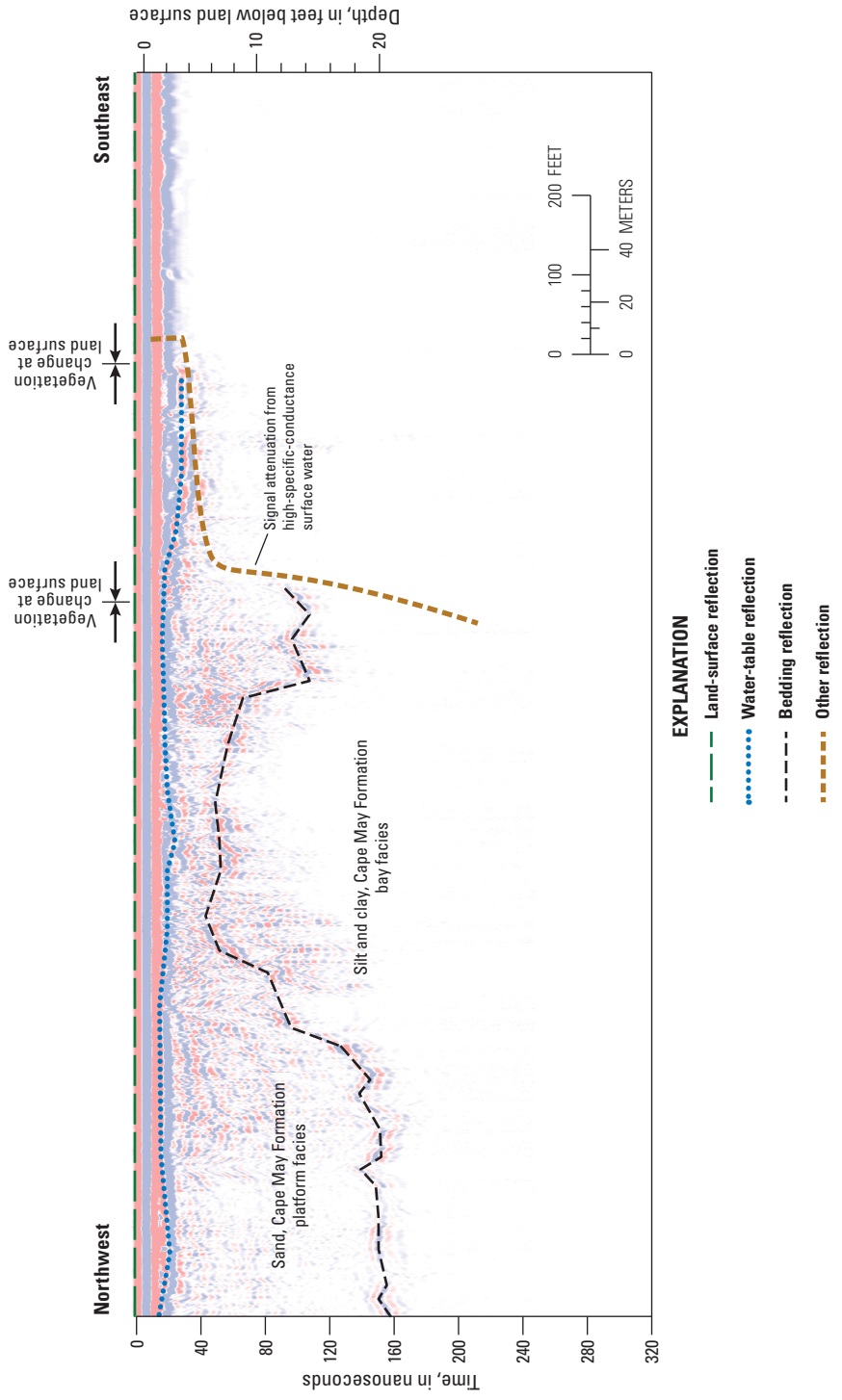

Figure 9. Ground-penetrating radar (GPR) line from Wescott Avenue study area, Ocean County, New Jersey, and reflection interpretations. Line includes direct current removal and time-varying gain filters. Depth scale is variable and not applicable to entire profile. GPR line shown in figure 7.

Stafford Avenue Area

Four drive-point sites were installed on Stafford Avenue (table 1, fig. 10). In the upland area, two nested drive-point holes were installed to test two shallow (ST-U3-S) and two deep (ST-U3-D) intervals (table 1). The holes are within 10 ft of each other and are discussed in this report as a single site (ST-U3).

Intervals G, H, K, and P maintained pumping at 600 mL/min (228.25 gal/d) (table 1) and are likely in the same permeable hydrologic unit (fig. 11). An underlying low-permeability layer was indicated by the failure of water levels to recover in interval L and the observation that interval M was pumped dry (table 1, fig. 11). Artesian conditions in permeable material were observed in intervals I, N, and Q (table 1), as indicated by measured hydraulic heads above land surface (table 1). The low-permeability layer at intervals L and M (fig. 11) is likely equivalent to the fine-grained unit on the gamma logs of other wells in the area (fig. 12). Stanford (2014) mapped Qcm2f in the adjacent West Creek quadrangle; this low-permeability layer at intervals L and M may be the eastward expression of that unit. The less permeable layer at intervals L and M extends about 3,000 ft southeastward to ST-M1 between the bottom of intervals P and Q and northwestward to ST-U3 between intervals H and I (fig. 12). Water levels in interval J did not fully recover after testing (table 1, fig. 11), which indicates a progression to finer grained material below the more permeable artesian unit that contains interval I (fig. 11). It is not clear whether this lower permeability layer at interval J is part of the same unit at about intervals L and M (as illustrated in fig. 12) or whether interval J is in a separate clay lens.

A strong reflection at about 230 ns on the GPR line near ST-U3 (fig. 13) may be caused by the top of the low-permeability layer penetrated in intervals L and M. Earlier (shallower) reflectors are subhorizontal and caused minimal signal attenuation (fig. 13), which indicates that no substantial fine-grained material is present above the 230-ns reflector. Mound-shaped reflectors, such as the reflector that appears over the first 520 ft on the western side of the GPR line (fig. 13), are similar in appearance to those interpreted as bay deposits in GPR lines at other locations in the Atlantic Coastal Plain (Seminack and Buynevich, 2013), which may further indicate a contact with the low-permeability bay deposits of Qcm2f. The 230-ns reflector, if caused by the contact with Qcm2f, must be below the bottom of interval H at 20.2 ft BLS (table 1; figs. 12 and 13). At the time the GPR data were collected, the surface water in the stream north of Stafford Avenue was about 3 ft below the side of the road near ST-U3. If the 15-ns water-table reflection is assumed to correspond to a depth of 3 ft BLS, and most of the streamflow is assumed to be base flow, then 215 ns of two-way travel time and at least 34.4 ft of two-way travel distance are present between the water table and the 230-ns reflection, if the reflection is assumed to occur at 20.2 ft. These parameters correspond to a ground velocity of at least 0.16 ft/ns, which is an appropriate estimate for freshwater-saturated sands (Beres and Haeni, 1991). Because the top of Qcm2f is likely several feet below the bottom of interval H rather than at equal depth at 20.2 ft, however, the ground velocity is most likely slightly greater than 0.16 ft/ns but still within the typical range for wave propagation through such media. Because the material at interval I is permeable and likely does not include this low-permeability layer, the thickness of this low-permeability layer at ST-U3 is likely no more than 15 ft (fig. 12).

A brackish-water SC value of 8,680 µS/cm was measured in interval O (table 1), as would be expected owing to its shallow depth below the marsh, making the interval susceptible to the effects of saline marsh surface water. However, the groundwater in underlying interval P was fresh, with a SC of 147 µS/cm (table 1). No low-permeability sediments that would impede downward flow between intervals O and P were indicated at ST-M1 (fig. 12). The disparity in SC values between intervals O and P may result from the recirculation of marsh-sourced groundwater through the shallow sediments (fig. 2) (Michael and others, 2005; Bratton, 2010), wherein the freshwater flow from the upland may be stronger than the gravitational downward flow of the higher SC groundwater, preventing brackish water in interval O from flowing downward and causing it instead to discharge back out to the marsh. Contours of equal hydraulic head in each test interval (fig. 11) indicate strong lateral groundwater flow from upland (higher heads) to marsh (lower heads) and vertical flow from deeper intervals (higher heads) to shallower intervals (lower heads), so recirculation of surficial saline or brackish water back to the marsh from a strong freshwater flow is plausible. The recirculation process is also heavily influenced by tides that change the hydraulic head in the marsh (Michael and others, 2005; Bratton, 2010). SC values of about 27,000 and 5,000 µS/cm were recorded for the marsh surface water on the north side of Stafford Avenue on February 12, 2015, and March 12, 2015, respectively; such variation is likely tidally driven, so the tidal regime at Stafford Avenue is likely sufficient to produce such a recirculation cell, as shown by Bratton (2010).

Most of the GPR signal from 1,640 ft eastward is attenuated at the water table (fig. 13). This distance corresponds to the end of the tree line on the aerial photo (fig. 10), which indicates a possible correlation with vegetation changes similar to those observed on Wescott Avenue (figs. 7 and 9). The reflection from the water table is also stronger in the marsh and produces a later time multiple (fig. 13), which is a duplicated reflection in the GPR line caused by a greater interface contrast between unsaturated marsh sediments and higher SC groundwater than that between unsaturated upland sediments and lower SC groundwater.

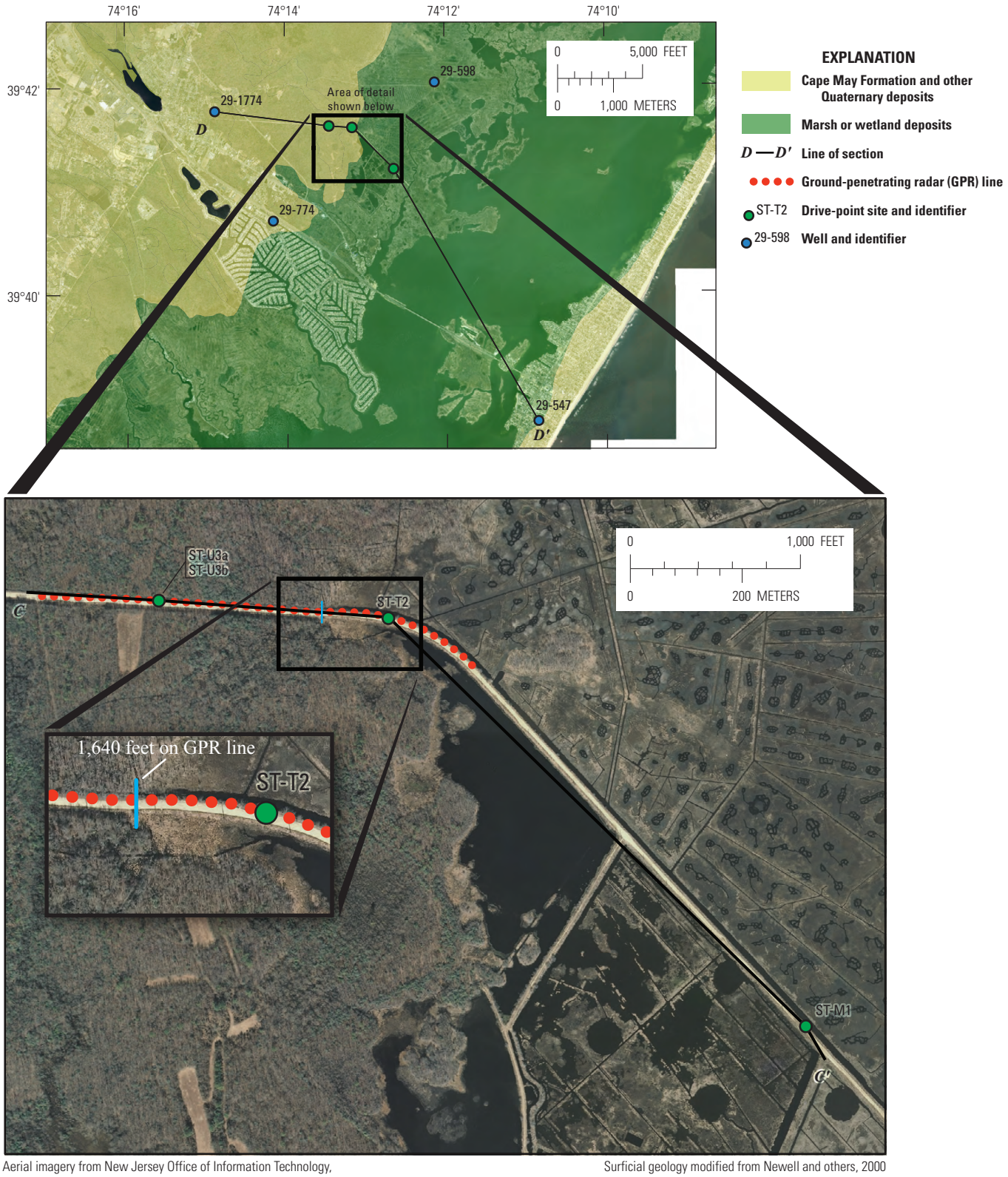

Figure 10. Surficial geology and locations of wells, drive-point sites, lines of section, and ground-penetrating radar line, Stafford Avenue study area, Ocean County, New Jersey.

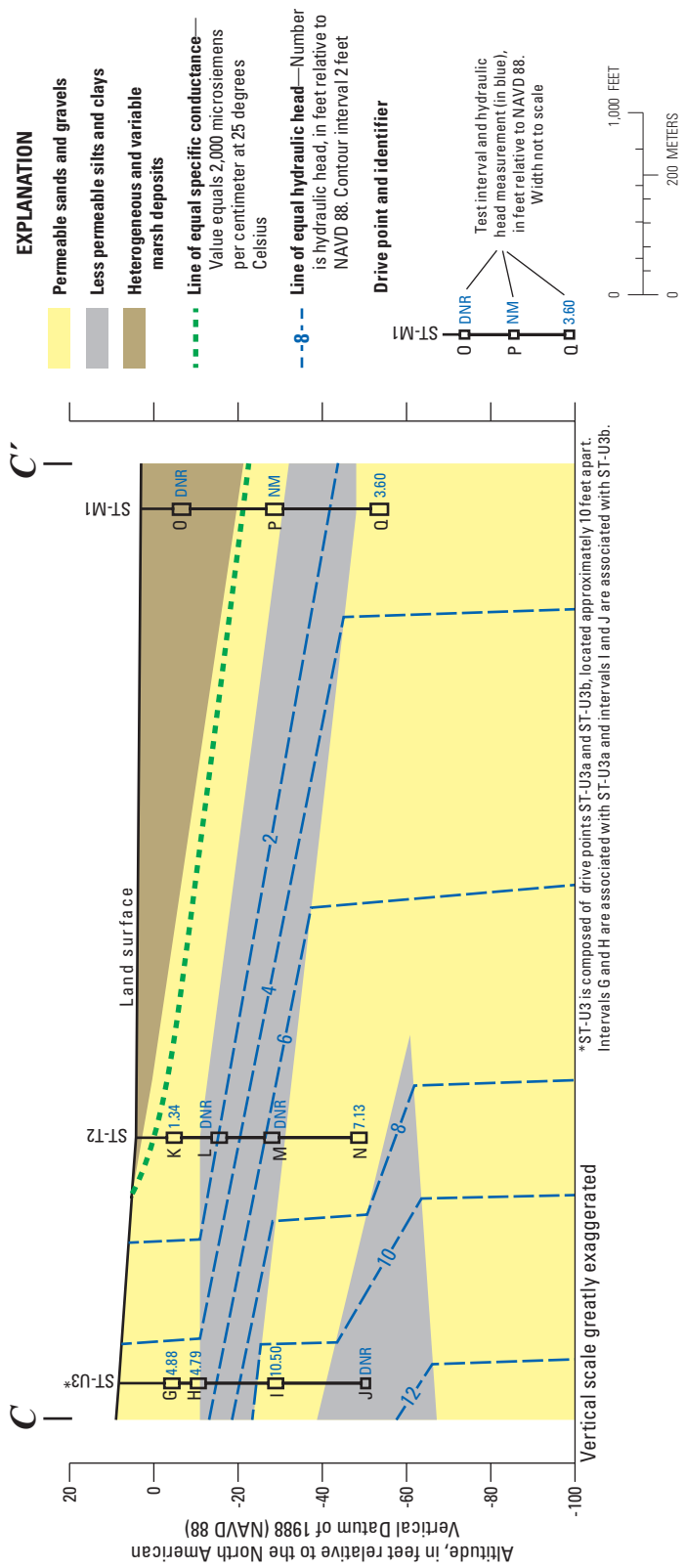

Figure 11. Hydrogeologic cross section *C-C′* at Stafford Avenue study area, Ocean County, New Jersey. Line of section shown in figure 10. (DNR, water level did not recover to a static condition; NM, water level not measured)

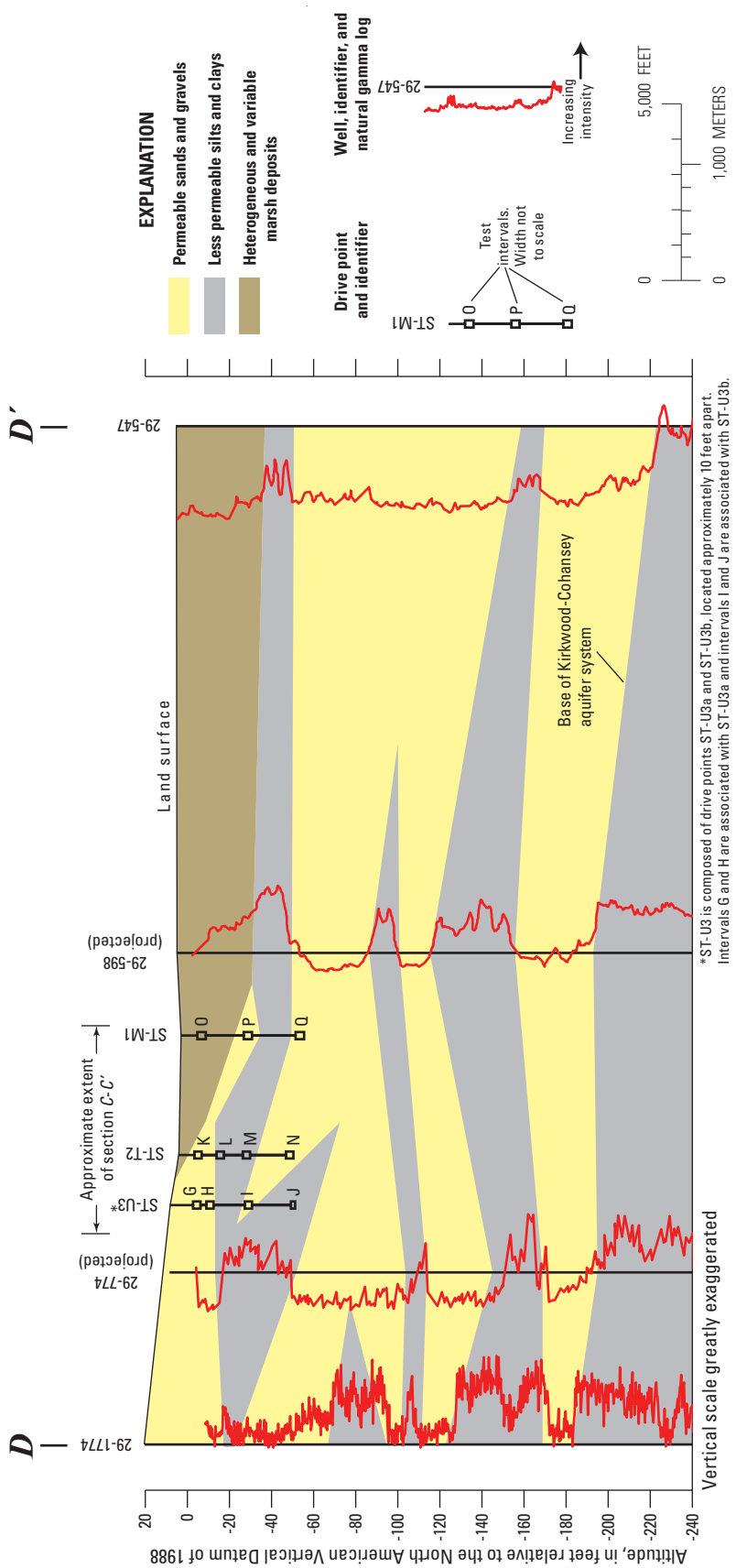

Figure 12. Hydrogeologic cross section *D-D´* at Stafford Avenue study area, Ocean County, New Jersey. Line of section shown in figure 10.

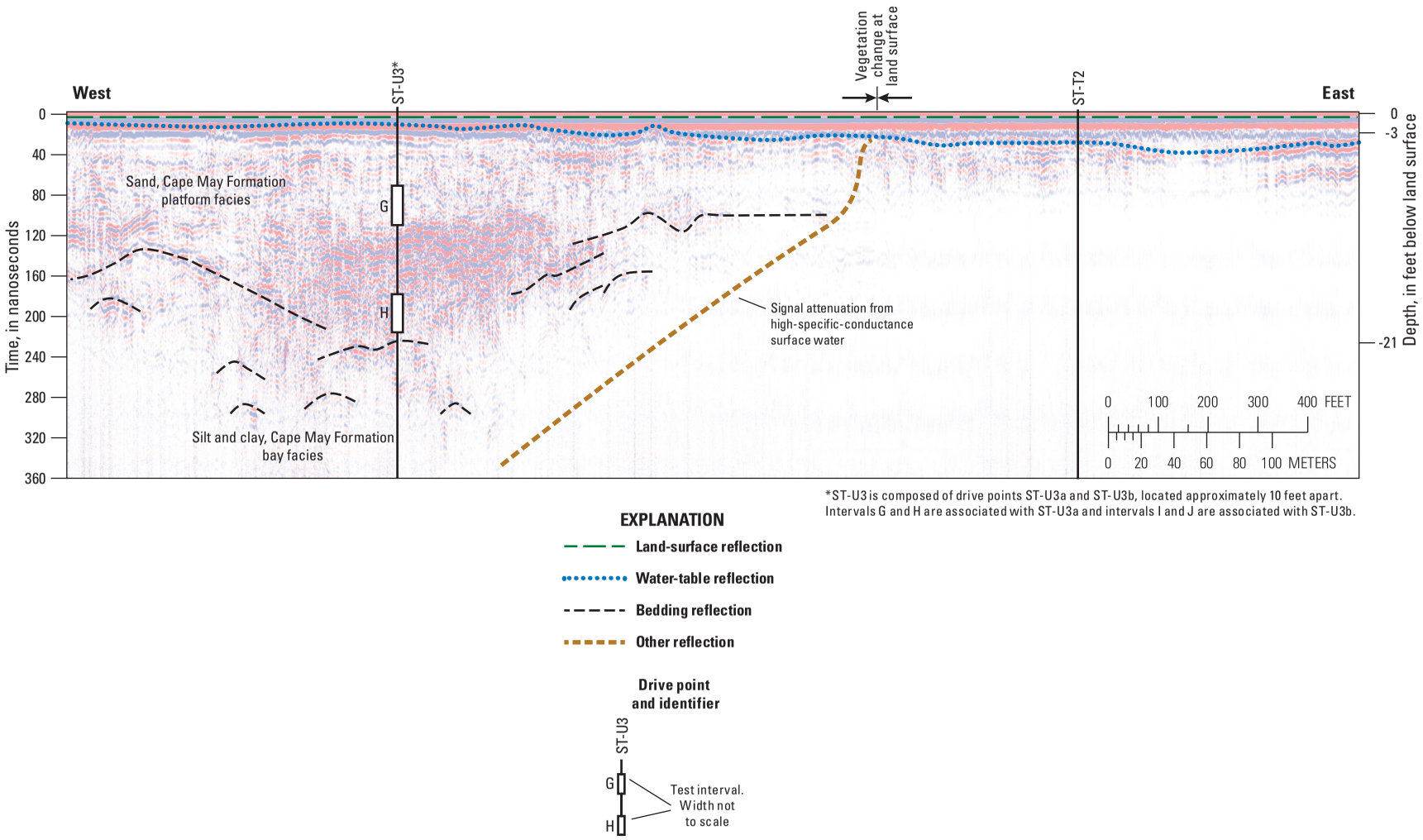

Figure 13. Ground-penetrating radar (GPR) line from Stafford Avenue study area, Ocean County, New Jersey, and reflection interpretations. Line includes direct current and time-varying gain filters. Depth scale is variable and not applicable to entire profile. GPR line shown in figure 10.

South Wildlife Drive Area

Three test holes were installed at South Wild Drive (table 1, fig. 14). Intervals R, S, T, U, V, and Y maintained similar pumping rates of 500 to 600 mL/min (190.20–228.25 gal/d) (table 1) and are likely hydraulically connected in the same permeable aquifer material (fig. 15). Water levels in intervals R (2.60 ft), S (2.53 ft), and T (2.28 ft) were higher than that in interval Y (1.57 ft) (table 1), indicating groundwater flow from upland to marsh as also indicated at the other locations. Water levels in intervals U and V were not measured (table 1), but the hydraulic-head values likely fall within that range, given their location in the flow path between SW-U3 and SW-M1.

Interval Z is open to a lower permeability layer (fig. 15). This interval had a lower pumping rate of 300 mL/min, and the water level failed to recover completely after pumping (table 1). The bottom of interval Z was set to 52.7 ft BLS (table 1) because the Geoprobe® was not able to hammer below that depth, which indicates denser and less permeable material below 52.7 ft (table 1). Because the SC at interval Z (2,880 µS/cm) indicates water is brackish (table 1), the unit above interval Z may be slightly coarser and sufficiently permeable to receive downward flow from overlying material. The clogging of the mill slot screen at SW-T2 likely occurred at some depth between intervals V and W, as intervals U and V maintained higher pumping rates than interval W (table 1) and fine-grained, low-permeability sediments are more likely to clog a screen. The low-permeability unit at interval W is likely the northwestern equivalent of the lower permeability unit at interval Z (fig. 15). Because testing at interval T indicated higher permeability than at interval Z, the low-permeability unit at Z either pinches out before reaching SW-U3 or is deeper than the bottom of interval T at SW-U3. Slightly high gamma counts on the log of well 1-180 at approximately the same altitudes as those of the low-permeability unit at interval Z (-55 to -58 [NAVD 88]) likely result from an extension of this unit and indicate the unit likely is present at a depth below that of interval T (fig. 15) rather than pinching out. This unit also extends across the bay to well 1-39 on the barrier island (figs. 14 and 16).

Peat was attached to the upper 18 ft of Geoprobe® rods at SW-M1, which indicates marsh deposits are present to a depth of about 18 ft at this location. A core collected by Kemp and others (2013) in a high marsh area less than 3 mi north of South Wildlife Drive indicated marsh deposits to a depth of about 14 ft. Interval X is likely situated within such deposits (fig. 15), and testing results indicate low-permeability material because the interval was pumped dry with no water-level recovery (table 1). This material differs from the more permeable marsh deposits at ST-M1 on Stafford Avenue (table 1); however, these results may be an artifact of the peat clogging the screen and preventing groundwater from entering the rods. If the sediments here are truly low permeability, the testing results are evidence of considerable hydrologic heterogeneity within marsh deposits that may result from differences in location in the marsh regime (upper marsh, lower marsh, and so on) and (or) geographical location along the coast of New Jersey.

SC measurements at South Wildlife Drive, like those at Stafford Avenue (table 1), indicate a process of high-SC groundwater recirculation described by Michael and others (2005) and Bratton (2010). Each interval tested in SW-M1 showed SC values indicative of brackish groundwater, and SC decreased with depth (table 1). Higher SC and more saline marsh-sourced water that enters the subsurface is likely discharged back to the marsh as a result of the stronger flow of fresh upland groundwater toward the marsh (fig. 2). The low-permeability unit at 52.7 ft BLS is deeper than low-permeability zones below the marsh at Stafford Avenue (figs. 11 and 12), so higher SC water can reach greater depths during the winter season when brackish recharge increases and groundwater discharge decreases (Michael and others, 2005). The brackish water that reaches interval Z will likely fail to infiltrate upon encountering the zone at 52.7 ft BLS and will eventually flow eastward and discharge farther from the upland.

Reflection shapes on the GPR line at South Wildlife Drive (fig. 17) are indicative of the Cape May Formation. Newell and others (2000) map the upland units at South Wildlife Drive as unit 1 of the Cape May Formation (Qcm1) and describe shoreward-dipping trough crossbeds as a feature of that unit. Westward-dipping crossbed reflections apparent on the GPR line (fig. 17) are consistent with the description of Qcm1 (Newell and others, 2000). Cross-stratification can be present in various depositional environments in the Cape May Formation as described by Stanford (2013a), but it is not clear to which specific unit these sediments belong. Crossbeds are generally typical in formations with high sand contents with moderate to high permeability. The gamma log of well 1-180 (fig. 15), about 300 ft south-southwest of drive point SW-U3 (fig. 14), indicates that some silt may also be present near land surface, which may be evident from the slightly lower pumping rates (500 mL/min) in test intervals R, S, U, and V (500 mL/min) than in shallow test intervals at other locations (600 mL/min) (table 1). The water table on the GPR line at South Wildlife Drive appears early in the profile at about 20 ns until a distance of about 1,080 ft, where the uplands end (figs. 14 and 17) and the signal is obscured by attenuation in the marsh, such as at Game Farm Road (fig. 6), Wescott Avenue (fig. 9), and Stafford Avenue (fig. 13). If GPR ground velocity in the upland below the water table is assumed to be 0.19 ft/ns, maximum penetration depth by the GPR is likely less than 30 ft, and the reflection from the top boundary of the crossbed reflections at SW-U3 is at a depth of about 10 ft (fig. 15).

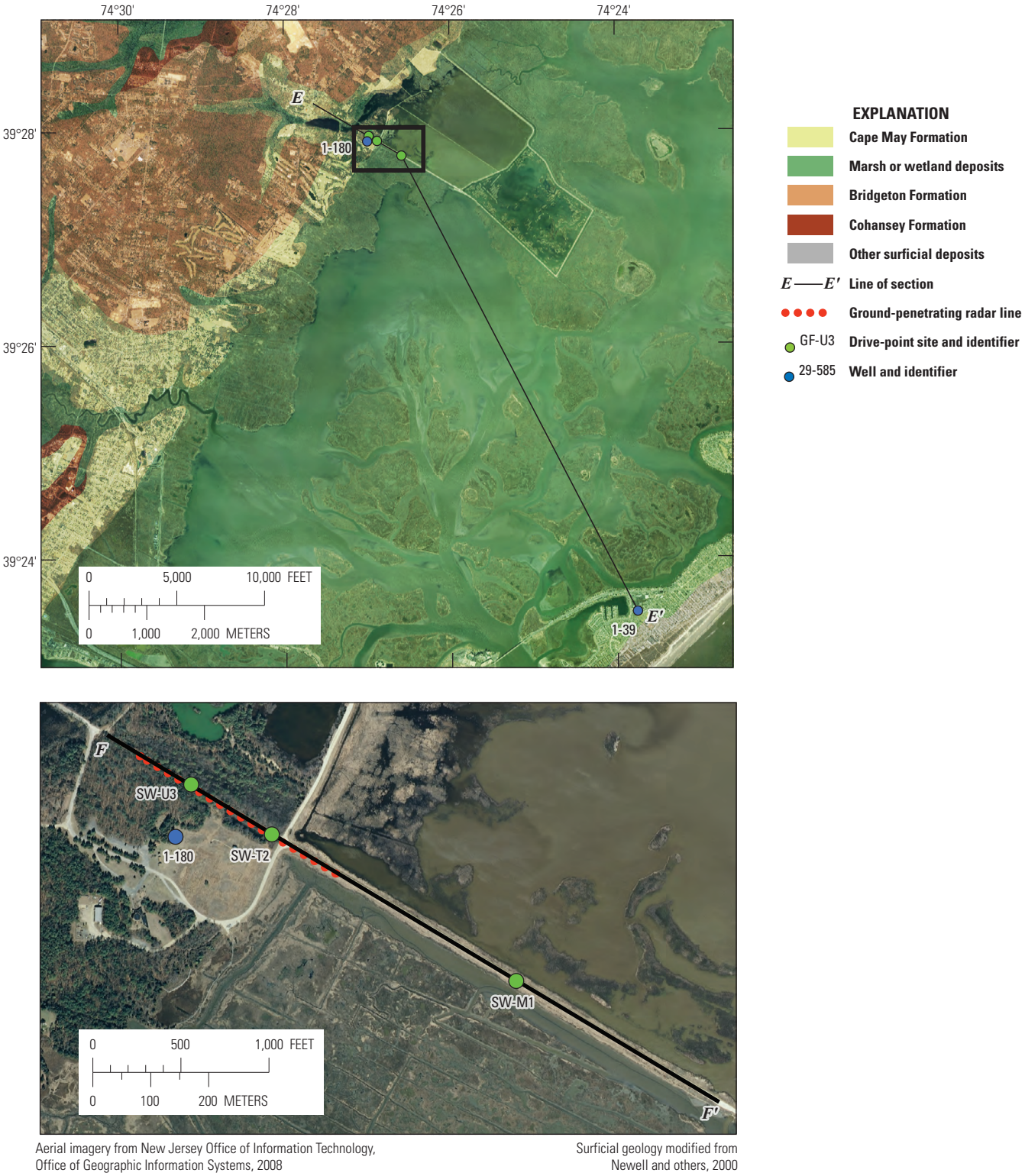

Figure 14. Surficial geology and locations of wells, drive-point sites, lines of section, and ground-penetrating radar line, South Wildlife Drive study area, Atlantic County, New Jersey.

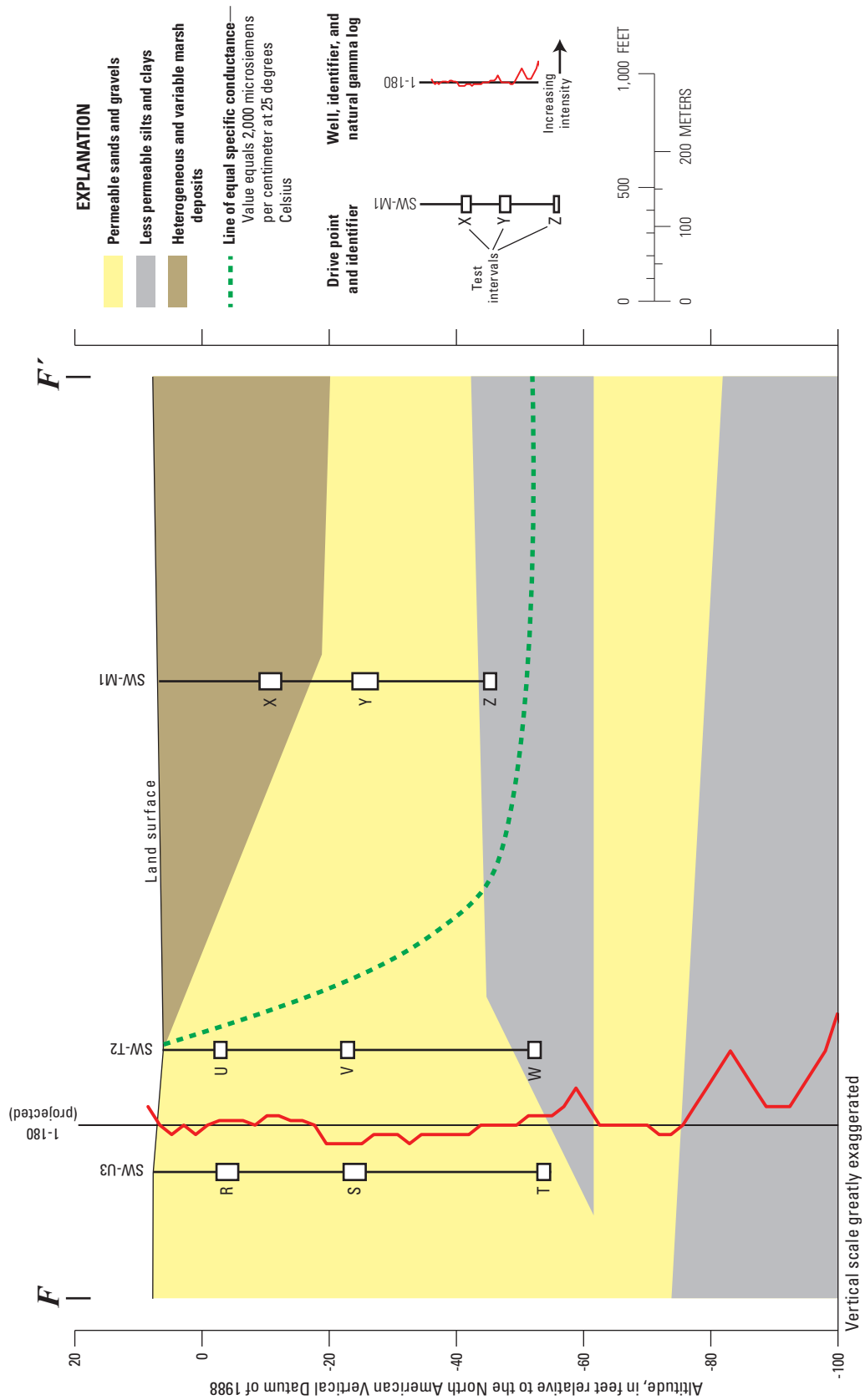

Figure 15. Hydrogeologic cross section *F-F′* at South Wildlife Drive study area, Atlantic County, New Jersey. Line of section shown in figure 14.

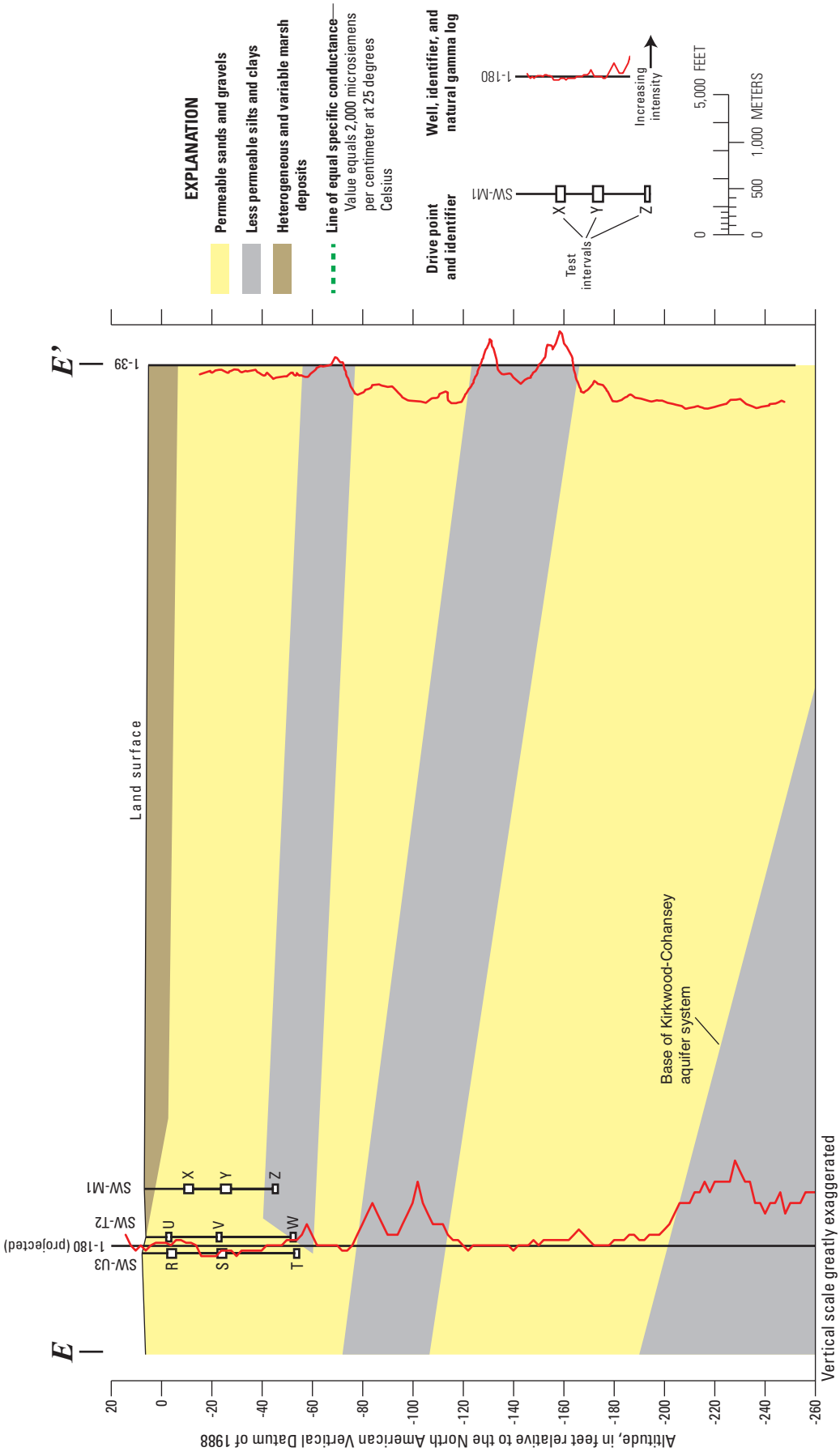

Figure 16. Hydrogeologic cross section *E-E'* at South Wildlife Drive study area, Atlantic County, New Jersey. Line of section shown in figure 14.

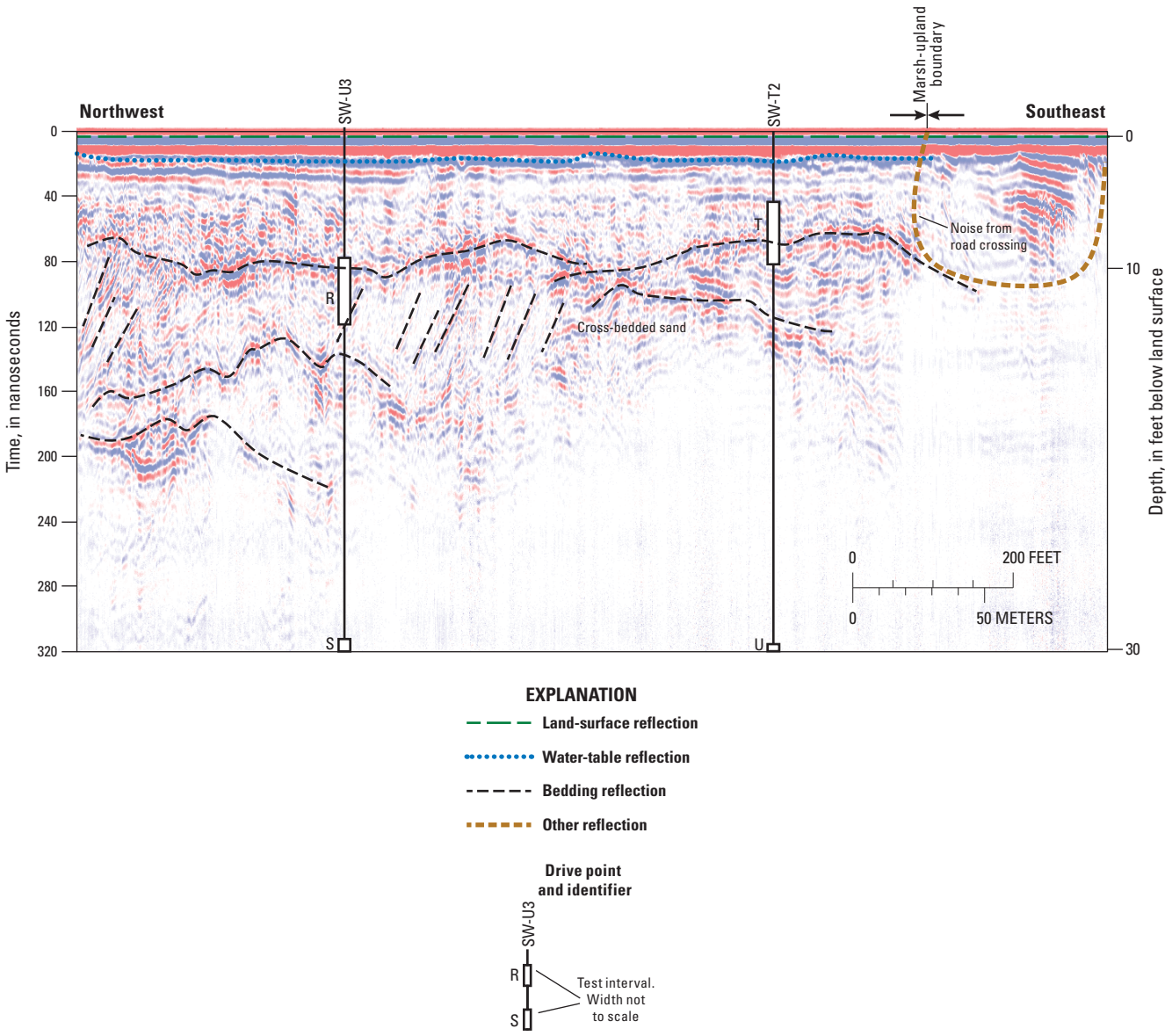

Figure 17. Ground-penetrating radar (GPR) line from South Wildlife Drive study area, Atlantic County, New Jersey, and reflection interpretations. Line includes direct current and time-varying gain filters. Depth scale is variable and not applicable to entire profile. GPR line shown in figure 14.

Water-Use Data

The New Jersey Department of Environmental Protection (NJDEP) Bureau of Water Supply requires well owners to report monthly withdrawals for all wells within the State that have a pump capable of extracting 70 gallons per minute or greater. Owners of private domestic wells are not required to report water use. Because withdrawals from these wells are much smaller than permitted withdrawals, domestic self-supply withdrawal data are not included in this study. The NJDEP maintains records for all reported withdrawal wells, categorized by type of water use and pump capacity. High-volume public-supply and industrial water users are metered, but wells with an agricultural certification are not. Agricultural users report estimated annual withdrawals. Annual and monthly water-use records with reported values for 2009, the most recent year for which water-use data are available, compiled by the NJDEP were used to calculate 2009 withdrawals from the 198 wells screened in the Kirkwood-Cohansey aquifer system in the Forsythe model area (fig. 18). Withdrawals from the Kirkwood-Cohansey aquifer system in the Forsythe model area by all water users averaged 16 million gallons per day (Mgal/d) in 2009. Groundwater withdrawals from individual wells ranged from 3.56×10^{-9} to 1.83 Mgal/d.

Simulation of Groundwater Flow

A three-dimensional numerical steady-state groundwater flow model was developed for the Kirkwood-Cohansey aquifer system in the Forsythe model area by creating a mathematical representation of the hydrogeologic framework and groundwater flow system. Model simulation files discussed herein are available as a data release (Fiore and Voronin, 2018). The USGS modular finite-difference groundwater flow model MODFLOW-2005 was used in this study (Harbaugh, 2005). The MODFLOW code consists of a main program and a series of independent subroutines called modules. The MODFLOW modules used in this study included Basic (BAS6), Discretization (DIS), Layer Property Flow (LPF), Recharge (RCH), Well (WEL), Drain (DRN), Evapotranspiration Segments (ETS), General Head Boundary (GHB), Flow and Head Boundary (FHB1), Saltwater Intrusion (SWI2), Zone (ZONE), and Multiplier (MULT). The FHB1 module is documented in Leake and Lilly (1997). The solver used for this model is the Geometric Multigrid Solver (GMG) (Wilson and Naff, 2004).

Model Discretization

The Forsythe model area was discretized horizontally into a variably spaced model grid that was rotated 42 degrees from north. The model grid was constructed with a variable spacing of 220 × 220 and 275 × 220 ft over the land mass. Grid-cell dimensions increased to the east over the Atlantic Ocean to 330 ft (fig. 19). Grid spacing in the Forsythe NWR is 275 × 220 ft, a cell size of 60,500 square feet (ft^2). There are 1,056 columns and 648 rows. The number of cells per layer is 684,288. The areal extent of the model grid is approximately 1,463 square miles (mi^2), 595 mi^2 onshore and 868 mi^2 including the ocean and Barnegat Bay, N.J. The model grid spacing and alignment were selected to provide relatively fine resolution of model input and output throughout the refuge and to minimize errors in the estimation of boundary flows simulated by using the USGS Regional Aquifer System Analysis (RASA) model grid (Spitz and others, 2008). The RASA grid-cell size ranges from 6.25 to 47.5 mi^2. The ratio of the number of model grid cells in the RASA model to the number in the Forsythe model is 1 to 144.

The Kirkwood-Cohansey aquifer system was discretized vertically into three layers of varying thickness (fig. 20). Model layer 1 includes the sediments of the upper part of the Kirkwood-Cohansey aquifer system and encompasses the shallow unconfined groundwater flow system. The thickness of model layer 1 is 45 or 100 ft. (These surficial sediments are described in the Hydrogeologic Framework section of this report.) Layer 2 consists of the sediments of the middle part of Kirkwood-Cohansey aquifer system and is 35 and 75 ft thick. Layer 3 consists of the sediments of the lower part of the Kirkwood-Cohansey aquifer system and ranges in thickness from 3 to 342 ft. The bottom of layer 3 contacts either the confining unit overlying the Rio Grande water-bearing zone or the basal Kirkwood confining unit (fig. 20). Model layer 3 is thicker in the northwestern part of the model area, above the basal Kirkwood confining unit, and is thinner in the southern part of the model area, above the confining unit overlying the Rio Grande water-bearing zone (Zapecza, 1989). In general, the fine-grained, relatively thin, low-permeability units in the Kirkwood-Cohansey aquifer system are too thin to be accurately interpolated for continuity beyond the topographic quadrangles in which they have been mapped. Therefore, the layer thicknesses are large to allow this high level of heterogeneity to be consistent across the relatively large size of the model domain.

Generally, groundwater flow paths move from recharge areas to discharge areas. In the Kirkwood-Cohansey aquifer system, recharge areas are at higher altitude and discharge areas include streams, lake, wells, and wetlands. The length of time required for groundwater to move from recharge to discharge areas depends on the length and depth of the flow path along which it travels. Groundwater traveling along shallow flow paths in the Kirkwood-Cohansey aquifer system may take days or years to reach a nearby stream, lake, or wetland. Water traveling along deeper, longer flow paths in the Kirkwood-Cohansey flow system may take hundreds of years to flow to a distant regional discharge point such as a large river, bay, or wetland.

Time in the groundwater flow model is simulated in units of seconds. The simulation period of the model is average 2005–15 hydraulic conditions. Hydrographs for wells 5-570, 5-628, and 29-1419 (fig. 21), which are part of the USGS

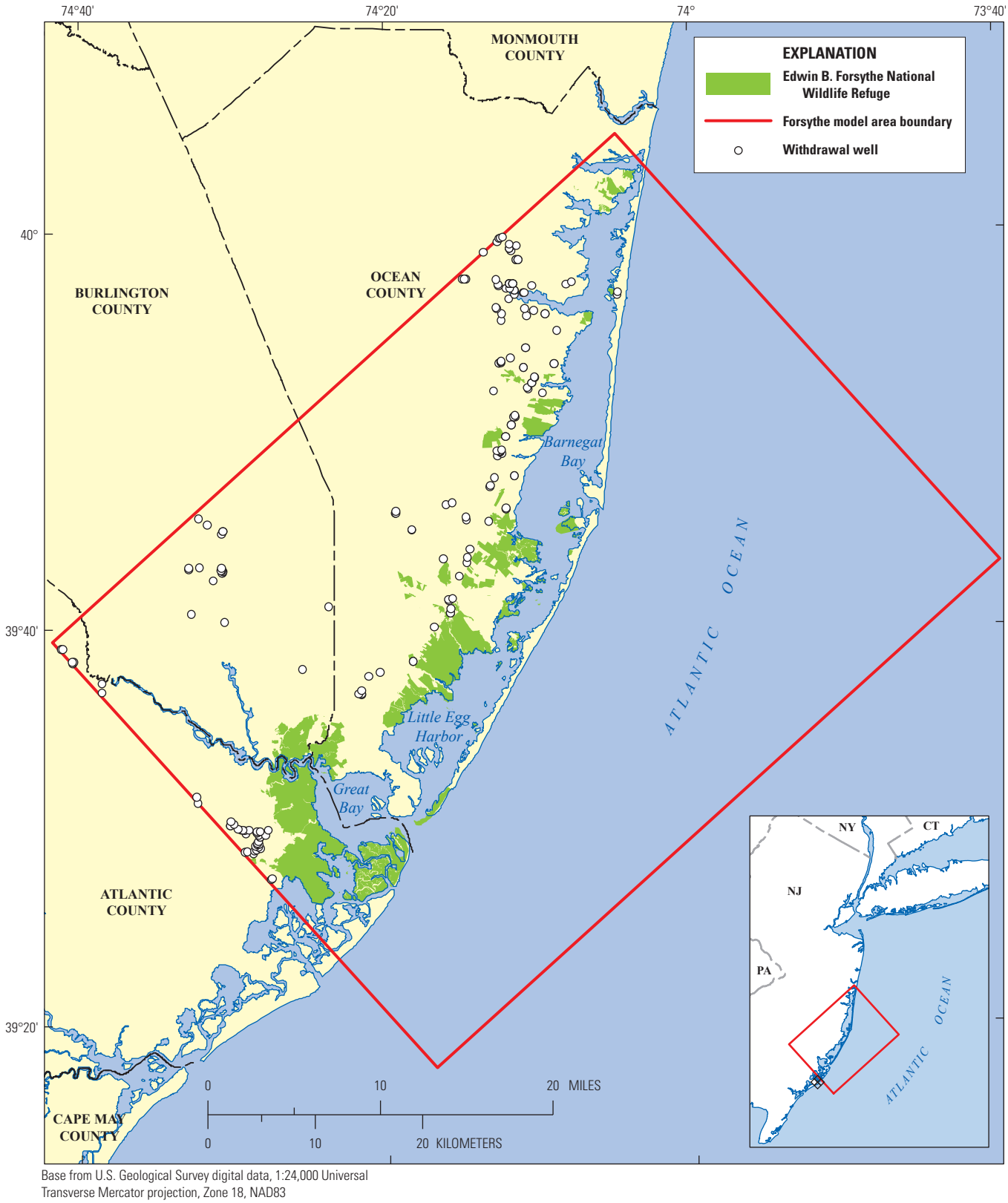

Base from U.S. Geological Survey digital data, 1:24,000 Universal Transverse Mercator projection, Zone 18, NAD83

Figure 18. Location of groundwater withdrawal wells with withdrawal records for 2009 and screened in the Kirkwood-Cohansey aquifer system, Forsythe model area, New Jersey.

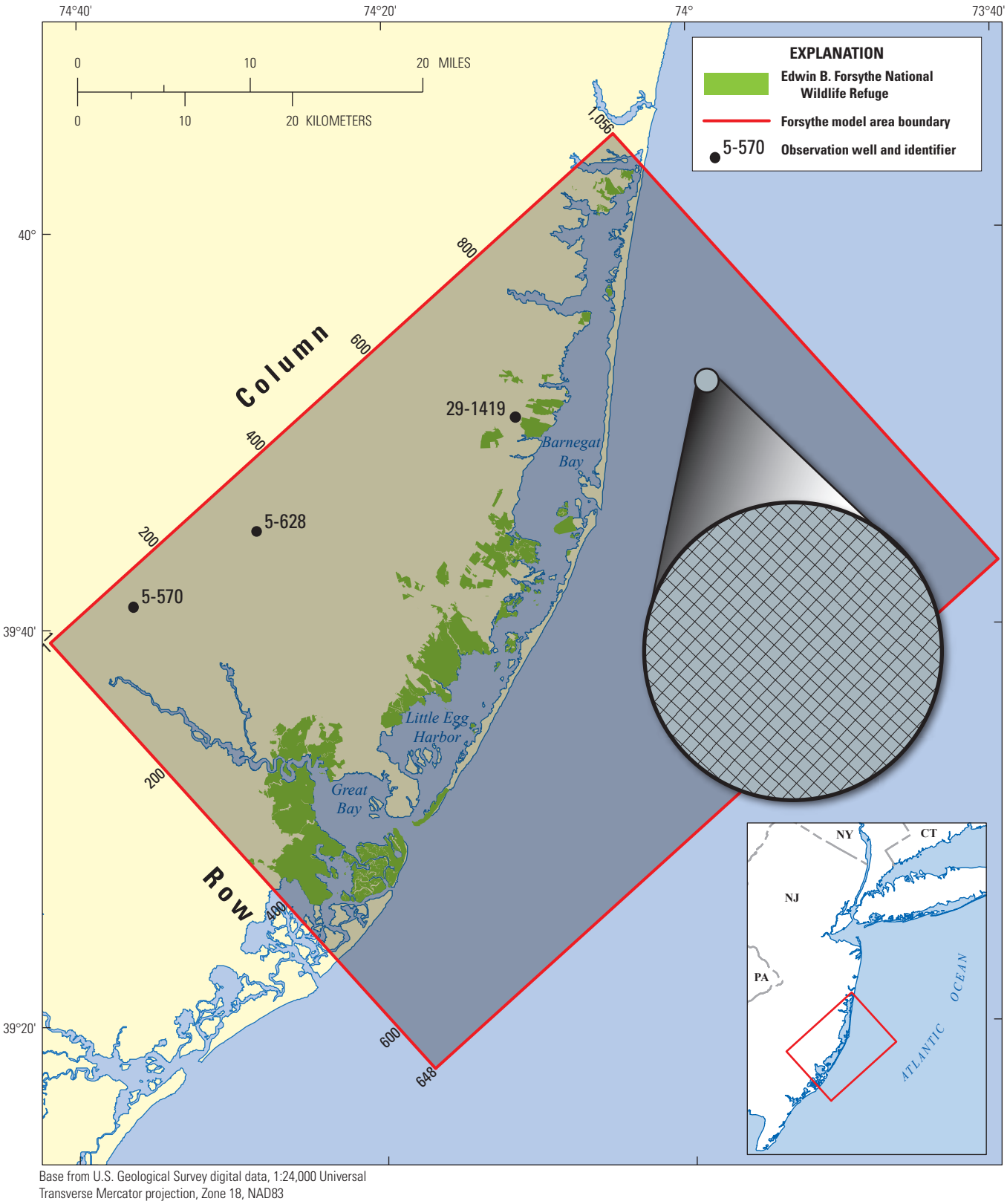

Figure 19. Variably spaced model grid in the Forsythe model area, New Jersey.

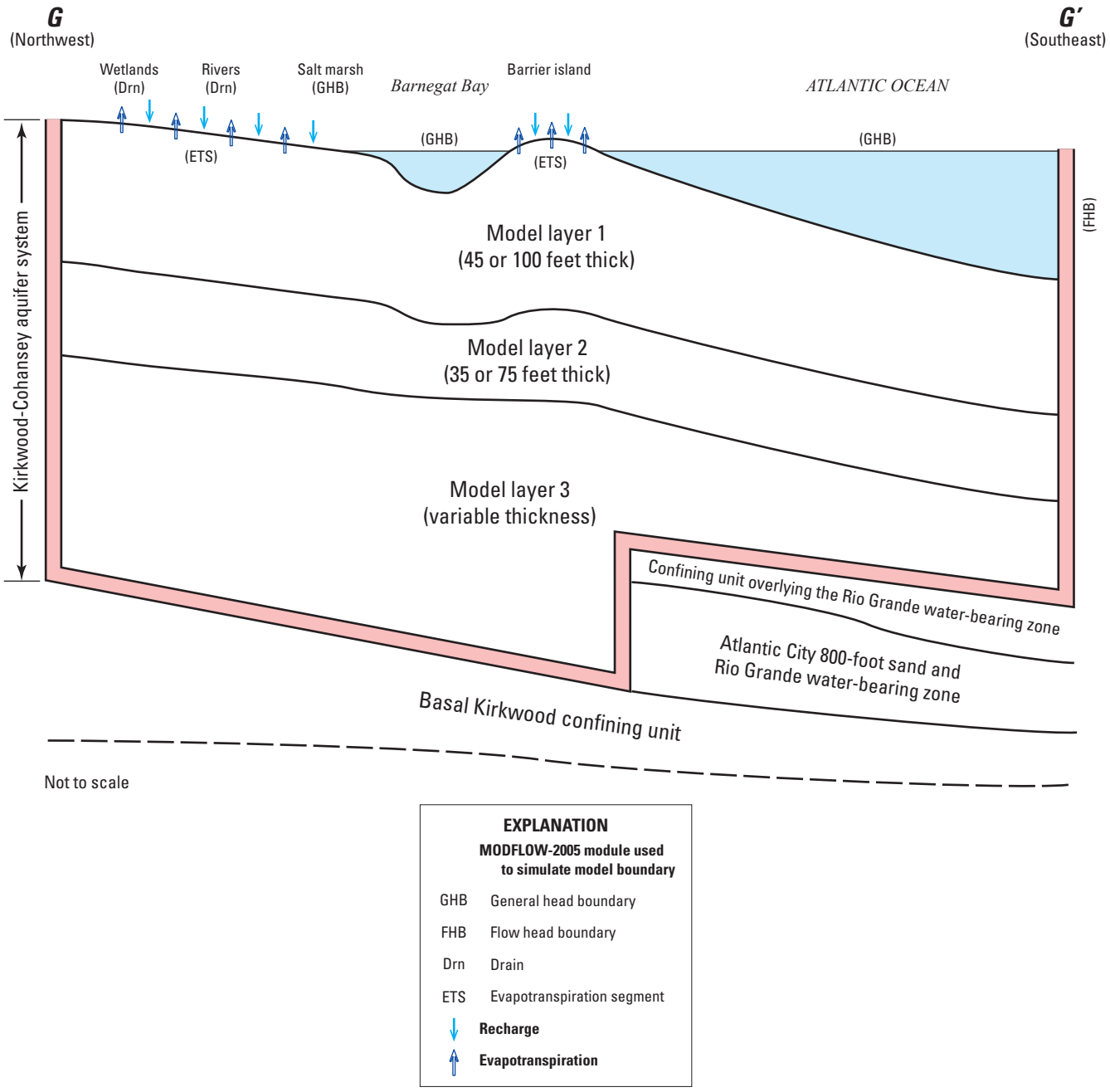

Figure 20. Section *G-G′* through the Kirkwood-Cohansey aquifer system illustrating the relation between model layers and aquifers and model boundaries, Forsythe model area, New Jersey. Line of section shown in figure 1.

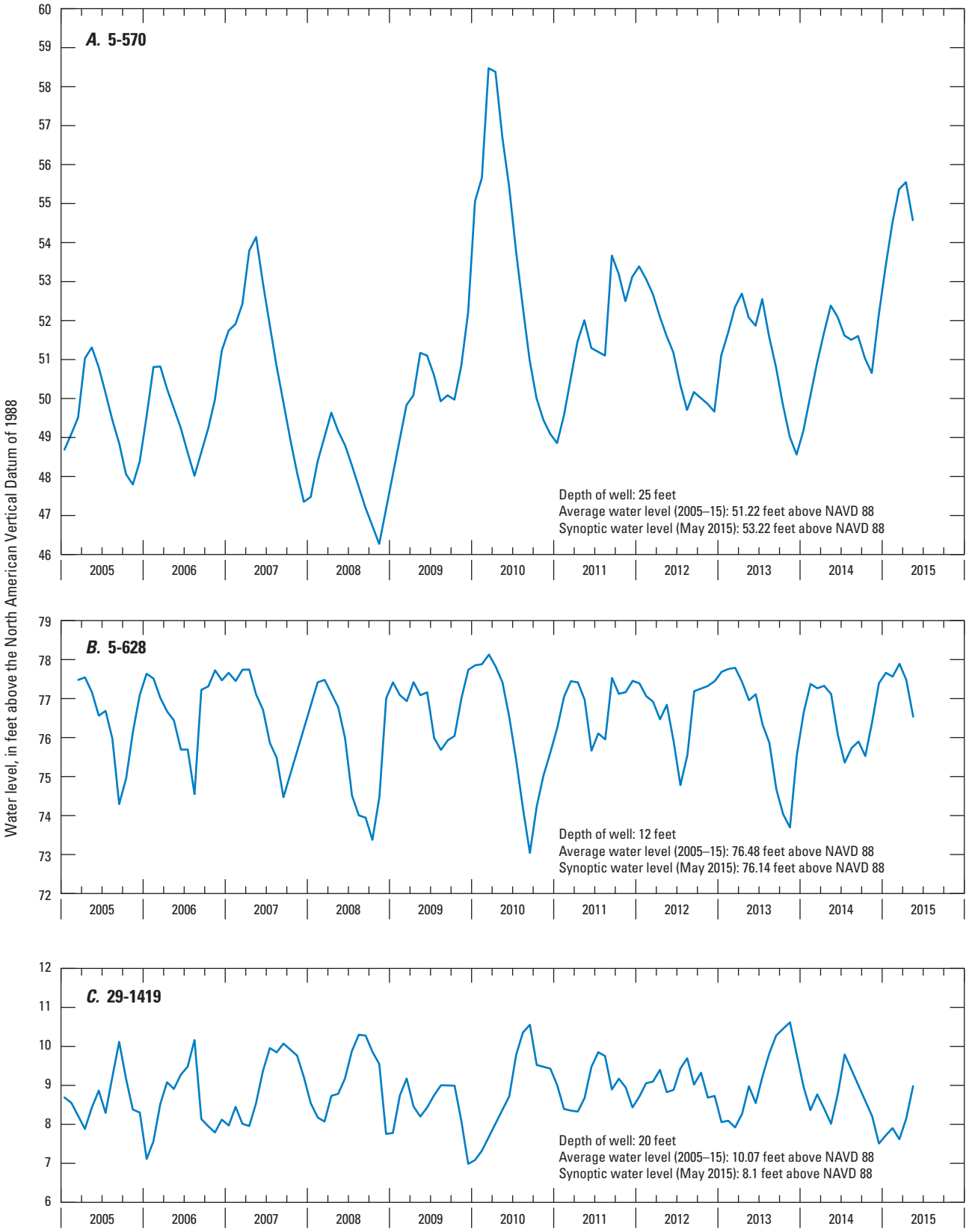

Figure 21. Hydrographs of wells *A*, 5-570, *B*, 5-628, and *C*, 29-1419, Forsythe model area, New Jersey. Location of wells shown in figure 19. (NAVD 88, North American Vertical Datum of 1988).

long-term water-level monitoring network and in the Forsythe model area in which water levels were measured during the spring 2015 synoptic survey, were used to determine whether the results of the spring 2015 survey are representative of 2005–15 average conditions. The average water levels in wells 5-570, 5-628, and 29-1419 are 51.22, 76.48, and 10.07 ft above NAVD 88, respectively. The spring 2015 synoptic water levels in wells 5-570, 5–628, and 29-1419 were 53.44, 76.14, and 8.1 ft above NAVD 88, respectively. The spring 2015 water level in well 5-570 was 2 ft higher than the average water level in this well; in well 5–628 it was 0.34 ft lower than the average water level; and in well 29-1419 it was 1.97 ft lower than the average water level. Therefore, the water levels measured during the spring 2015 synoptic survey are considered to be representative of 2005–15 average hydrologic conditions in the Forsythe model area.

Hydrologic Boundary Conditions

The location and quantity of flow into and out of the model were represented with hydrologic boundaries. These boundaries represent surface-water features, evapotranspiration, recharge, groundwater withdrawals, and lateral and vertical flow.

Surface-Water Features

The streams and freshwater wetland areas in the model area are represented with the DRN module (fig. 22). Streams in the groundwater flow model are derived from the geographical representation of their extent in the USGS 1:24,000-scale National Hydrography Dataset (U.S. Geological Survey, 2015). The stream conductance for each cell is calculated as a product of the area of the stream within the cell, the streambed hydraulic conductivity, and the streambed thickness.

Streambed hydraulic conductivity was divided into five groups on the basis of altitude in feet with respect to NAVD 88: greater than 50, 20 to 49, 10 to 19, 1 to 9, and 0. These groups were established to account for the differences in hydraulic conductivity of the various sediments in the study area. For example, in the upland area, a low-permeability layer that is resistant to erosion impedes the flow of groundwater discharge to streams. In addition, at high altitudes where the steep slope of the stream is not conducive to the accumulation of fine-grained sediments in the streambed, the streambed hydraulic conductivity reflects the characteristics of the sediments at that location. At lower altitudes, where the stream is less steep, fine-grained sediments can accumulate in the streambed, thereby impeding groundwater discharge to streams.

The initial estimate of streambed hydraulic conductivity, 0.25 feet per day (ft/d), is similar to values used in a simulation of the water table in the Mullica River (Harbaugh and Tilley, 1984) and Toms River (Cauller and others, 2016) Basins. Final calibrated hydraulic-conductivity values, calculated by using the automated parameter estimation software UCODE-2005 (Poeter and others, 2005), ranged from 0.0022 to 17.28 ft/d (table 4).

Streambed thickness is assumed to be 3 ft. For stream reaches located above an altitude of 50 ft, the length of the stream within the cell and a stream width of 4 ft were used to calculate the area within a cell. For stream reaches located below an altitude of 50 ft, the stream reach was assumed to occupy the entire cell. This assumption is reasonable because extensive wetlands in the model area are typically located adjacent to stream reaches (fig. 22). The altitude of the streambed was estimated from the digital topobathymetric maps from the USGS Earth Resources and Observation Science Center (EROS) (Danielson and others, 2016).

The land-surface boundary beneath Barnegat Bay, Great Bay, Little Egg Harbor, and the Atlantic Ocean is represented by the GHB module. The GHB module was used to simulate a head-dependent flux boundary—in this study, flow between the bays or ocean and the underlying sediments. Model input for the GHB module includes hydraulic head at the boundary; for this study, the freshwater equivalent head was used in Barnegat Bay, Great Bay and Little Egg Harbor, and the Atlantic Ocean. The following equation, adapted from Hubbert (1940), was used to calculate the freshwater equivalent head:

$$h_f = (P_s / P_f)\, h_{msl} - [(P_s - P_f) / P_f]\, Z \qquad (2)$$

where

h_f is the freshwater equivalent head,
P_s is the density of seawater,
P_f is the density of freshwater,
h_{msl} is mean sea level, and
Z is the bathymetric altitude.

F.J. Spitz (U.S. Geological Survey, written commun., 2016) estimated the mean salinity of the water in Barnegat Bay to be 26 parts per thousand (ppt), which is approximately equivalent to 75 percent seawater and 25 percent freshwater; this value was used in equation 2 to calculate the density of seawater in Barnegat Bay and Great Bay and Little Egg Harbor. Digital bathymetric maps from EROS were used to define the depth of the bay and ocean (Danielson and others, 2016). The mean sea level value of -0.4 ft was based on the mean sea level for the 1983–2001 tidal epoch at National Oceanic and Atmospheric Administration (NOAA) gage 8534720 at Atlantic City, N.J. (National Oceanic and Atmospheric Administration, 2013a), and was used for the h_{msl} value in the ocean. The mean sea level value of -0.02 ft in Barnegat Bay is based on mean sea level for the 1983–2001 tidal epoch at the NOAA gages 8533615 at Barnegat Inlet (inside) (National Oceanic and Atmospheric Administration, 2013b) and 8533987 at West Creek, N.J. (National Oceanic and Atmospheric Administration, 2013c).

The salt marsh areas in the model area were simulated with the GHB module. The hydraulic head value of -0.02 ft was based on mean sea level for the 1983–2001 tidal epoch

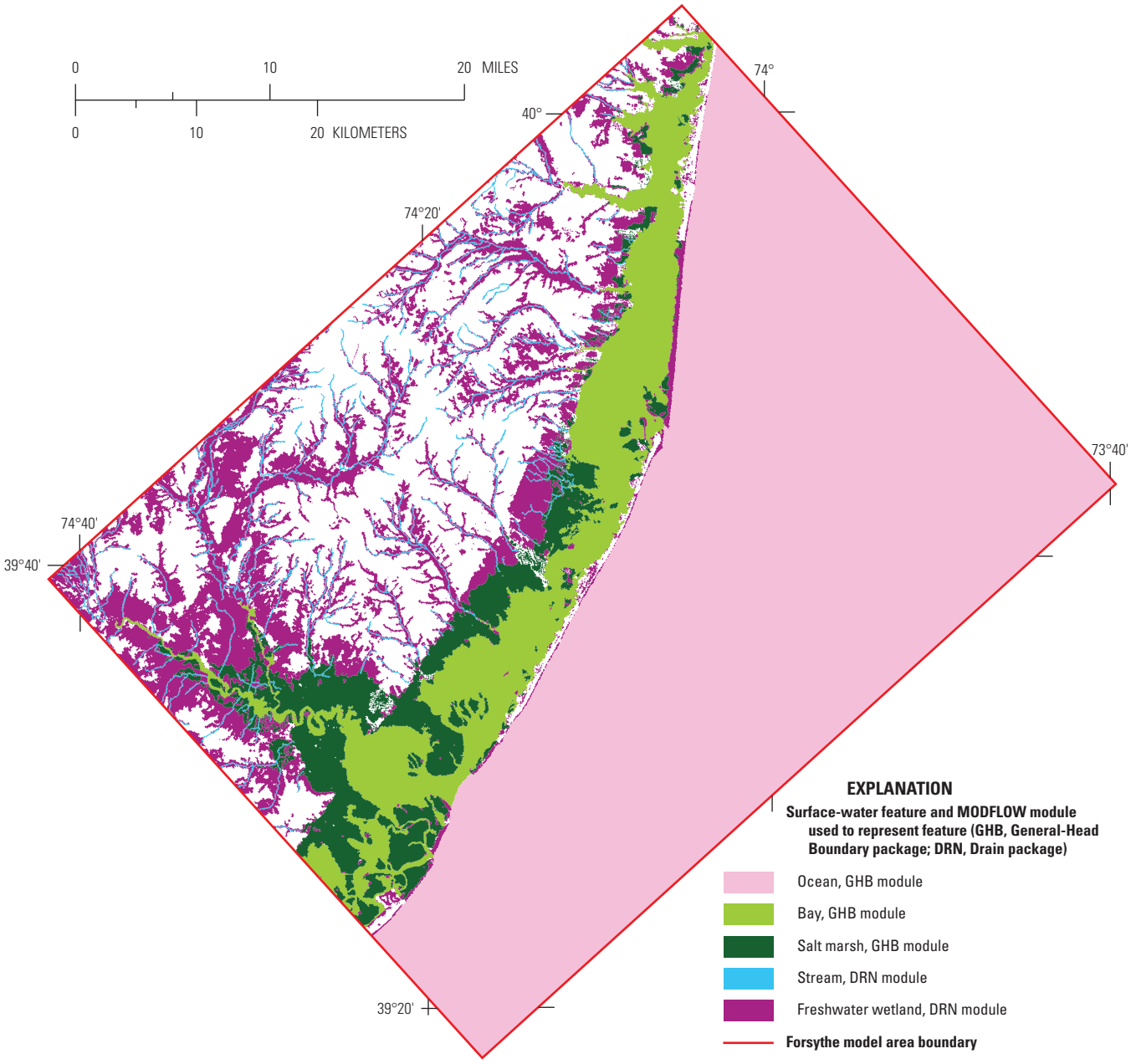

Figure 22. Location of surface-water features and MODFLOW module used to represent feature in the Forsythe model area, New Jersey.

at the NOAA gages at Barnegat Inlet (inside) (8533615) and West Creek, N.J. (8533987). A freshwater equivalent head was not used in the salt marsh areas because these areas are inundated only during high tide with a thin layer of saltwater; hence, a freshwater equivalent head was not warranted.

The hydraulic conductance of the interface between the aquifer sediments and the boundary (freshwater equivalent head or head) also was input to the GHB package. The conductance for each cell was calculated as a product of the area of the cell, the sediment hydraulic conductivities, and the thickness of the sediments. The sediment hydraulic conductivities for the bay, ocean, and salt marsh are 0.5, 0.014, and 0.05 ft/d, respectively. The thickness of the sediments is assumed to be 10 ft.

Evapotranspiration

Evapotranspiration (ET) in the abundant (256 mi²) freshwater wetlands in the model area (fig. 22) and where the water table is within 5 ft of the land surface was simulated by using the ETS module. Nicholson and Watt (1997) conducted a detailed analysis of ET for the Toms River study area, N.J., and concluded that groundwater ET is likely an important process in the shallow groundwater budget in wetland areas. Charles and Nicholson (2012), in their analysis of ET for the New Jersey Pinelands area that includes the Morses Mill watershed, part of which is located in the Forsythe model area, also concluded that ET is an important process in the shallow groundwater budget. They used the ETS module in their simulation, and their model input for the ET module was used as a template for the Forsythe model input for the ET module.

The following parameters were defined for the ET module. The depth to the ET surface was calculated by subtracting 3.28 ft from the altitude of land surface. ET was varied vertically: up to 3.28 ft BLS, 100 percent of initial ET; 3.29 to 3.36 ft BLS, 100 to 66 percent of initial ET; 3.36 to 5 ft BLS, 66 to 60 percent of initial ET; and greater than 5 ft BLS, zero ET. The initial ET value, taken from Charles and Nicholson (2012), was 8.2×10^{-8}. Published ET values are summarized in table 3.

Recharge

Recharge was applied to the top surface of the model in onshore land areas without surface-water features by using the RCH module. A variety of methods have been used by researchers to estimate recharge in the New Jersey Coastal Plain. Estimated recharge rates are summarized in table 3. On the basis of geology of the underlying sediments and the percentage of urban land use in the Metedeconk and Toms River Basins, Nicholson and Watt (1997) estimated recharge rates that ranged from 13.4 to 17.3 inches per year (in/yr) for urban land and 16.8 to 21.6 in/yr for nonurban land. In an analysis of the water resources of Ocean County that includes the Cedar Creek, Forked River, Oyster Creek, Mill Creek, Cedar Run, Dinner Point Creek, Westecunk Creek, and Tuckerton Creek Basins, Gordon (2004) estimated a recharge rate of 17.5 in/yr. Charles and Nicholson (2012) used a water-budget analysis to estimate a recharge rate of 46 in/yr. The model that Charles and Nicholson constructed included the ET module and an annual ET rate of 31 in/yr was estimated by the ET module. Pope and others (2012) estimated recharge that ranged from 10 to 30 in/yr. Cauller and others (2016) used a modified water-balance method that incorporates the effect of land use by factoring in spatially uniform estimated monthly recharge rates with the spatially variable annual recharge data;

Table 3. Published recharge, annual evapotranspiration, and hydraulic properties of the Kikwood-Cohansey aquifer system, New Jersey.

[ft/d, feet per day; in., inch; in/yr, inch per year; NA, not available]

Horizontal hydraulic conductivity (ft/d)	Vertical hydraulic conductivity (ft/d)	Recharge (in/yr)	Annual evapotranspiration (in.)	Citation
0.03 to 394.00	0.03 to 20.00	[1,2]46.00	[1]31.20	Charles and Nicholson, 2012
[3]15.00 to 100.00	NA	16.00 to 20.00	NA	Martin, 1998; Voronin, 2004
18.00 to 150.00	0.2 to 1.8	12.42 to 21.20	NA	Cauller and others, 2016
20.00 to 100.00	0.2 to 1.00	13.40 to 21.60[b]	10.2	Nicholson and Watt, 1997
60.00	10	10.00 to 30.00	NA	Pope and others, 2012
90.00 to 250.00	NA	NA	NA	Gill, 1962; Rhodehamel, 1973
NA	NA	18.94	22.15	Johnson and Watt, 1996
131.00 to 200.00	NA	17.5	23.4	Gordon, 2004

[1]Average rate.

[2]Simulated evapotranspiration separately; net recharge is less than values shown.

[3]Hydraulic conductivity estimated from aquifer thickness and transmissivity in the Forsythe study area.

they estimated an annual 2000–03 recharge rate that ranged from a low of 12.42 in/yr in 2001 to a high of 21.20 in/yr in 2002.

Wieben and Chepiga (2018) calculated the mean precipitation in the Forsythe model area from the National Oceanic and Atmospheric Administration (2015) National Climatic Data Center (NCDC) for 2004–13 for three weather stations: Atlantic City and Atlantic City International Airport, N.J., in the southern part of the Forsythe model area, and Freehold-Marlboro, N.J., in the northern part (fig. 1). Mean precipitation at Freehold-Marlboro is 48.9 in/yr; mean precipitation for the Atlantic City and Atlantic City International Airport weather stations is 46.5 in/yr.

On the basis of the previously mentioned studies and the mean precipitation in the Forsythe model area, an initial recharge rate of 20 in/yr was used. This value is within the range used in the previously mentioned studies. The final simulated recharge rate used in the model, estimated with UCODE-2005, ranges from 6.27 to 42.65 in/yr. The lower rate was applied in wetland areas, and the higher rate was applied in upland areas with no surface-water features, which make up about 10 percent of the model area. Wetlands receive less recharge than uplands because some recharge is rejected as runoff, rather than lost to ET, during times of the year when the water table is high. Groundwater discharge to ET will increase where simulated sea-level rise (SLR), described later in this report, causes the water table to rise within the simulated 3.29- to 5-ft BLS ET transition zone. Therefore, explicit simulation of recharge and ET is appropriate to account for changes in ET associated with SLR.

Groundwater Withdrawals

Groundwater withdrawals in the Forsythe model area were represented in the model by using the WELL module. Groundwater withdrawals within the model area were obtained from the NJDEP Bureau of Water Supply as described previously in the Water Use section of this report. A model layer was assigned to each withdrawal well on the basis of the location and depth of the well screen. All wells were screened in model layer 3.

Lateral and Vertical Flow

The FHB1 module provides a means to apply specified heads or specified flow at boundary cells from a larger scale model, such as the RASA model (Voronin, 2004). A steady-state version of the RASA model was revised and included 2003 groundwater withdrawals (Spitz and others, 2008). Flows generated by the revised simulations of the RASA were used at corresponding cells as input to the FHB1 module to incorporate flow at lateral and bottom model boundaries (fig. 20).

Hydraulic Properties

Hydraulic properties include streambed hydraulic conductivity, and horizontal and vertical hydraulic conductivity for each model layer. The hydraulic properties were grouped into zones of similar geologic units that were defined with a single value. Delineation of the hydraulic-property zone was based on lithologic logs and geologic maps that were available for the model area as described in the Hydrogeologic Framework section of this report. Model layer 1 was divided into seven hydraulic-property zones, model layer 2 was divided into six zones, and model layer 3 was divided into five zones (fig. 23). Initial estimates for each of the hydraulic-property zones were determined on the basis of the geologic and hydrologic data compiled from previous studies.

Estimates of the initial hydraulic conductivities for the Kirkwood-Cohansey aquifer system that were based on previous studies in the model area are shown in table 4. These estimates served as starting points for the calibration process. Initial hydraulic-conductivity values ranged from 15 to 150 ft/d. One horizontal hydraulic-conductivity value was calibrated for each of the hydraulic-property zones in each model layer (fig. 23). Final horizontal hydraulic conductivities for the Kirkwood-Cohansey aquifer system range from 8.64 ft/d for zone 2 in layer 1 to 238.43 ft/d for zone 5 in layer 2 (table 4).

The hydraulic connection (vertical leakance, leakage) between model layers is calculated with the MODFLOW program by using the thickness and the vertical hydraulic conductivity of the model layer to calculate the vertical leakage for each model cell (Harbaugh, 2005). For this model, the vertical hydraulic conductivity was calculated as a fraction of the horizontal hydraulic conductivity. The ratio of horizontal hydraulic conductivity (K_h) to vertical hydraulic conductivity (K_v)—vertical anisotropy—was calibrated to be 1:10.

Model Calibration

Reilly and Harbaugh (2004) state that when evaluating the adequacy of model calibration, “a reasonable representation of the conceptual model and sources of water is more important than blindly minimizing the discrepancy between simulated and observed heads.” For this study, several types of data were used to compare measured and simulated values to support the representation of the conceptual model, including water levels, groundwater discharge to streams, and flow budgets.

Initially, the model was calibrated by a trial-and-error approach until a reasonable match between measured and simulated data was achieved. Hydraulic properties were adjusted during model calibration to minimize the differences between simulated and measured values of the following: (1) estimated base flow at five streamflow-gaging stations, (2) water levels in 44 temporary piezometers and 28 existing wells measured in spring 2015, and (3) potentiometric surfaces in May 2015.

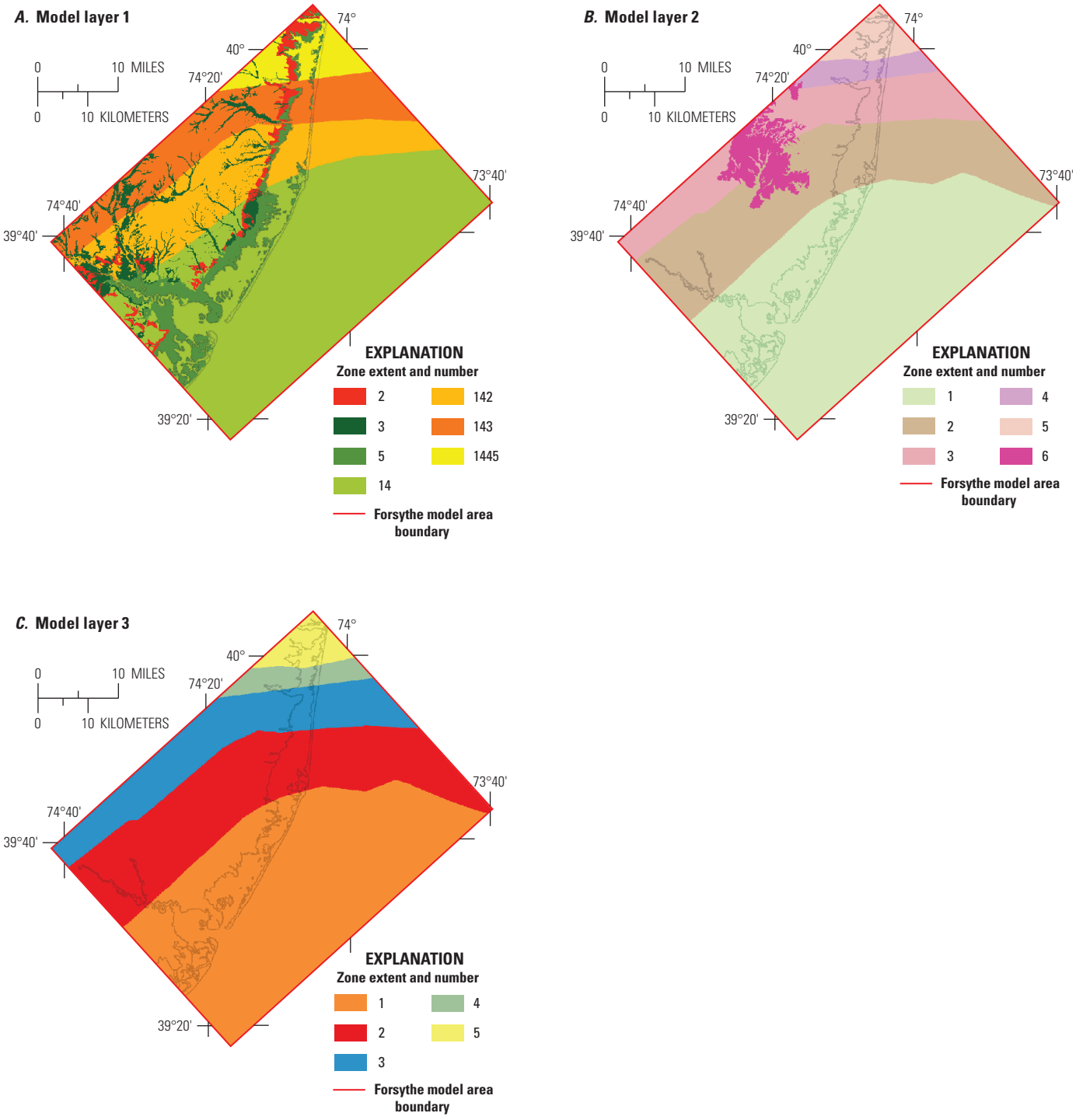

Figure 23. Hydraulic property zones used during the calibration process for estimating hydraulic conductivity, Forsythe model area, New Jersey: *A*, model layer 1, *B*, model layer 2, and *C*, model layer 3. Zones were delineated on the basis of geologic and hydrogeologic features.

Table 4. Final parameter values for the calibrated model of the Kirkwood-Cohansey aquifer system and composite scaled sensitivities, Forsythe model area, New Jersey.

[Location of Forsythe model area is shown in figure 1; ft/d, feet per day; NA, not applicable; Fig., Figure]

Parameter name	Parameter value	Units	Model layer	Reference for parameter extent	Composite scaled sensitivity
Horizontal hydraulic conductivity					
KH_z14	9.18	ft/d	1	Fig. 23A, zone 14	3.43
KH_z142	28.49	ft/d	1	Fig. 23A, zone 142	3.70
KH_z143	25.23	ft/d	1	Fig. 23A, zone 143	8.10
KH_z1445	40.88	ft/d	1	Fig. 23A, zone 1445	2.63
KH_z2	20.25	ft/d	1	Fig. 23A, zone 2	3.06
KH_z3	8.95	ft/d	1	Fig. 23A, zone 3	3.71
KH_z5	35.00	ft/d	1	Fig. 23A, zone 5	1.03
KH_z1a	14.67	ft/d	2	Fig. 23B, zone 1	2.86
KH_z2a	8.64	ft/d	2	Fig. 23B, zone 2	3.29
KH_z3a	86.50	ft/d	2	Fig. 23B, zone 3	6.22
KH_z4a	24.86	ft/d	2	Fig. 23B, zone 4	1.13
KH_z5a	238.43	ft/d	2	Fig. 23B, zone 5	3.36
KH_z6a	11.68	ft/d	2	Fig. 23B, zone 6	3.49
KH_z1b	229.41	ft/d	3	Fig. 23C, zone 1	9.16
KH_z2b	31.02	ft/d	3	Fig. 23C, zone 2	7.56
KH_z3b	8.64	ft/d	3	Fig. 23C, zone 3	5.02
KH_z4b	33.96	ft/d	3	Fig. 23C, zone 4	0.96
KH_z5b	44.86	ft/d	3	Fig. 23C, zone 5	1.44
Vertical anisotropy					
VANIall	10	Dimensionless	1–3	NA	4.57
Streambed hydraulic conductivity					
DrnBedK50	17.28	ft/d	NA	NA	0.54
DrnBedK20	2.68	ft/d	NA	NA	0.15
DrnBedK10	0.002	ft/d	NA	NA	0.08
DrnBedK0	2.33	ft/d	NA	NA	0.13
DrnBdKEq0	0.37	ft/d	NA	NA	0.21
FreshWtLnd	1.37	ft/d	NA	NA	0.82
General head boundary hydraulic conductivity					
SaltMshGHB	0.050	ft/d	NA	NA	2.14
Bay	0.500	ft/d	NA	NA	0.09
Ocean	0.014	ft/d	NA	NA	0.01
Recharge					
RechParm	1.14	multiplier, dimensionless	NA	NA	171.37
Evapotranspiration					
ETS_Par1	0.518	multiplier, dimensionless	NA	NA	38.88

Final model calibration was accomplished by using the automated parameter estimation software, UCODE-2005.

A weighting factor for the observation value can be defined and used by the automated parameter estimation software UCODE-2005. The weighting factor is commonly based on measurement errors. Errors that contribute most to the uncertainty of water-level observations are associated with potential inaccuracies in the altitude and location of a well and in the measurement of a water level (San Juan and others, 2004). Streamflow measurements were weighted the highest (100) and all hydraulic-head observations were weighted the same (50). Hydraulic-head observations were assigned a smaller weight to prevent them from dominating the calibration process. Hydraulic-head observations were weighted the same because the measurements were made during a 3-week time frame and were made with a steel tape. The altitudes at 13 of the temporary piezometers were surveyed and compared to Digital Elevation Model (DEM) data for these locations. The surveyed altitude and DEM data compared closely (table 5). The DEM data were used for the altitudes at all of the temporary piezometers. For consistency, DEM data also were used for the altitude at all of the wells.

Highly correlated parameters, such as ET and recharge, cannot be reliably estimated by UCODE. For highly correlated parameters, one of the parameters was fixed and the parameter estimation proceeded with the other parameter estimated by UCODE. The fixed parameter was chosen on the basis of whether that parameter had more reasonable estimates than the other. For example, ET was fixed on the basis of evapotranspiration values in Charles and Nicholson (2012), and it was assumed there was more confidence in evapotranspiration than in independent recharge estimates.

Hydraulic-Head Observations

The difference (measured water level minus simulated water level, or residual) (table 5, fig. 24), average of the residual, median of the residual, average absolute residual, and the root mean square error (RMSE) between measured and simulated water levels at 72 wells were used to evaluate model calibration (table 5). The RMSE for 72 water-level measurements in the model area is 2.73 ft, indicative of a reasonable fit between measured and simulated water levels. The RMSE was small compared to the approximately 144-ft range in observed water levels in the model area. The average of the residual, 0.34 ft, and the average absolute residual, 1.99 ft, also are indicative of a reasonable fit between simulated and measured water levels (table 5).

The relation between the simulated hydraulic heads and measured water levels closely matches a 1:1 correlation line (fig. 25). A graph of simulated equivalent and measured water levels for an unbiased model ideally shows a random distribution above and below a 1:1 correlation line. The measured and simulated equivalent water levels for the Forsythe model area are randomly distributed above and below the 1:1 correlation line. There is a very small model bias to underpredict measured water levels.

Base-Flow Observations

Estimated average 2004–13 base flows at five streamflow-gaging stations were used in model calibration (table 6, fig. 26). Wieben and Chepiga (2018) used hydrograph separation to estimate average base flow from January 2004 to December 2013 at five continuous-record stations (table 6) in the Forsythe model area. Simulated base-flow values were calculated by summing the simulated flow to drain cells (used to represent streams and wetlands adjacent to stream reaches) from each streamflow-gaging station in the model. Simulated base flows evaluated at the five streamflow-gaging stations match the estimated base flows very closely, within 1.65 cubic feet per second. The simulated and measured base flows for the five streamflow-gaging stations are distributed on the 1:1 correlation line (fig. 25) and indicate a good model fit and little model bias.

Sensitivity Analysis

The results of model calibration demonstrate that the groundwater flow model, as defined by its combination of boundary conditions, boundary flows and heads, hydrologic-unit definitions, geometry, and values of hydraulic parameters, reasonably reproduces the measured base flows and potentiometric surfaces in the aquifer system in the model area. The purpose of sensitivity analysis is to quantify the uncertainty in the calibrated model due to uncertainty in the estimates of aquifer parameters, stresses, and boundary conditions (Anderson and Woessner, 1992). The objective is to determine how readily and excessively water-level altitudes are affected by a change in hydraulic parameters in the calibrated model. A sensitivity analysis was conducted for the groundwater flow model by using UCODE-2005. The composite scaled sensitivities (CSSs) are used to evaluate the sensitivity of the simulated model parameters and determine whether the calibration data are sufficient to estimate a parameter (Hill and Tiedeman, 2007). CSSs summarize all the sensitivities for each parameter and are used to evaluate the relative sensitivity of the simulated model parameters (Hill and Tiedeman, 2007). Parameters with large CSSs compared to those of other parameters indicate that simulation results are more sensitive to those parameters, given the observations used in this model.

CSSs were calculated for 30 parameters as part of the model sensitivity analysis (table 4, fig. 27). Table 4 presents the value for each parameter zone and a brief description of the hydrogeologic unit that makes up the zone. A weighting factor for the observation value was used in the calculation

Table 5. Difference between simulated and water levels measured in spring 2015, Forsythe model area, New Jersey.

[Location of Forsythe model area shown in figure 1; Water-level and land-surface measurements are relative to the North American Vertical Datum of 1988; UID, unique identifier; USGS, U.S. Geological Survey; ft, foot; DEM, Interpolated from 1-meter Digital Elevation Model; NWIS, USGS National Water Information System database]

UID	Local name	Measured water level (ft)	Simulated water level (ft)	Difference between measured and simulated water level (ft)	Model layer	Type of well	Land-surface[1] altitude from DEM (ft)	Land-surface altitude in NWIS (ft)
1-721	Ac 11 Obs	21.31	14.68	6.63	1	Existing well	32.5	29.74
1-726	Ac 12 Obs	13.2	3.97	9.23	1	Existing well	24.8	23.73
1-756	Slf MW-1-1980	20.54	20.60	-0.06	1	Existing well	27.4	28.53
1-757	Slf MW-2-1980	21.76	24.10	-2.34	1	Existing well	33.2	40.93
5-511	Mullica 6D	29.9	27.12	2.78	2	Existing well	37.9	41.1
5-570	Mount Obs	53.25	50.49	2.76	1	Existing well	62.7	62
5-613	Mullica 45S	36.7	34.61	2.09	2	Existing well	41.2	39.82
5-628	Penn Sf Shallow Obs	76.16	69.84	6.32	1	Existing well	78.6	77.53
5-630	Penn Sf Deep Obs	80.18	78.61	1.57	2	Existing well	106.1	103.05
5-1102	Bass R Sf-Pz-2	17.69	17.36	0.33	1	Existing well	23.0	21.74
5-1103	Bass R Sf-MW-1	17.71	17.27	0.44	2	Existing well	23.0	21.74
5-1138	Cedar Ave-MW1	13.16	14.25	-1.09	1	Existing well	20.8	21.73
5-1156	MW 1	0.01	3.03	-3.02	1	Existing well	3.2	6.33
29-17	Island Beach 1 Obs	0.44	2.83	-2.39	3	Existing well	4.8	7.26
29-20	Island Beach 4 Obs	1.28	0.18	1.10	1	Existing well	4.8	6.95
29-58	PW 21	-1.99	2.81	-4.80	2	Existing well	6.1	8.77
29-513	Garden St Pky 1 Obs	43.24	35.79	7.45	1	Existing well	49.5	43.01
29-514	Garden St Pky 2 Obs	40.79	35.20	5.59	3	Existing well	49.5	42.58
29-773	Bass R Sf 1	26.98	29.47	-2.49	1	Existing well	45.2	43.74
29-789	Cedar Brg Twr1	144.14	144.37	-0.23	2	Existing well	199.1	198.74
29-1249	Lf MW-4A	27.56	34.26	-6.70	1	Existing well	49.9	52.74
29-1251	Lf MW-2A	31.5	35.59	-4.09	1	Existing well	51.5	52.74
29-1257	Slf MW-2	32.65	33.50	-0.85	1	Existing well	52.0	48.75
29-1258	Slf MW-3	34.5	31.08	3.42	2	Existing well	50.1	48.75
29-1419	MW61	8.06	7.57	0.49	1	Existing well	17.2	17.76
29-1431	Service MW-118S	28.82	28.22	0.60	1	Existing well	38.6	38.75
29-2273	WLT-1	7.9	11.40	-3.50	1	Existing well	26.4	26
29-2274	MW8	25.3	26.34	-1.04	1	Existing well	44.2	44
1-2250	EBF-PZ-01	2.6	3.70	-1.10	1	Temporary piezometer	6.8	7
1-2252	EBF-PZ-02	7.76	5.82	1.94	1	Temporary piezometer	13.6	13
1-2251	EBF-PZ-03	2.88	1.33	1.55	1	Temporary piezometer	5.8	6
1-2253	EBF-PZ-04	5.85	3.52	2.33	1	Temporary piezometer	13.9	14
29-2255	EBF-PZ-05	5.51	5.79	-0.28	1	Temporary piezometer	6.8	7
29-2256	EBF-PZ-06	11.3	11.15	0.15	1	Temporary piezometer	13.5	13
29-2254	EBF-PZ-07	2.13	1.53	0.60	1	Temporary piezometer	3.8	4
29-2252	EBF-PZ-08	3.14	3.52	-0.38	1	Temporary piezometer	5.1	5
29-2253	EBF-PZ-09	5.17	6.05	-0.88	1	Temporary piezometer	6.4	6
29-2266	EBF-PZ-10	6.38	5.36	1.02	1	Temporary piezometer	9.1	9
29-2257	EBF-PZ-11	4.76	3.06	1.70	1	Temporary piezometer	7.8	8
29-2267	EBF-PZ-12	26.33	28.35	-2.02	1	Temporary piezometer	38.1	38

Table 5. Difference between simulated and water levels measured in spring 2015, Forsythe model area, New Jersey.—Continued

[Location of Forsythe model area shown in figure 1; Water-level and land-surface measurements are relative to the North American Vertical Datum of 1988; UID, unique identifier; USGS, U.S. Geological Survey; ft, foot; DEM, Interpolated from 1-meter Digital Elevation Model; NWIS, USGS National Water Information System database]

UID	Local name	Measured water level (ft)	Simulated water level (ft)	Difference between measured and simulated water level (ft)	Model layer	Type of well	Land-surface[1] altitude from DEM (ft)	Land-surface altitude in NWIS (ft)
29-2259	EBF-PZ-13	19.18	18.35	0.83	1	Temporary piezometer	22.0	22
29-2258	EBF-PZ-14	3.58	2.29	1.29	1	Temporary piezometer	5.3	5
29-2260	EBF-PZ-15	13.91	13.27	0.64	1	Temporary piezometer	16.1	16
29-2265	EBF-PZ-16	20.16	20.51	-0.35	1	Temporary piezometer	28.9	29
29-2263	EBF-PZ-17	0.92	0.33	0.59	1	Temporary piezometer	3.4	3
29-2262	EBF-PZ-18	5.7	7.91	-2.21	1	Temporary piezometer	13.1	13
29-2264	EBF-PZ-19	15.5	16.24	-0.74	1	Temporary piezometer	16.1	16
29-2261	EBF-PZ-20	15.84	14.29	1.55	1	Temporary piezometer	18.7	19
29-2271	EBF-PZ-21	10.35	7.18	3.17	1	Temporary piezometer	13.6	13
29-2270	EBF-PZ-22	0.93	0.03	0.90	1	Temporary piezometer	1.2	1
29-2272	EBF-PZ-23	30.22	33.21	-2.99	1	Temporary piezometer	38.8	39
1-2258	EBF-PZ-24	7.88	10.19	-2.31	1	Temporary piezometer	22.9	23
1-2259	EBF-PZ-25	10.02	13.07	-3.05	1	Temporary piezometer	40.7	41
1-2256	EBF-PZ-26	3.92	3.86	0.06	1	Temporary piezometer	5.1	5
1-2257	EBF-PZ-27	4.89	5.50	-0.61	1	Temporary piezometer	14.1	14
1-2255	EBF-PZ-28	8.24	9.03	-0.79	1	Temporary piezometer	24.3	23
5-1926	EBF-PZ-29	3.18	1.74	1.44	1	Temporary piezometer	4.3	5
5-1927	EBF-PZ-30	5.12	2.82	2.30	1	Temporary piezometer	8.5	9
5-1928	EBF-PZ-31	7.72	6.49	1.23	1	Temporary piezometer	13.2	13
5-2254	EBF-PZ-32	16.69	20.67	-3.98	1	Temporary piezometer	21.5	22
29-2269	EBF-PZ-33	2.25	4.19	-1.94	1	Temporary piezometer	5.4	5
29-2268	EBF-PZ-34	0.87	0.16	0.71	1	Temporary piezometer	3.7	4
29-2276	EBF-PZ-35	1.56	-0.02	1.58	1	Temporary piezometer	3.2	3
29-2278	EBF-PZ-36	8.41	6.40	2.01	1	Temporary piezometer	11.1	11
29-2250	EBF-PZ-37	4.29	1.61	2.68	1	Temporary piezometer	8.2	8
29-2249	EBF-PZ-38	2.45	0.69	1.76	1	Temporary piezometer	4.2	4
29-2248	EBF-PZ-39	1.99	2.07	-0.08	1	Temporary piezometer	7.3	8
29-2251	EBF-PZ-40	0.4	0.10	0.30	1	Temporary piezometer	1.9	2
29-2275	EBF-PZ-41	0.18	-0.44	0.62	1	Temporary piezometer	1.6	2
29-2277	EBF-PZ-42	0.73	2.23	-1.50	1	Temporary piezometer	2.9	3
29-2280	EBF-PZ-43	0.6	0.22	0.38	1	Temporary piezometer	4.2	4
29-2279	EBF-PZ-44	6.23	7.81	-1.58	1	Temporary piezometer	11.0	11
Average of residual				0.34				
Median of residual				0.38				
Root Mean Square Error				2.73				
Average absolute residual				1.99				

[1]Values from Wieben and Chepiga (2018).

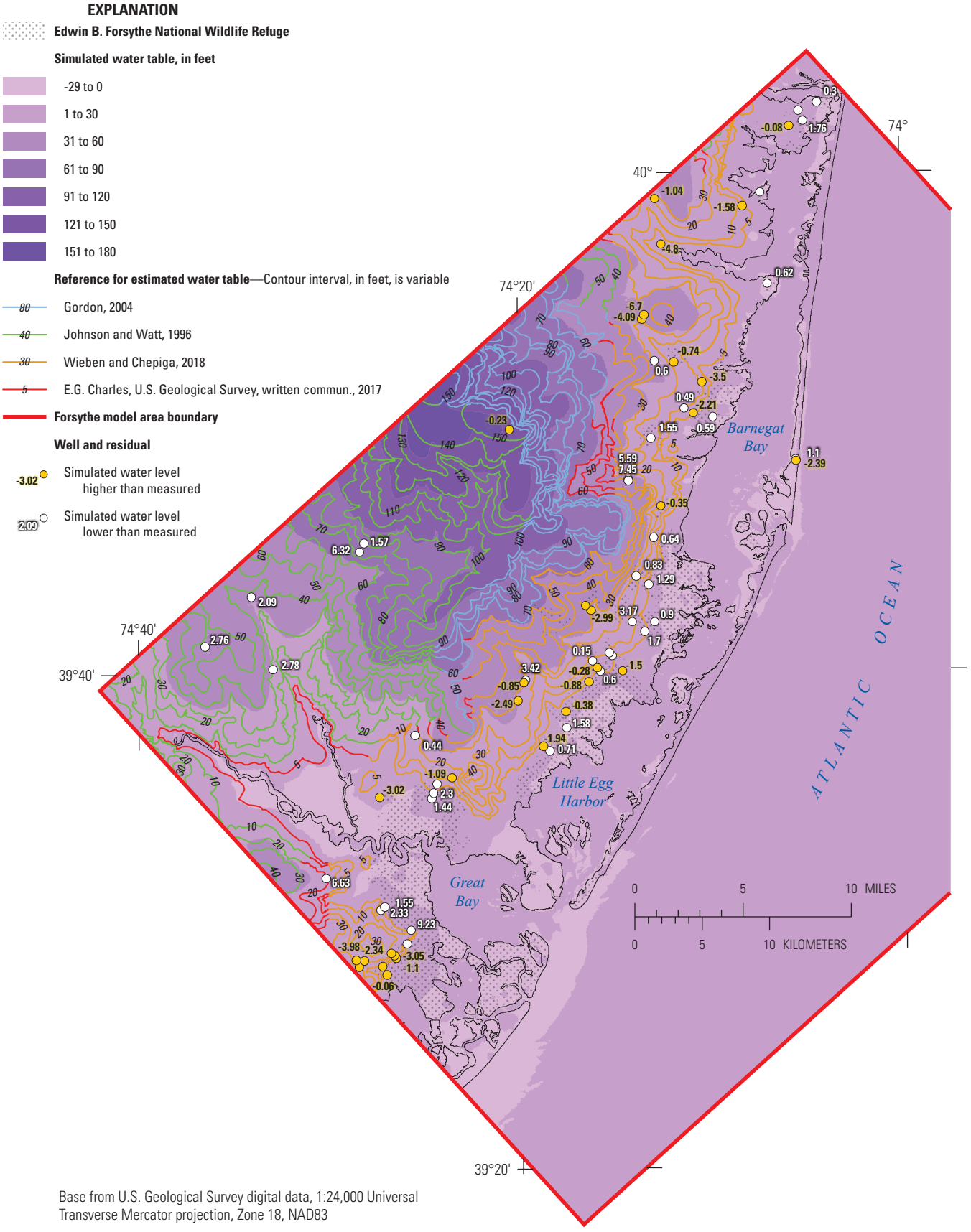

Figure 24. Estimated and simulated water table, location of wells measured during the spring 2015 synoptic study, and residuals in the Kirkwood-Cohansey aquifer system, Forsythe model area, New Jersey.

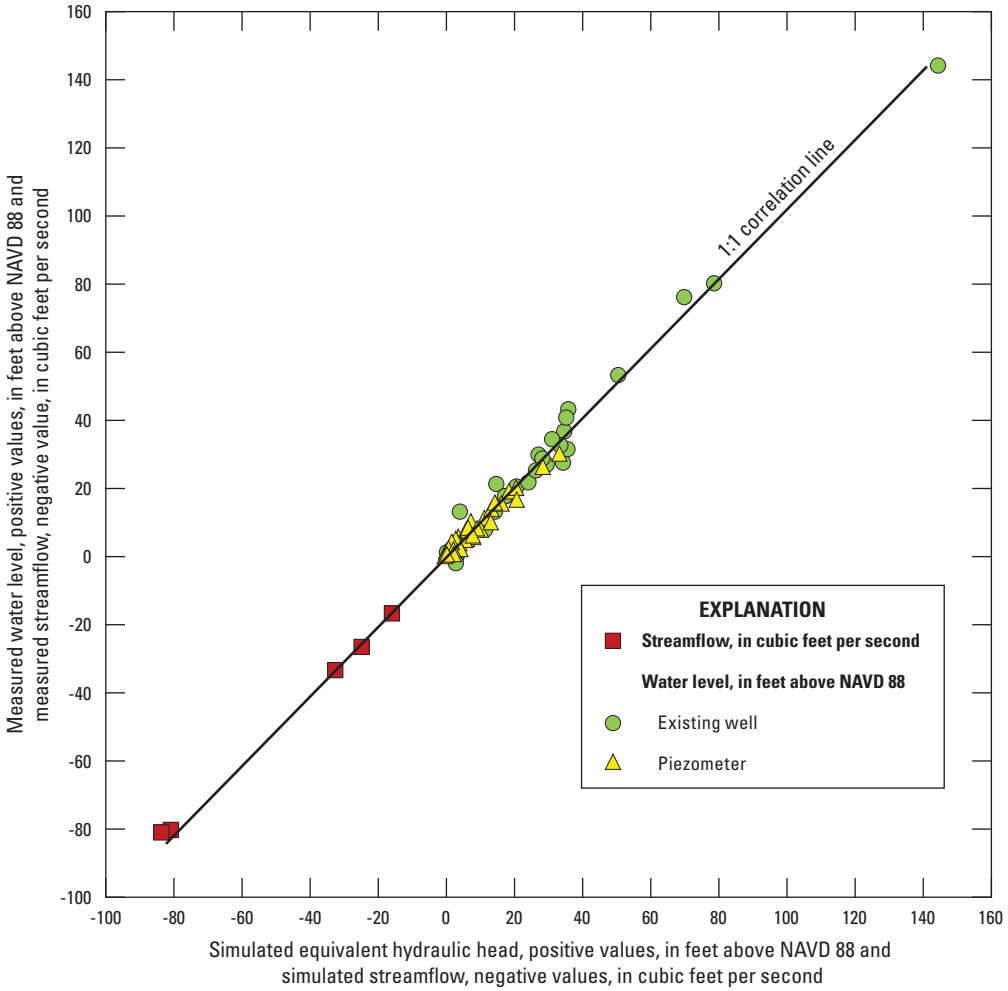

Figure 25. Measured water levels, simulated equivalent water levels, and measured and simulated streamflow, Forsythe model area, New Jersey. (NAVD 88, North American Vertical Datum of 1988)

Table 6. Estimated and simulated average base flow at five streamflow-gaging stations, Forsythe model area, New Jersey.

[Location of Forsythe model area shown in figure 1; location of streamflow-gaging station shown in figure 26; USGS, U.S. Geological Survey; HS, hydrograph separation; mi^2, square miles; ft^3/s, cubic feet per second]

USGS streamflow-gaging station number	Streamflow-gaging station name	Drainage area (mi^2)	Period of record	Average 2004–2013 base flow estimated by HS (ft^3/s)	Simulated average base flow (ft^3/s)	Difference between simulated and estimated average base flow (ft^3/s)
01409000	Cedar Creek at Lanoka Harbor, N.J.	53.3	1933–1958, 1971, 2003–present	84.00	83.62	0.38
01409100	Oyster Creek near Waretown, N.J.	7.43	1965–1984	26.50	24.85	1.65
01409280	Westecunk Creek at Stafford Forge, N.J.	15.8	1974–1987, 2004–2013	33.29	32.57	0.72
01410000	Oswego River at Harrisville, N.J.	72.5	1931–2013	80.20	80.85	-0.65
01410150	East Branch Bass River near New Gretna, N.J.	8.11	1979–2012	16.70	15.94	0.76

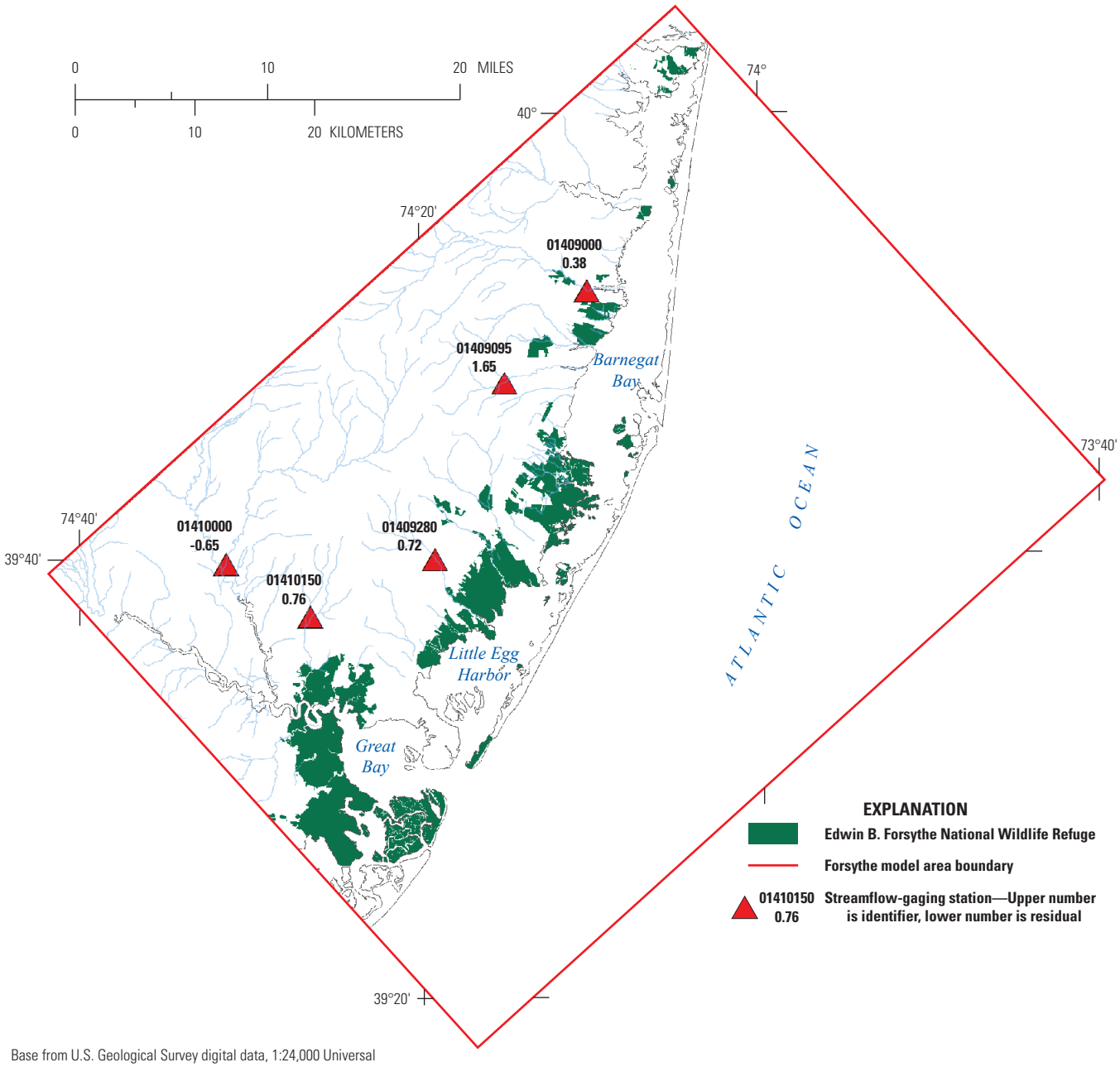

Base from U.S. Geological Survey digital data, 1:24,000 Universal Transverse Mercator projection, Zone 18, NAD83

Figure 26. Location of streamflow-gaging stations in the Forsythe model area, New Jersey.

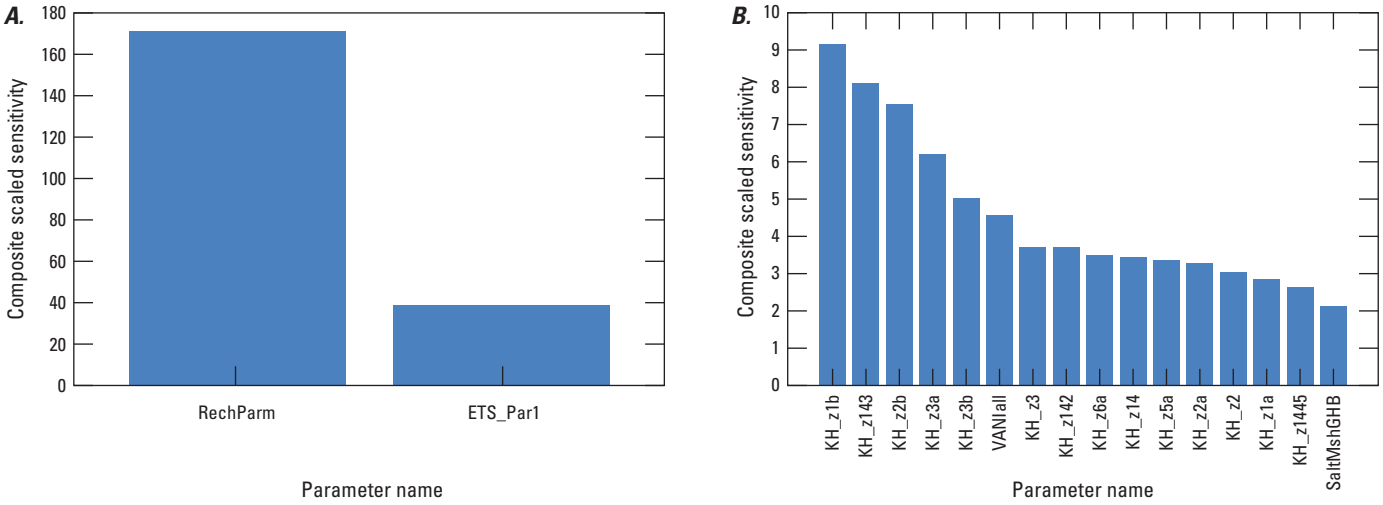

Figure 27. Composite scaled sensitivity values, by parameter, Forsythe model area, New Jersey: *A*, parameters with values greater than 38.88, and *B*, parameters with values greater than 1.7 and less than 38.88. (Model parameter prefixes: RechParm, recharge; ETS_Par1, evapotranspiration; KH, horizontal conductivity; VANIall, vertical anisotropy; SaltMshGHB, salt marsh hydraulic conductivity)

of the CSS. Hill and Tiedeman (2007) state that parameter values with a CSS less than 1.0 are more likely to be poorly estimated. Twenty of the 30 parameters estimated in this study are considered sensitive (CSS values greater than 1.0), indicating they are reasonably estimated by model calibration. The sensitive parameters, shown in order of sensitivity in figure 27 (*A* and *B*), are as follows: RechParm (recharge); ETS_Par1 (evapotranspiration); KH_z1b (KH; horizontal hydraulic conductivity); KH_z143; KH_z2b; KH_z3a; KH_z3b; VANIall (vertical anisotropy of all model layers); KH_z3; KH_z142; KH_z6a; KH_z14; KH_z5a; KH_z2a; KH_z2; KH_z1a; KH_z1445; SALTMshGHB (salt marsh hydraulic conductivity); KH_Z5, and KH_Z4a.

Model Limitations

A numerical model is useful for testing and refining a conceptual model of a groundwater flow system, developing an understanding of the system, guiding data collection, and projecting aquifer responses to changes in aquifer stresses within specified limits. A model can only approximate the actual system and is based on simplified assumptions and estimated conditions, however, and therefore can only approximate the actual system. The results of model simulations are only as accurate as the input data and assumed boundary conditions used to constrain the simulations, and are limited by the quantity and type of data available for calibration; other data types (such as groundwater age) can be used as additional calibration targets to constrain the model further. The groundwater flow model developed for this study is an approximation of a dynamic, real-world groundwater flow system that covers 1,463 mi² of land and water and extends at its deepest point to nearly 600 ft BLS. The area of study is divided into discrete model cells, most of which are 220 ft x 220 ft and of variable thickness. Because of the number of model cells in each model layer (684,288), the number of model layers (3), and the limited availability of data that describe the hydrologic properties of each layer, the hydrologic parameters in the flow model are generalized and, therefore, do not reflect all of the variability and transience that exists in the actual flow system. In other words, the groundwater flow model is calibrated to available data, but simulated parameter values may not be a unique representation of the groundwater flow system.

Data on the location of the freshwater-seawater interface in the vicinity of the Forsythe model area are limited. SC measurements made at three drive-point test hole sites—Game Farm Road, Stafford Avenue, and South Wildlife Drive—were used to estimate the location of the freshwater-seawater interface for this study. The drive-point test holes installed at these three locations were approximately 60 ft deep. SC measurements at the drive-point sites indicate that the freshwater-seawater interface is more than 60 ft BLS at all three sites and, therefore, the SC data could be used only to estimate where the interface was not present.

As designed and calibrated, the groundwater flow model of the Edwin B. Forsythe NWR was most appropriately used for analyzing site-specific issues related to changes in the groundwater flow system. Site-specific issues include, but are not limited to, estimating changes in groundwater levels and flows in response to SLR.

Simulation of Freshwater-Seawater Interface

Groundwater flow in coastal areas can be affected by seawater, whose density is 2.5 percent greater than that of freshwater. Fresh groundwater that flows toward the ocean or other coastal features, such as Barnegat Bay, mixes with seawater and forms a transition zone. The size and location of the transition zone depends on aquifer properties and groundwater flow in the area of the transition zone (Hughes and White, 2014).

The SWI2 module (Bakker and others, 2013) developed for MODFLOW was used to estimate the location of the freshwater-seawater interface in the vicinity of the Forsythe model area. The SWI2 module simulates the multidensity groundwater flow, treating the freshwater-seawater transition zone as a sharp interface. The SWI2 input requires an estimate of the location of the initial freshwater-seawater interface. Because limited data on the location of the freshwater-seawater interface are available, the initial freshwater-seawater interface was estimated by using the Ghyben-Herzberg relation (Ghyben, 1889; Herzberg, 1901). When the model was considered to be calibrated after all modules, including the SWI2 module, had been used, the water-level solution from a MODFLOW-2005 simulation that did not include the SWI2 variable-density module (J.D. Hughes, U.S. Geological Survey, written commun., 2015) was used to calculate an initial freshwater-seawater interface location. The freshwater-seawater interface location estimated with the Ghyben-Herzberg relation was used as the initial freshwater-seawater interface location for the first SWI2 model simulation. The freshwater-seawater interface estimated from the first SWI2 simulation was then used as the initial freshwater-seawater interface location in the second SWI2 simulation, and the freshwater-seawater interface location estimated from the second SWI2 simulation was used as the initial freshwater-seawater interface location in a third SWI2 simulation, referred to as the "calibrated baseline simulation." To ensure that the freshwater-seawater interface reached steady-state conditions, the location of the freshwater-seawater interface resulting from the third SWI2 model simulation was compared to the location of the freshwater-seawater interface resulting from the second SWI2 model simulation. Inasmuch as the locations obtained from both simulations were identical, the interface was considered to have reached steady-state conditions and the freshwater-seawater interface estimated from the second SWI2 model simulation was used as the initial freshwater-seawater interface for the three SLR scenarios.

Simulated Effects of Sea-Level Rise

Three SLR scenarios—20 cm (0.656 ft), 40 cm (1.312 ft), and 60 cm (1.968 ft)—were simulated. These values of SLR are consistent with scenarios being evaluated by the USGS of the effects of SLR on fresh groundwater resources at U.S. Department of Interior lands on Fire Island, N.Y., Sandy Hook, N.J., and Assateague Island, Md., National Seashores for the National Park Service. These values of SLR are also consistent with the estimated range of SLR in New Jersey of 28 to 65 cm (0.919–2.133 ft) by 2050 (Miller and others, 2013). Estimating changes in the shape of the shoreline from erosion or deposition associated with SLR is beyond the scope of this study; only shoreline change associated with inundation is considered, as in Masterson and others (2013). For each SLR scenario, the increase in hydraulic head with each simulated rise in sea level at the surface of the salt marsh areas (coinciding with 78 percent of the refuge area) is simulated with the GHB module and is independent of the increase in the altitude of the salt marsh caused by the sedimentation that may result from SLR. Kemp and others (2013) estimated marsh altitudes for the past 2,500 years from core samples collected at 12 sites in New Jersey, including 5 sites in the vicinity of Great Egg Harbor (1 site at Leeds Point in the Edwin B. Forsythe NWR). Kirwan and others (2016) used core-sample data from Kemp and others (2013) in their analysis of SLR and the building of marshes. Kirwan and others (2016) concluded that "global measurements of marsh-elevation change indicate that marshes are generally building at rates similar to or exceeding historical sea-level rise, and that process-based models predict survival under a wide range of future sea level scenarios."

Digital topobathymetric maps from the USGS EROS (Danielson and others, 2016) were used to identify areas that could become inundated with seawater in each SLR scenario. The freshwater wetland areas in the model area are above 60 cm (1.968 ft) and will not become inundated with seawater in any of the three SLR scenarios; therefore, the hydraulic heads in the freshwater wetland areas were not changed for any of the SLR scenarios. Only areas in the salt marsh, bay, and ocean were identified as having land-surface altitudes equal to or below 60 cm and are simulated as inundated with seawater in the SLR scenarios.

The boundary head in the GHB module was calculated by adding the current land-surface altitude and the increase in sea level for areas that currently are above sea level but were simulated as inundated with seawater in the SLR scenarios. It was assumed that only a thin veneer of seawater would overlie the inundated areas; therefore, a freshwater equivalent head was not calculated for areas that currently are above sea level and will be inundated with seawater during SLR. Areas that currently are above sea level but were simulated as inundated during a SLR scenario are located in the salt marsh.

For areas that underlie Barnegat Bay, Great Bay, and the Atlantic Ocean, the freshwater equivalent head was calculated and used as the boundary head in the GHB module for each

SLR scenario. The freshwater equivalent head was calculated by using equation 2 with the rise in sea level added to the equation:

$$h_f = [(P_s / P_f)h_{msl} + SLR_s] - [(P_s - P_f) / P_f](Z + SLR_s) \quad (3)$$

where

h_f is the freshwater equivalent head,
P_s is the density of seawater,
P_f is the density of freshwater,
h_{msl} is mean sea level,
Z is the bathymetric altitude, and
SLR_s is the rise in sea level for each scenario.

The change in flow to streams, wetlands, salt marsh, and bay was calculated for each scenario and compared to the calibrated baseline simulation of average 2005–15 conditions (table 7). The initial freshwater-seawater interface location that was used in the calibrated baseline simulation was used in all three scenarios. As simulated SLR increases from 20 cm (0.656 ft) to 60 cm (1.968 ft), simulated groundwater discharge (flow from the aquifer system to the salt marsh, bay, and ocean) is projected to decrease accordingly (table 7). The largest decrease in groundwater discharge is noted for the salt marsh and bay—from 21 (baseline simulation) to 12 (scenario 3) Mgal/d and from 16 (baseline simulation) to 8 (scenario 3) Mgal/d, respectively. The simulated change (increase) in ET is minimal (less than 3 Mgal/d), probably as a result of the small change between the calibration baseline simulation and the scenarios in the extensive wetlands areas in the Forsythe model area where the water table is high. Simulated groundwater discharge to the freshwater wetlands and streams increases, from 243 (baseline simulation) to 303 (scenario 3) Mgal/d and from 240 (baseline simulation) to 251 (scenario 3) Mgal/d, respectively. Flow from the salt marsh, bay, and ocean to the aquifer system is projected to increase as sea level rises (table 7). Flow from the bay to the aquifer system is projected to increase most, from 40 (baseline simulation) to 85 (scenario 3) Mgal/d.

As sea level rises, the water-table altitude is projected to increase (fig. 28). The projected increase from the baseline simulation to scenarios 1 and 2 (fig. 28*A* and *B*) is small compared to the projected increase in the water-table altitude for scenario 3 (fig. 28*C*). The projected increase in water-table altitude ranges from 0.19 to 0.8 ft in scenario 1 (fig. 28*A*) and from 0.19 to 1.35 ft in scenario 2 (fig. 28*B*). The projected increase in the water-table altitude ranges from 0.19 to 2 ft from the baseline simulation to scenario 3 (fig. 28*C*).

The simulated freshwater-seawater interface in columns 63, 399, and 697 of the model grid (fig. 29) for the baseline simulation and scenario 3 is shown in figure 30 (*A*, *B*, and *C*, respectively). Figure 30*B* shows the freshwater-seawater interface in column 399 for scenarios 1, 2, and 3. These columns were selected because they are along groundwater flow paths and are near the test sites. The section along column 399 (fig. 30*B*) is representative of the maximum simulated increase in the landward movement of the freshwater-seawater interface in the Forsythe model area. In the vicinity of column 399, the simulated interface moved inland about 200 ft and downward about 5 ft in each scenario (fig. 30*B*). The downward movement of the interface is assumed to result from the 0.0033 hydraulic-head gradient in the vicinity of column 399. The hydraulic head in the baseline simulation is 23.54 ft at the onshore location and 1.72 ft at the landward beginning of the salt marsh, and the distance between the two locations is about 6,600 ft. Hydraulic-head locations used in the calculation of

Table 7. Simulated water budgets from the calibrated baseline model and three sea-level rise scenarios in the Forsythe model area, New Jersey.

[Location of Forsythe model area shown in figure 1; all values in million gallons per day; cm, centimeter; 20 cm, 0.656 feet; 40 cm, 1.312 feet; 60 cm, 1.968 feet]

Scenario	Flow from aquifer system into boundary										Flow from boundary into aquifer system				
	Evapotranspiration			Specified flows[1]	Salt marsh	Bay	Ocean	Freshwater wetlands	Streams	Wells	Recharge	Specified flows[1]	Salt marsh	Bay	Ocean
	Stream	Freshwater wetlands	Onshore												
Baseline model	21	97	47	16	21	16	2	243	240	16	630	42	4	40	6
Scenario 1, 20-cm sea-level rise	21	98	48	16	17	13	1	259	242	16	630	42	5	50	6
Scenario 2, 40-cm sea-level rise	21	99	49	16	14	10	1	279	246	16	630	42	8	65	8
Scenario 3, 60-cm sea-level rise	21	99	50	16	12	8	1	303	251	16	630	42	12	85	9

[1]Values calculated from the Regional Aquifer System Analysis model.

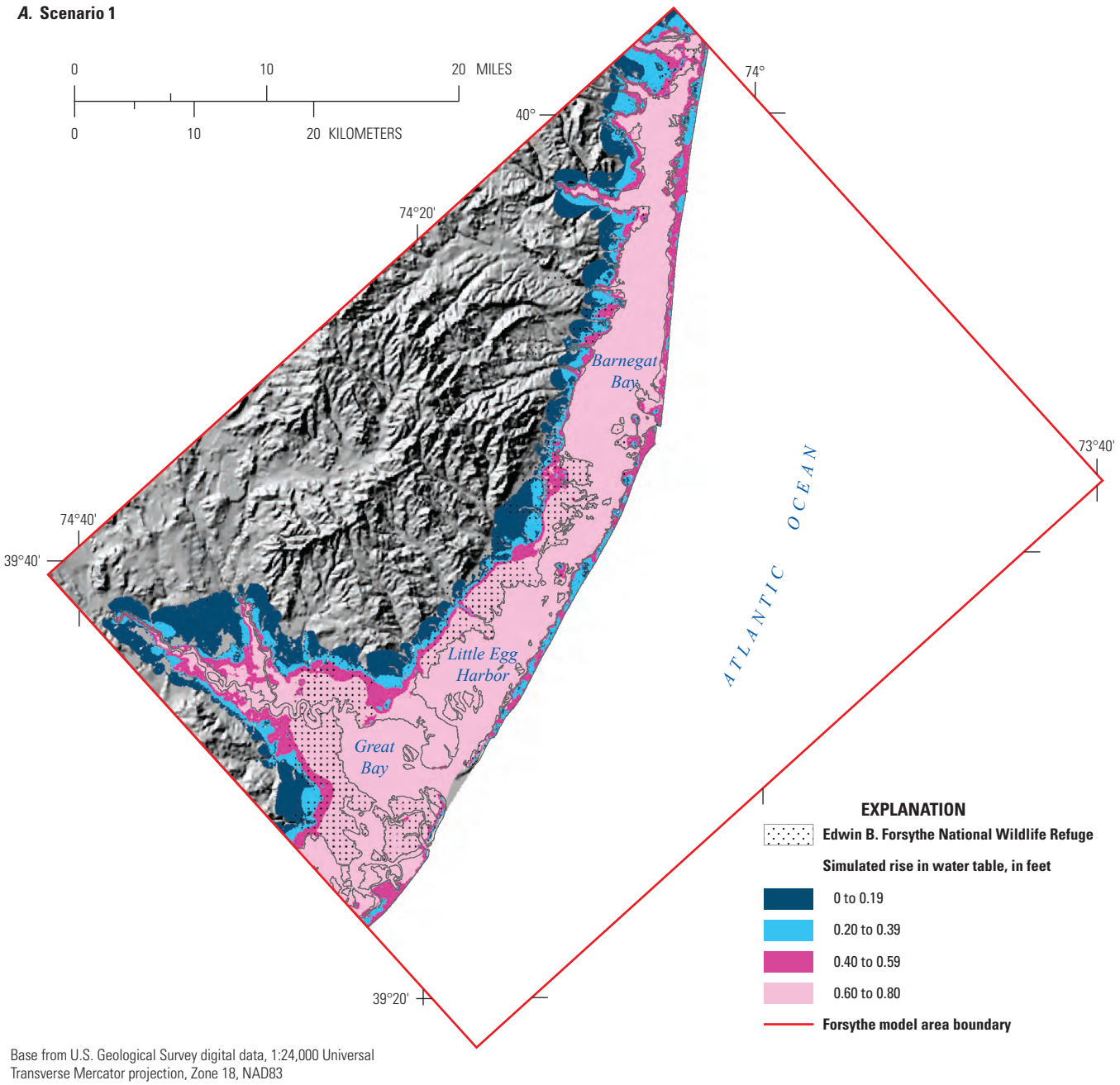

Figure 28. Simulated rise in water table from the baseline scenario to *A*, scenario 1 simulation with sea-level rise of 20 centimeters 0.656 feet), *B*, scenario 2 simulation with sea-level rise of 40 centimeters (1.312 feet), and *C*, scenario 3 simulation with sea-level rise of 60 centimeters (1.968 feet), Forsythe model area, New Jersey.

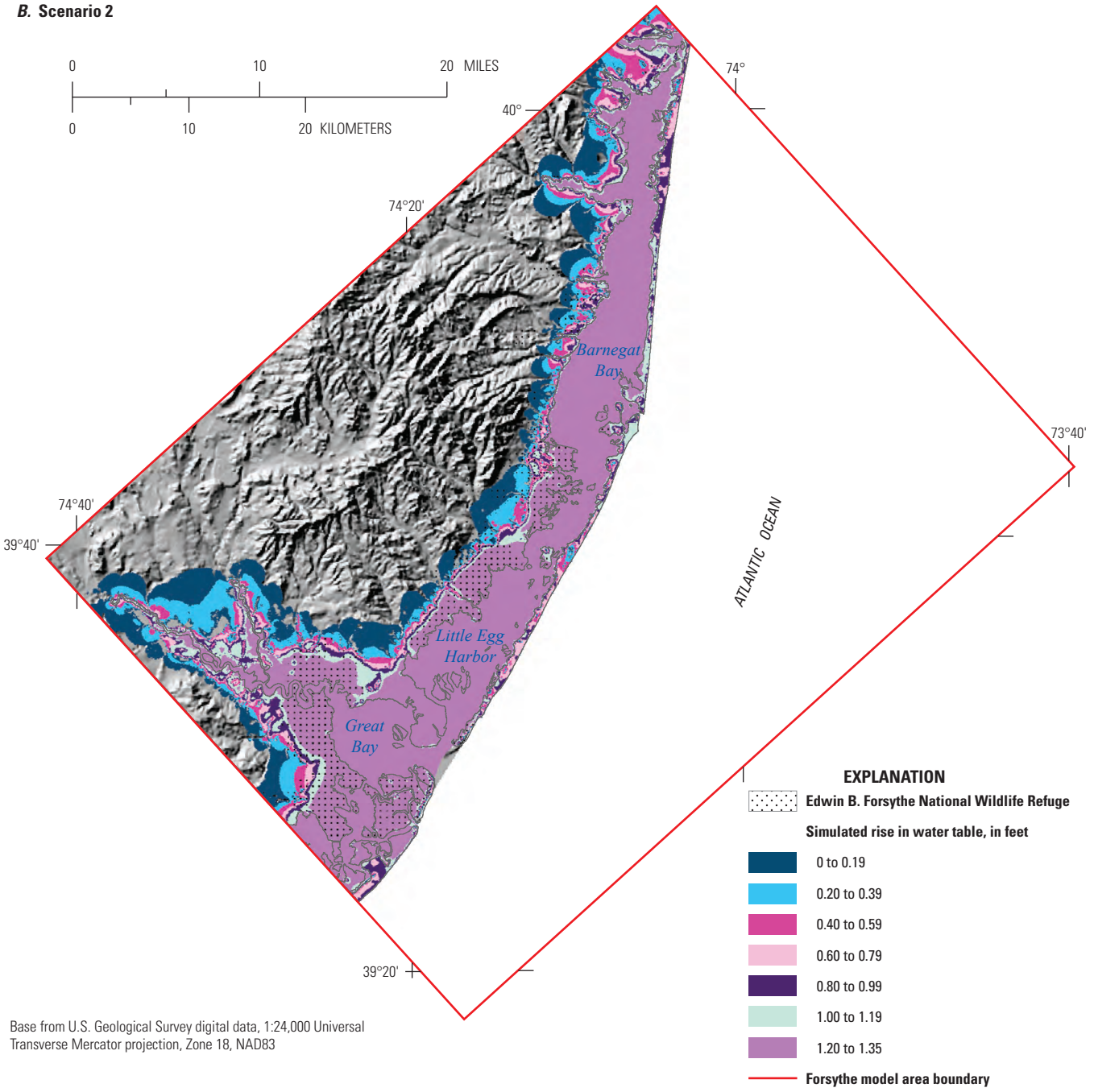

Figure 28. Simulated rise in water table from the baseline scenario to *A*, scenario 1 simulation with sea-level rise of 20 centimeters (0.656 feet), *B*, scenario 2 simulation with sea-level rise of 40 centimeters (1.312 feet), and *C*, scenario 3 simulation with sea-level rise of 60 centimeters (1.968 feet), Forsythe model area, New Jersey.—Continued

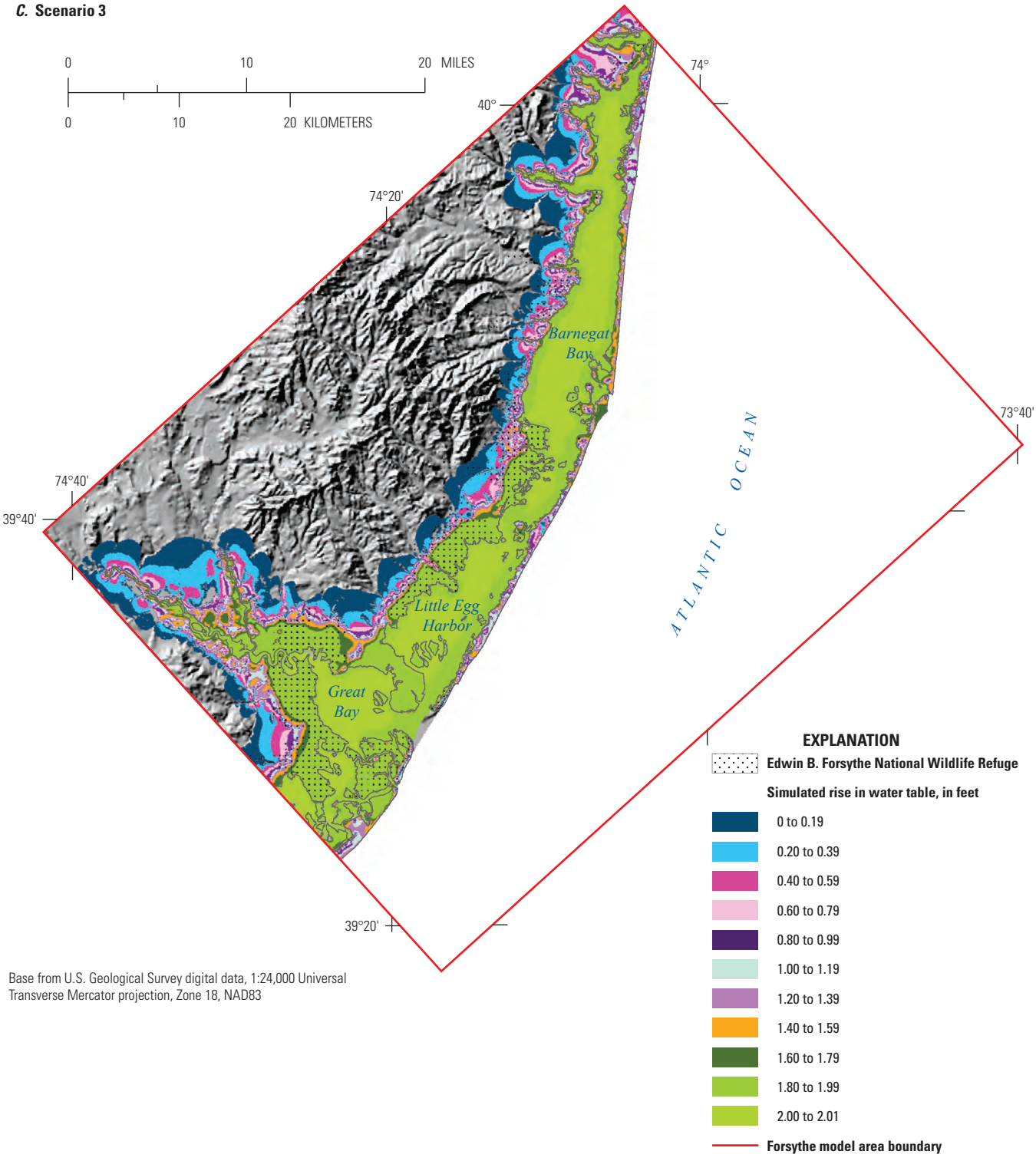

Figure 28. Simulated rise in water table from the baseline scenario to *A*, scenario 1 simulation with sea-level rise of 20 centimeters (0.656 feet), *B*, scenario 2 simulation with sea-level rise of 40 centimeters (1.312 feet), and *C*, scenario 3 simulation with sea-level rise of 60 centimeters (1.968 feet), Forsythe model area, New Jersey.—Continued

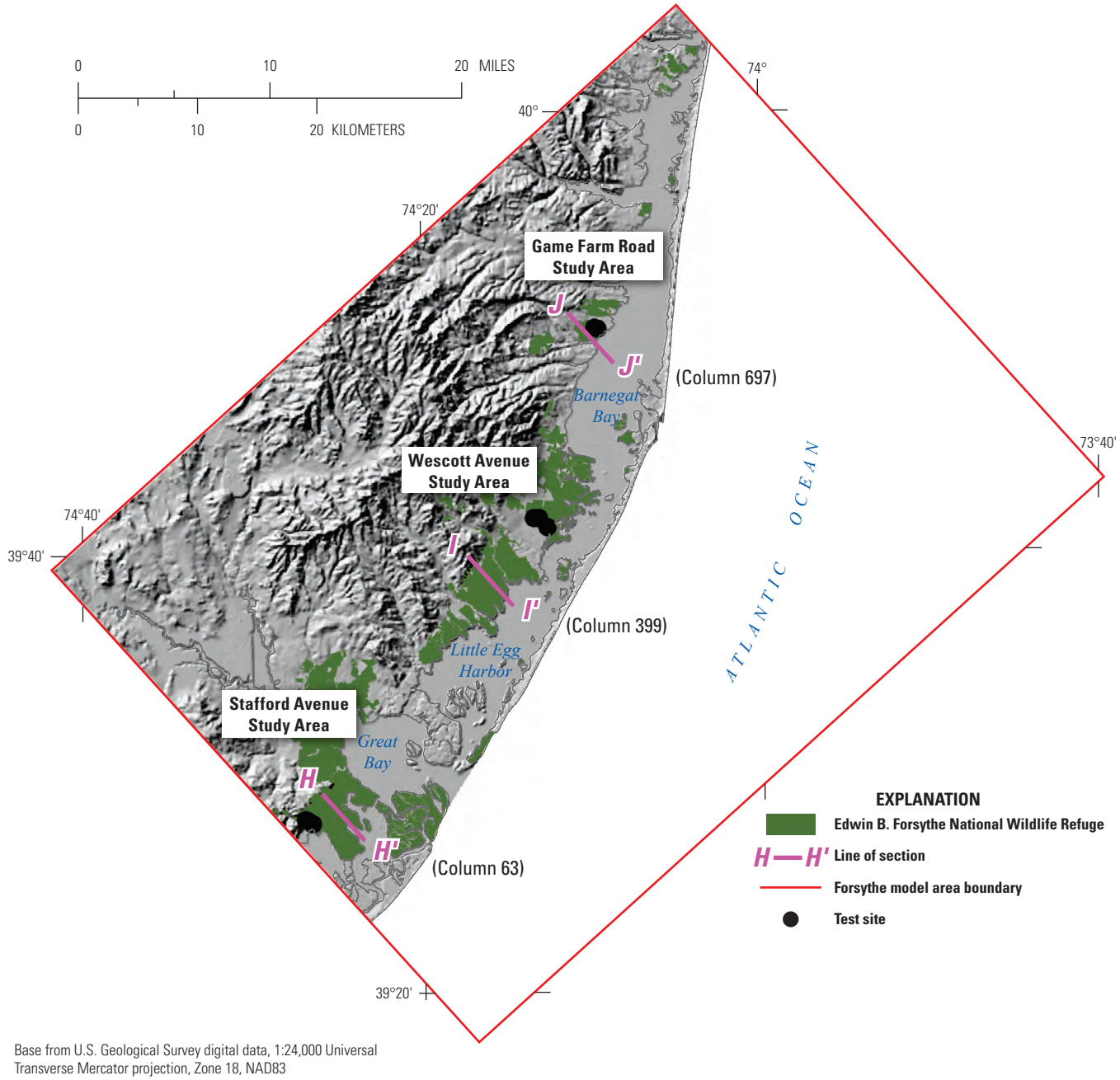

Figure 29. Location of lines of section *H-H′*, *I-I′*, and *J-J′* in the Forsythe model area, New Jersey.

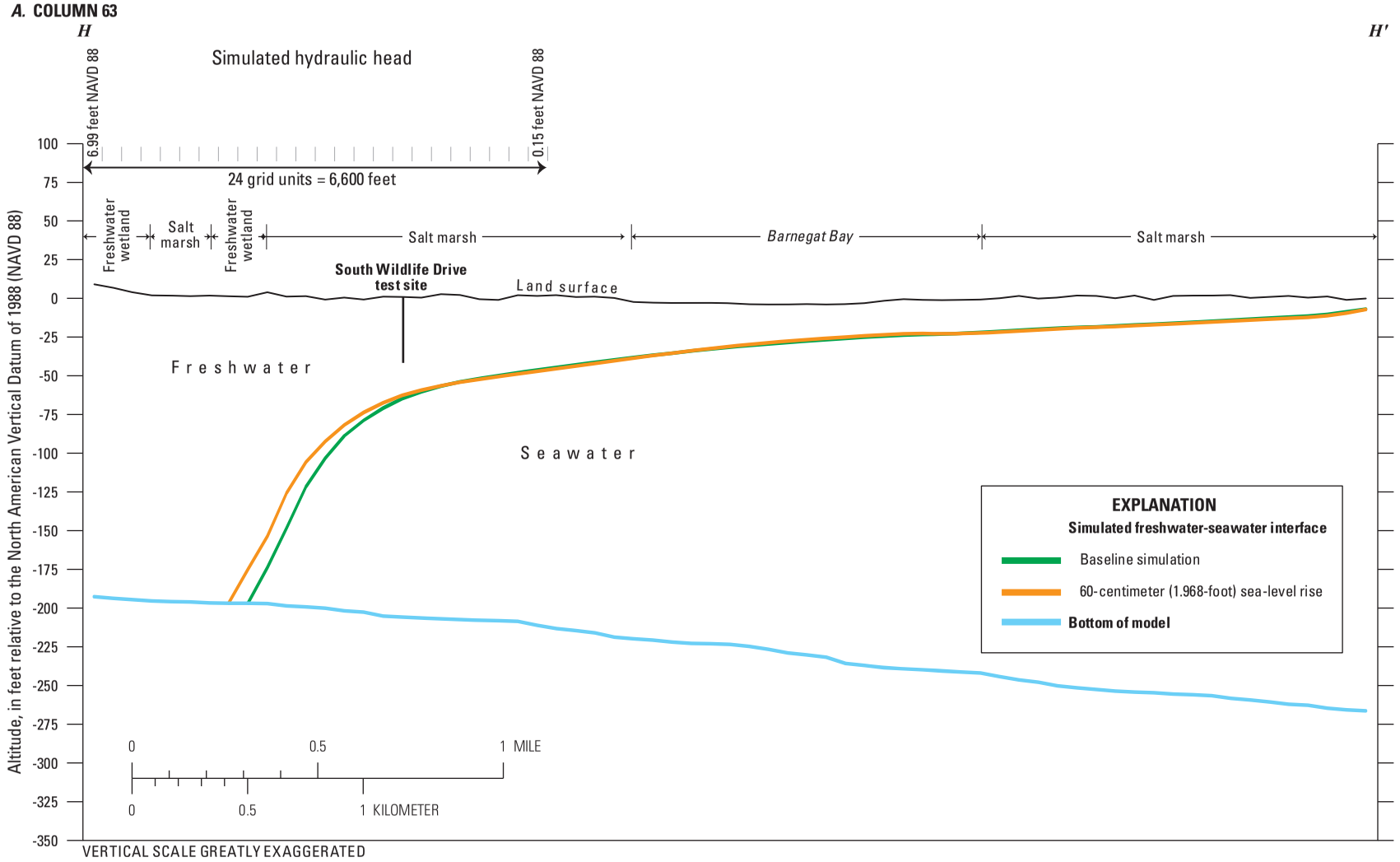

Figure 30. Freshwater-seawater interface from the baseline simulation for *A*, *H-H′* (model column 63), *B*, *I-I′* (model column 399), and *C*, *J-J′* (model column 697) in the Forsythe model area, New Jersey. Lines of section shown in figure 29.

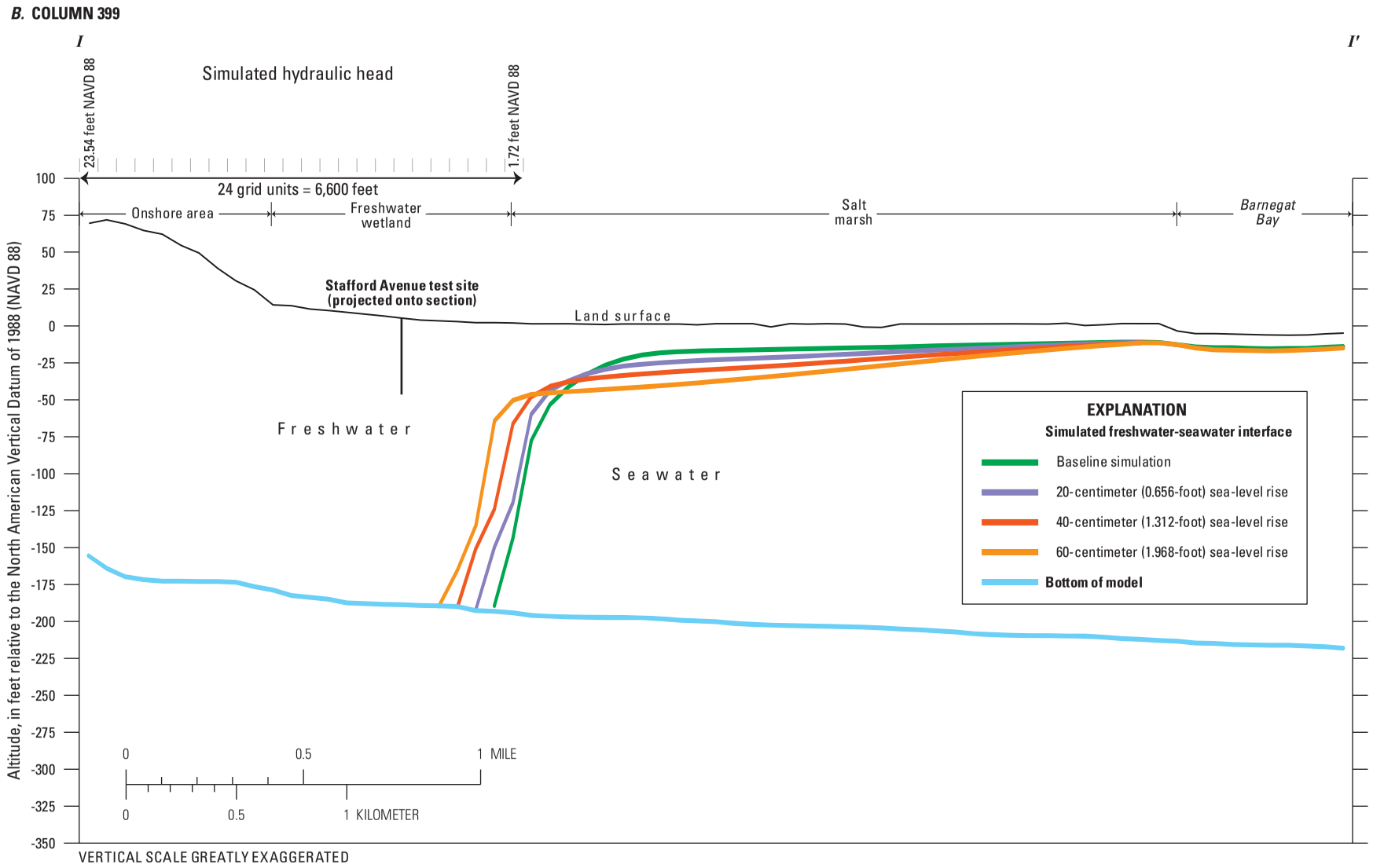

Figure 30. Freshwater-seawater interface from the baseline simulation for *A*, *H-H'* (model column 63), *B*, *I-I'* (model column 399), and *C*, *J-J'* (model column 697) in the Forsythe model area, New Jersey. Lines of section shown in figure 29.—Continued

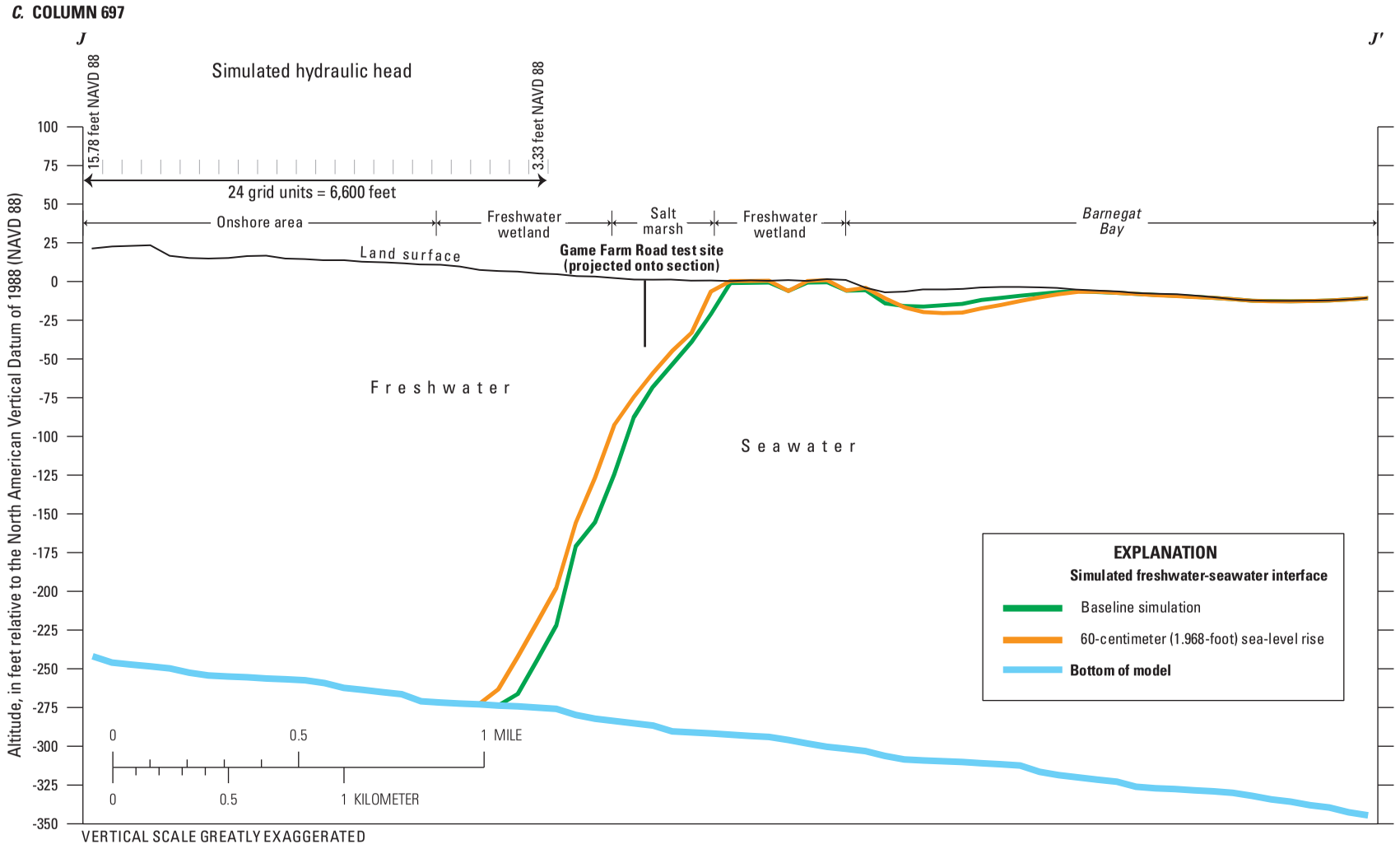

Figure 30. Freshwater-seawater interface from the baseline simulation for *A*, *H-H′* (model column 63), *B*, *I-I′* (model column 399), and *C*, *J-J′* (model column 697) in the Forsythe model area, New Jersey. Lines of section shown in figure 29.—Continued

the hydraulic gradient are shown in figure 30 (*A*, *B*, and *C*). As sea level rises, the simulated hydraulic head in scenario 3 increases 0.07 ft at the onshore location, 0.3 ft at the landward beginning of the salt marsh, and 2 ft under the bay (fig. 30*B*). Because the simulated head under the bay is higher in scenario 3 than in the baseline simulation, groundwater discharge into the bay decreases; the groundwater mixes with the water in the transition zone and moves the interface downward.

In the vicinity of column 63, the topography is flatter than it is near column 399, and the hydraulic-head gradient is 0.001. The hydraulic head in the baseline simulation is 6.99 ft at the onshore location and 0.15 ft at the salt marsh, and, again, the distance between the two locations is about 6,600 ft. In the vicinity of column 63, the interface in scenario 3 is about 200 ft farther inland than in the baseline simulation, and has not moved downward (fig. 30*A*).

In the vicinity of column 697, the hydraulic-head gradient is 0.00188. The hydraulic head is 15.78 ft at the onshore location and 3.33 ft near the salt marsh, and the distance between the two locations, again, is about 6,600 ft. In the vicinity of column 697, the simulated interface has moved inland about 200 ft from the baseline simulation to scenario 3. The simulated interface has moved downward about 6 ft at the landward edge of the bay, but farther seaward, beneath the bay, the interface is at the same depth as in the baseline simulation (fig. 30*C*).

The location of the simulated interface in layers 1, 2, and 3 for the baseline simulation and in layer 3 in scenario 3 is shown in figure 31. The projected inland movement of the interface is minor in all three scenarios and layers. Therefore, for layer 3 only the projected freshwater-seawater interface for scenario 3 is shown in figure 31. The projected location of the freshwater-seawater interface in layer 3 in scenario 3 is represented by the thin red area that extends beyond the interface in layer 3 in the baseline simulation in figure 31. Generally, the simulated freshwater-seawater interface in the baseline simulation is more than 5 ft below land surface in the Edwin B. Forsythe NWR (fig. 32). The simulated freshwater-seawater interface is less than 5 ft below land surface in minor areas of the refuge (fig. 32). The simulated interface is not present beneath the more inland parts of the refuge.

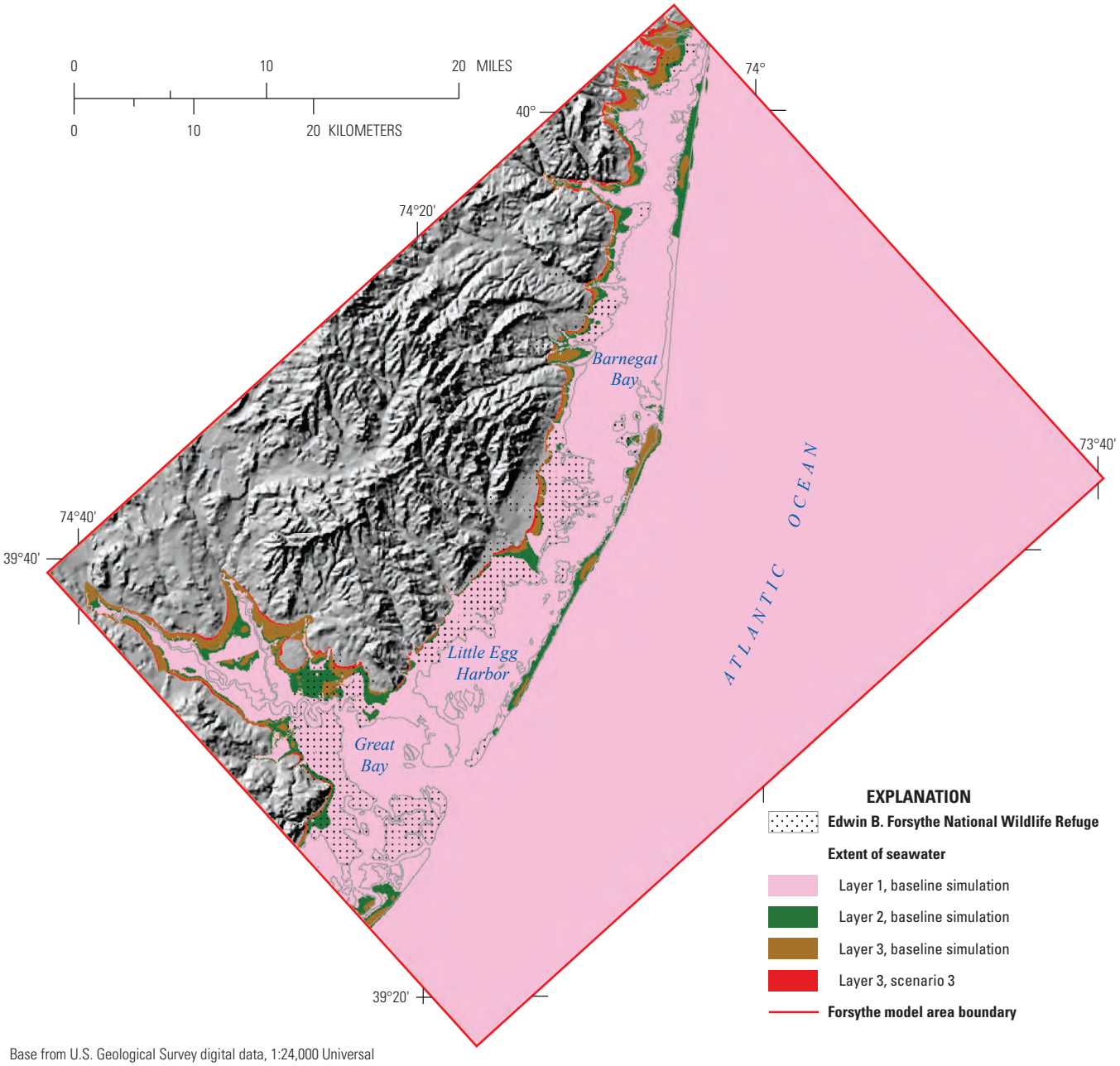

Base from U.S. Geological Survey digital data, 1:24,000 Universal Transverse Mercator projection, Zone 18, NAD83

Figure 31. Simulated extent of the freshwater-seawater interface, baseline simulation and scenario 3, Forsythe model area, New Jersey.

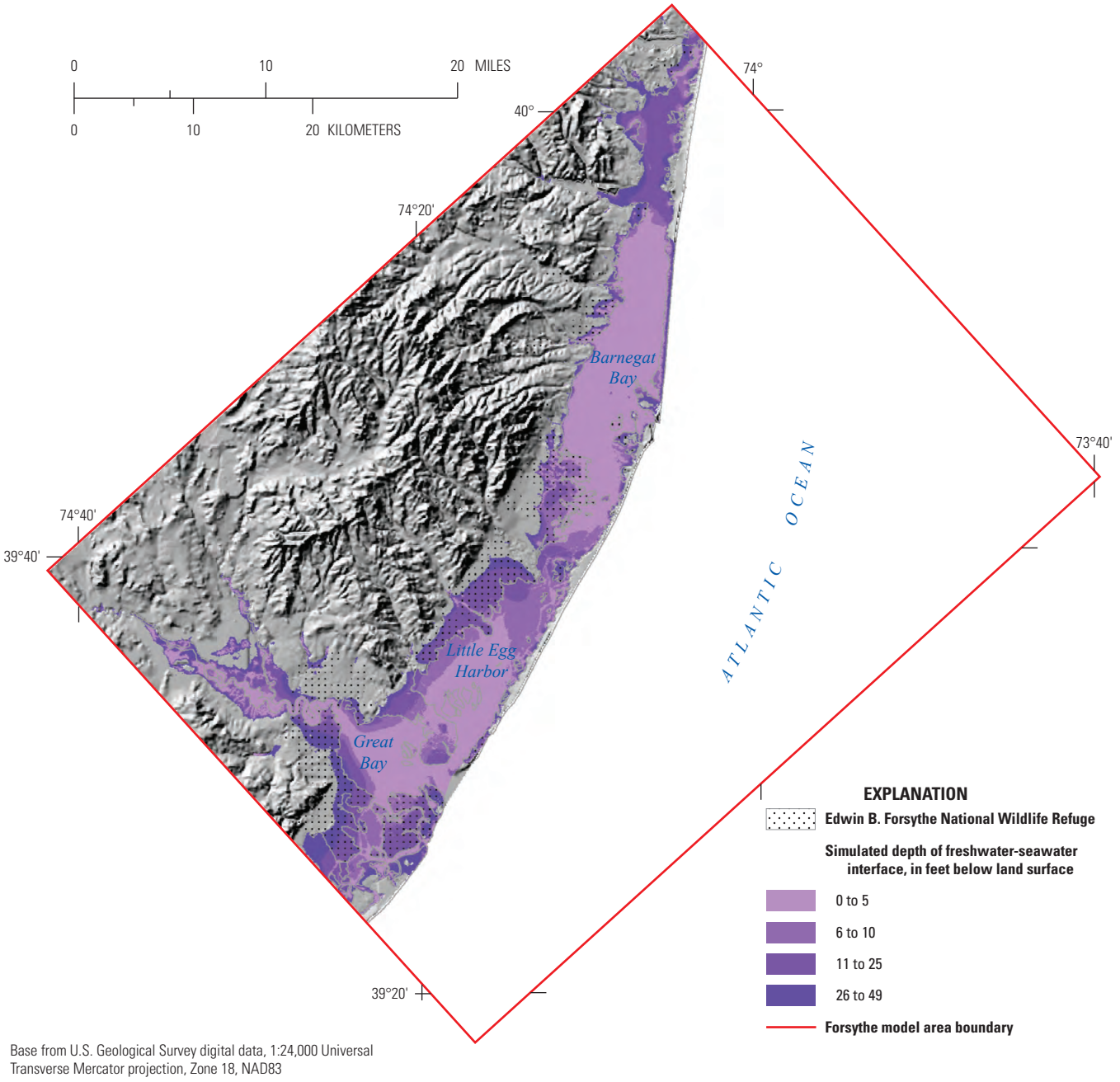

Figure 32. Simulated depth of the freshwater-seawater interface, baseline simulation, Forsythe model area, New Jersey.

Summary and Conclusions

The Edwin B. Forsythe National Wildlife Refuge (NWR) encompasses more than 47,000 acres of New Jersey coastal habitats including salt marshes, freshwater wetlands, tidal wetlands, barrier beaches, woodlands, and swamps. The refuge is an important area along the Atlantic Flyway and provides breeding habitat for fish, migratory birds, and other wildlife species. The refuge area may be threatened by global climate change, including sea-level rise (SLR).

The Kirkwood-Cohansey aquifer system underlies the Edwin B. Forsythe NWR. Groundwater is an important source of freshwater flow into the refuge, but information about the interaction of surface water and groundwater in the refuge area and the potential effects of SLR on the underlying aquifer system is limited. The U.S. Geological Survey (USGS), in cooperation with the U.S. Fish and Wildlife Service (USFWS), conducted a hydrologic assessment of the refuge in New Jersey and developed a groundwater flow model to improve understanding of the geohydrology of the refuge area and to serve as a tool to evaluate changes in groundwater-level altitudes that may result from a rise in sea level.

A numerical steady-state groundwater flow model was developed for the Kirkwood-Cohansey aquifer system in the refuge area by creating a mathematical representation of the hydrogeologic framework and flow system. Given the hydrologic and lithologic heterogeneity of the Kirkwood-Cohansey aquifer system, the hydrogeology was field evaluated at specific sites to improve the accuracy of the model hydrogeologic framework. Field investigation methods included conducting ground-penetrating radar surveys, measuring water levels and water-quality parameters in drive-point test intervals, and incorporating available borehole geophysical and lithologic data from other boreholes within the model area to the data collected. The shallow groundwater flow system and interaction with surrounding saltwater boundaries was constructed by using the USGS modular finite-difference groundwater flow model MODFLOW-2005 with the Saltwater Intrusion module, which explicitly simulates multidensity groundwater flow, treating the freshwater-saltwater transition zone as a sharp interface. The model, representing average 2005–15 conditions, was initially calibrated by a trial-and-error approach that minimized the difference between simulated and measured values of the following: (1) estimated base flow at five streamflow-gaging stations, (2) water levels in 44 temporary piezometers and 28 existing wells measured in spring 2015, and (3) potentiometric surfaces in May 2015. Final model calibration was accomplished by using the automated parameter estimation software UCODE-2005 and the above-mentioned measured data. A reasonable match between measured and simulated data was achieved.

Three SLR scenarios were simulated: 20 centimeters (cm) (0.656 ft), 40 cm (1.312 ft), and 60 cm (1.968 ft). For each SLR scenario, the increase in hydraulic head (from current conditions to the rise in sea level) at the surface of the salt-marsh areas (which account for 78 percent of the refuge area) is simulated with the General Head Boundary and is independent of the increase in the altitude of the salt marsh as a result of the sedimentation or erosion that may occur with SLR. Results of previous research on global marsh-altitude change indicate that marshes are generally building at rates similar to or exceeding historical SLR and are likely to survive under a range of future SLR scenarios. A previous study has shown that marsh vertical accretion depends on the rate of mineral and organic sediment accretion.

The change in flow to streams, wetlands, salt marsh, and bay was calculated for each scenario and compared to the results of the calibrated baseline simulation. As the simulated rise in sea level increases, simulated groundwater discharge to the salt marsh, bay, and ocean is projected to decrease. This decrease is largest for flow to the salt marsh and bay—from 21 (baseline simulation) to 12 (scenario 3, a SLR of 60-cm [1.968-ft]) million gallons per day (Mgal/d) and from 16 (baseline simulation) to 8 (scenario 3) Mgal/d, respectively. The change in the evapotranspiration rate estimated from the baseline simulation to scenario 1, 2, or 3 is projected to be minimal (less than 3 Mgal/d), probably as a result of the small change in the extensive wetlands in the Forsythe model area where the water table is high. In the onshore areas, simulated groundwater discharge to the freshwater wetlands and streams increases from 243 (baseline simulation) to 303 (scenario 3) Mgal/d and from 240 (baseline simulation) to 251 (scenario 3) Mgal/d, respectively. Flow from the salt marsh, bay, and ocean to the fresh groundwater flow system is projected to increase as sea level rises. Flow from the bay is projected to increase most, from 40 (baseline simulation) to 85 (scenario 3) Mgal/d.

As sea level rises, the water table is projected to rise. The projected increase in the water-table altitude from the baseline simulation to scenarios 1 and 2 is small compared to the projected increase from the baseline simulation to scenario 3. The projected water-table altitudes increase 0.8 ft in the bay, 0.2 to 0.4 ft in onshore areas from the baseline simulation to scenario 1, and 0.2 to 1.35 ft from the baseline simulation to scenario 2. The projected increase in the water-table altitude from the baseline simulation to scenario 3 ranges from 2 ft in the bay to about 0.19 to 1 ft in onshore parts of the model area.

Analysis of the results of the baseline simulation and three SLR scenarios indicates the movement of the freshwater-seawater interface is dependent on the hydraulic-head gradient and the change in the hydraulic-head gradient of the groundwater flow system. In the center of the Forsythe model area, topographic relief is high and the hydraulic-head gradient is 0.0033. As sea level rises, the simulated hydraulic head (scenario 3) increases 0.07 ft at the onshore location, 0.3 ft at the salt marsh, and 2 ft under the bay. Because the head is higher under the bay than in the baseline simulation, less groundwater discharges into the bay; the groundwater mixes with the water in the transition zone and moves the interface downward. In the center of the Forsythe model area, the simulated interface moves inland about 600 ft and downward about 15 ft from the baseline simulation to scenario 3. In the southern part of the Forsythe model area, where the topography is flatter, the

hydraulic-head gradient is 0.001. The hydraulic head is 6.66 ft at the onshore location and 0.15 ft at the salt marsh, and the distance between the two locations is about 6,600 ft. In the southern part of the Forsythe model area, the interface is projected to move inland about 200 ft from the baseline simulation to scenario 3 and does not move downward.

The objective of this study was to quantify the effects of three SLR scenarios on simulated groundwater flow to and from the Forsythe Refuge area. The hydrologic data collected as part of this study do not allow for an assessment of the effects of changes in groundwater flow on wetland and stream habitats. For such an assessment to be conducted, data on the hydrogeologic characteristics of the study area, including hydraulic properties, would need to be known on a much finer scale than was provided for in the scope of this study. Because local variations in hydrogeology are likely to have a large effect on groundwater discharge in the study area, additional, site-specific data collection and analysis would be needed to address the effects of changes in groundwater flow related to SLR on the biological and ecological habitats in the refuge area.

Acknowledgments

The authors are grateful for technical reviews by U.S. Geological Survey (USGS) hydrologists Martha Watt and Linda Woolfenden, who improved the quality and technical accuracy of the report. We thank Mary Chepiga, Glen Carleton, Susan Colarullo, and Joseph Hughes (USGS) for providing technical suggestions and assistance over many hours of meetings. Andrew Leaf (USGS) provided software to calculate stream altitudes and verify that they decrease in downstream order. Robert Rosman, Timothy Wilson, Eric Jacobsen, and Peter Joesten (USGS) provided assistance and technical support for the field efforts.

References Cited

Anderson, H.R., and Appel, C.A., 1969, Geology and groundwater resources of Ocean County, New Jersey: New Jersey Department of Conservation and Economic Development Special Report 29, 74 p., 2 maps, accessed March 9, 2018, at https://pubs.er.usgs.gov/publication/70047881.

Anderson, M.P., and Woessner, W.W., 1992, Applied groundwater modeling—Simulation of flow and advective transport: San Diego, Calif., Academic Press, Inc., 381 p.

Bakker, Mark, Schaars, Frans, Hughes, J.D., Langevin, C.D., and Dausman, A.M., 2013, Documentation of the Seawater Intrusion (SWI2) package for MODFLOW: U.S. Geological Survey Techniques and Methods, book 6, chap. A46, 47 p., accessed March 9, 2018, at http://pubs.usgs.gov/tm/6a46/.

Beres, Milan, Jr., and Haeni, F.P., 1991, Application of ground-penetrating radar methods in hydrogeologie studies: Ground Water, v. 29, no. 3, p. 375–386, accessed March 9, 2018, at https://doi.org/10.1111/j.1745-6584.1991.tb00528.x.

Bratton, J.F., 2010, The three scales of submarine groundwater flow and discharge across passive continental margins: Journal of Geology, v. 118, no. 5, p. 565–575, accessed March 9, 2018, at https://doi.org/10.1086/655114.

Cauller, S.J., Voronin, L.M., and Chepiga, M.M., 2016, Simulated effects of groundwater withdrawals from aquifers in Ocean County and vicinity, New Jersey: U.S. Geological Survey Scientific Investigations Report 2016–5035, 77 p., accessed March 9, 2018, at https://doi.org/10.3133/sir20165035.

Charles, E.G., and Nicholson, R.S., 2012, Simulation of groundwater flow and hydrologic effects of groundwater withdrawals from the Kirkwood-Cohansey aquifer system in the Pinelands of southern New Jersey: U.S. Geological Survey Scientific Investigations Report 2012–5122, 219 p., accessed March 9, 2018, at https://pubs.usgs.gov/sir/2012/5122/.

Danielson, J.J., Poppenga, S.K., Brock, J.C., Evans, G.A., Tyler, D.J., Gesch, D.B., Thatcher, C.A., and Barras, J.A., 2016, Topobathymetric elevation model development using a new methodology—Coastal National Elevation Database: Journal of Coastal Research, Special Issue 76 on the Advances in Topobathymetric Mapping, Models, and Applications, p. 75–89, accessed March 10, 2016, at https://doi.org/10.2112/SI76-008.

Fiore, A.R., 2018, Raw ground-penetrating radar data, Edwin B. Forsythe National Wildlife Refuge, New Jersey, 2014–15: U.S. Geological Survey data release, https://doi.org/10.5066/F7JH3KBD.

Fiore, A.R., and Voronin, L.M., 2018, MODFLOW-2005 model used to evaluate the potential effects of sea-level rise on the Kirkwood-Cohansey aquifer system in the vicinity of Edwin B. Forsythe National Wildlife Refuge, New Jersey: U.S. Geological Survey data release, https://doi.org/10.5066/F76W98JB.

Ghyben, W.B., 1889, Nota in verband met de voorgenomen putboring nabij Amsterdam: Tijdschrift van het Koninklijk Instituut van Ingenieurs, p. 8–22.

Gill, H.E., 1962, Ground-water resources of Cape May County, New Jersey—Salt-water invasion of principal aquifers: New Jersey Department of Conservation and Economic Development Special Report 18, 171 p.

Gordon, A.D., 2004, Hydrology of the unconfined Kirkwood-Cohansey aquifer system, Forked River and Cedar, Oyster, Mill, Westecunk, and Tuckerton Creek Basins and adjacent basins in the southern Ocean County area, New Jersey, 1998–99: U.S. Geological Survey Water-Resources Investigations Report 03–4337, 5 pls., accessed March 9, 2018, at https://pubs.er.usgs.gov/publication/wri034337.

Harbaugh, A.W., 2005, MODFLOW–2005, the U.S. Geological Survey modular ground-water model—The ground-water flow process: U.S. Geological Survey Techniques and Methods 6–A16 [variously paged], accessed March 9, 2018, at https://pubs.usgs.gov/tm/2005/tm6A16/.

Harbaugh, A.W., and Tilley, C.L., 1984, Steady-state computer model of the water-table aquifer in the Mullica River basin, the Pine Barrens, New Jersey: U.S. Geological Survey Water-Resources Investigations Report 84–4295, 38 p., accessed March 9, 2018, at https://pubs.er.usgs.gov/publication/wri844295.

Herzberg, A., 1901, Die Wasserversorgung einiger Nordseebäder: Journal für Gasbeleuchtung und Wasserversorgung, v. 44, p. 815–819.

Hill, M.C., and Tiedeman, C.R., 2007, Effective groundwater model calibration, with analysis of data, sensitivities, predictions and uncertainty: New York, John Wiley and Sons, 455 p.

Hubbert, M.K., 1940, The theory of ground-water motion: Journal of Geology, v. 48 no. 8, part 1, p. 785–944, accessed March 9, 2018, at https://doi.org/10.1029/TR021i002p00648-1.

Hughes, J.D., and White, J.T., 2014, Hydrologic conditions in urban Miami-Dade County, Florida, and the effect of groundwater pumpage and increased sea level on canal leakage and regional groundwater flow: U.S. Geological Survey Scientific Investigations Report 2014–5162, 175 p., accessed March 9, 2018, at http://dx.doi.org/10.3133/sir20145162.

Isphording, W.C., 1970, Petrology, stratigraphy, and redefinition of the Kirkwood Formation (Miocene) of New Jersey: Journal of Sedimentary Petrology, v. 40, no. 3, p. 986–997, accessed March 9, 2018, at https://doi.org/10.1306/74D720FE-2B21-11D7-8648000102C1865D.

Johnson, M.L., and Watt, M.K., 1996, Hydrology of the unconfined aquifer system, Mullica River basin, New Jersey, 1991–92: U.S. Geological Survey Water-Resources Investigations Report 94–4234, 6 sheets, accessed March 9, 2018, at https://pubs.er.usgs.gov/publication/wri944234.

Kemp, A.C., Horton, B.P.,, Vane, C.H., Bernhardt, C.E., Corbett, D.R., Engelhart, S.E., Anisfeld, S.C., Parnell, A.C., Cahill, Niamh, 2013, Sea-level change during the last 2500 years in New Jersey, USA: Quaternary Science Reviews, v. 81, p. 90–104, accessed March 9, 2018, at https://doi.org/10.1016/j.quascirev.2013.09.024.

Keys, W.S., 1990, Borehole geophysics applied to groundwater investigations: U.S. Geological Survey Techniques of Water-Resources Investigation, book 2, chap. E-2, 150 p., accessed March 9, 2018, at https://pubs.er.usgs.gov/publication/twri02E2.

Kirwan, M.L., Temmerman, Stijn, Skeenhan, E.E., Guntenspergen, G.R., and Fagherazzi, Sergio, 2016, Overestimation of marsh vulnerability to sea level rise: Nature Climate Change, v. 6, p. 253–260, accessed March 9, 2018, at https://doi.org/10.1038/nclimate2909.

Leake, S.A., and Lilly, M.R., 1997, Documentation of a computer program (FHB1) for assignment of transient specified-flow and specified-head boundaries in applications of the modular finite-difference ground-water flow model (MODFLOW): U.S. Geological Survey Open-File Report 97–571, 56 p., accessed March 9, 2018, at https://pubs.er.usgs.gov/publication/ofr97571.

Masterson, J.P., Fienen, M.N., Gesch, D.B., and Carlson, C.S., 2013, Development of a numerical model to simulate groundwater flow in the shallow aquifer system of Assateague Island, Maryland and Virginia: U.S. Geological Survey Open-File Report 2013–1111, 34 p., accessed March 9, 2018, at http://pubs.usgs.gov/of/2013/1111/.

Martin, Mary, 1998, Ground-water flow in the New Jersey Coastal Plain: U.S. Geological Survey Professional Paper 1404-H, 146 p., accessed March 9, 2018, at https://pubs.er.usgs.gov/publication/pp1404H.

Michael, H.A., Mulligan, A.E., and Harvey, C.F., 2005, Seasonal oscillations in water exchange between aquifers and the coastal ocean: Nature, v. 436, p. 1145–1148, accessed March 9, 2018, at https://doi.org/10.1038/nature03935.

Miller, R.L., Bradford, W.L., and Peters, N.E., 1988, Specific conductance—Theoretical considerations and application to analytical quality control: U.S. Geological Survey Water-Supply Paper 2311, 16 p., accessed March 9, 2018, at https://pubs.er.usgs.gov/publication/wsp2311.

Miller, K.G., Kopp, R.E., Horton, B.P., Browning, J.V., and Kemp. A.C., 2013, A geological perspective on sea-level rise and its impacts along the U.S. mid-Atlantic coast: Earth's Future, accessed March 9, 2018, at https://doi.org/10.1002/2013EF000135.

National Oceanic and Atmospheric Administration, 2013a, Tides & currents—Datums for 8534720, Atlantic City, NJ: National Oceanic and Atmospheric Administration, accessed June 3, 2016, at https://tidesandcurrents.noaa.gov/datums.html?id=8534720.

National Oceanic and Atmospheric Administration, 2013b, Tides & currents—Datums for 8533615, Barnegat Inlet (inside), NJ: National Oceanic and Atmospheric Administration, accessed June 3, 2016, at https://tidesandcurrents.noaa.gov/datums.html?id=8533615.

National Oceanic and Atmospheric Administration, 2013c, Tides & currents—Datums for 8533987, West Creek, Westecunk Creek, NJ: National Oceanic and Atmospheric Administration, accessed June 3, 2016, at https://tidesandcurrents.noaa.gov/datums.html?id=8533987.

National Oceanic and Atmospheric Administration, 2015, National Centers for Environmental Information (formerly National Climatic Data Center), Climate Data Online, accessed July 13, 2015, at http://www.ncdc.noaa.gov/cdo-web/.

Newell, W.L., Powars, D.S., Owens, J.P., Stanford, S.D., and Stone, B.D., 2000, Surficial geologic map of central and southern New Jersey: U.S. Geological Survey Miscellaneous Investigations Series Map I-2450-D, 21 p., 3 sheets., accessed March 9, 2018, at https://pubs.er.usgs.gov/publication/i2540D.

Nicholson, R.S., and Watt, M.K., 1997, Simulation of groundwater flow in the unconfined aquifer system of the Toms River, Metedeconk River, and Kettle Creek basins, New Jersey: U.S. Geological Survey Water-Resources Investigations Report 97–4066, 100 p., accessed March 9, 2018, at https://pubs.er.usgs.gov/publication/wri974066.

Poeter, E.P., Hill, M.C., Banta, E.R., Mehl, Steffen, and Christensen, Steen, 2005, UCODE_2005 and six other computer codes for universal sensitivity analysis, calibration, and uncertainty evaluation constructed using the Jupiter API: U.S. Geological Survey Techniques and Methods, book 6, chap. A11, 283 p., accessed March 9, 2018, at https://pubs.usgs.gov/tm/2006/tm6a11/.

Pope, D.A., Carleton, G.B., Buxton, D.E., Walker, R.L., Shourds, J.L., and Reilly, P.A., 2012, Simulated effects of alternative withdrawal strategies on groundwater flow in the unconfined Kirkwood-Cohansey aquifer system, the Rio Grande water-bearing zone, and the Atlantic City 800-foot sand in the Great Egg Harbor and Mullica River Basins, New Jersey: U.S. Geological Survey Scientific Investigations Report 2012–5187, 139 p., accessed March 9, 2018, at https://pubs.usgs.gov/sir/2012/5187/.

Reilly, T.E., and Harbaugh, A.W., 2004, Guidelines for evaluating ground-water flow models: U.S. Geological Survey Scientific Investigations Report 2004–5038, 37 p., accessed March 9, 2018, at https://pubs.usgs.gov/sir/2004/5038/.

Rhodehamel, E.C., 1973, Geology and water resources of the Wharton tract and the Mullica River basin in southern New Jersey: New Jersey Department of Environmental Protection Special Report 36, 58 p., accessed March 9, 2018, at https://pubs.er.usgs.gov/publication/70106983.

San Juan, C.A., Belcher, W.R., Laczniak, R.J., and Putnam, H.M., 2004, Hydrologic components for model development, in Belcher, W.R., ed., Hydrogeologic framework and transient ground-water flow model, chap. C, Death Valley regional ground-water flow system, Nevada and California: U.S. Geological Survey Scientific Investigations Report 2004–5205, p. 95–132, accessed March 9, 2018, at https://pubs.usgs.gov/pp/1711/.

Seminack, C.T., and Buynevich, I.V., 2013, Sedimentological and geophysical signatures of a relict tidal inlet complex along a wave-dominated barrier—Assateague Island, Maryland, USA: Journal of Sedimentary Research, v. 82, p. 132–144, accessed March 9, 2018, at https://doi.org/10.2110/jsr.2013.10.

Spitz, F.J., Watt, M.K., and dePaul, V.T., 2008, Recovery of ground-water levels from 1988 to 2003 and analysis of potential water-supply management options in Critical Area 1, east-central New Jersey: U.S. Geological Survey Scientific Investigations Report 2007–5193, 40 p., accessed March 9, 2018, at https://pubs.usgs.gov/sir/2007/5193/.

Stanford, S.D., 2015, Geology of the Millville quadrangle, Cumberland and Salem Counties, New Jersey: New Jersey Geological Survey Open-File Map Series OFM-105, scale 1:24,000, accessed December 11, 2015, at http://www.state.nj.us/dep/njgs/pricelst/ofmap/ofm105.pdf.

Stanford, S.D., 2014, Geology of the West Creek quadrangle, Ocean County, New Jersey: New Jersey Geological Survey Open-File Map Series OFM-103, scale 1:24,000, accessed December 11, 2015, at http://www.state.nj.us/dep/njgs/pricelst/ofmap/ofm103.pdf.

Stanford, S.D., 2013a, Geology of the Forked River and Barnegat Light quadrangles, Ocean County, New Jersey: New Jersey Geological Survey Geologic Map Series GMS 13–2, scale 1:24,000, accessed December 11, 2015, at http://www.state.nj.us/dep/njgs/pricelst/gmseries/gms13-2.pdf.

Stanford, S.D., 2013b, Geology of the Keswick Grove quadrangle, Ocean County, New Jersey: New Jersey Geological Survey Open-File Map Series OFM–100, scale 1:24,000, accessed December 11, 2015, at http://www.state.nj.us/dep/njgs/pricelst/ofmap/ofm100.pdf.

Stanford, S.D., 2012, Geology of the Chatsworth quadrangle, Burlington County, New Jersey: New Jersey Geological Survey Open-File Map Series OFM–97, scale 1:24,000, accessed December 11, 2015, at http://www.state.nj.us/dep/njgs/pricelst/ofmap/ofm97.pdf.

Stanford, S.D., 2011, Geology of the Brookville quadrangle, Ocean County, New Jersey: New Jersey Geological Survey Open-File Map Series OFM–81, scale 1:24,000, accessed December 11, 2015, at http://www.state.nj.us/dep/njgs/pricelst/ofmap/ofm81.pdf.

Stanford, S.D., 2010, Geology of the Woodmansie quadrangle, Burlington County, New Jersey: New Jersey Geological Survey Geologic Map Series GMS 10–2, scale 1:24,000, accessed December 11, 2015, at http://www.state.nj.us/dep/njgs/pricelst/gmseries/gms10-2.pdf.

Sugarman, P.J., 2001, Hydrostratigraphy of the Kirkwood and Cohansey formations of Miocene age in Atlantic County and vicinity, New Jersey: New Jersey Geological Survey Report 40, 26 p., accessed October 14, 2010, at http://www.state.nj.us/dep/njgs/pricelst/gsreport/gsr40.pdf.

Uptegrove, Jane, Waldner, J.S., Stanford, S.D., Monteverde, D.H., Sheridan, R.E., and Hall, D.W., 2012, Geology of the New Jersey offshore in the vicinity of Barnegat Inlet and Long Beach Island: New Jersey Geological Survey Geologic Map Series GMS 12–3, scale 1:80,000, accessed December 11, 2015, at http://www.state.nj.us/dep/njgs/pricelst/gmseries/gms12-3.pdf.

U.S. Fish and Wildlife Service, 2009, Edwin B. Forsythe National Wildlife Refuge, 10 p., accessed January 5, 2015, at https://www.fws.gov/uploadedFiles/Region_5/NWRS/North_Zone/Edwin_B_Forsythe/ForsytheBrochure.pdf (brochure).

U.S. Geological Survey, 2015, The National Map—Hydrography—National Hydrography Dataset, Watershed Boundary Dataset, accessed May 3, 2015, at http://nhd.usgs.gov.

U.S. Geological Survey, 2016, USGS water data for the Nation: U.S. Geological Survey National Water Information System database, accessed March 9, 2018, at https://doi.org/10.5066/F7P55KJN.

U.S. Geological Survey, 2017, USGS GeoLog Locator database, accessed March 9, 2018, at https://doi.org/10.5066/F7X63KT0.

Voronin, L.M., 2004, Documentation of revisions to the regional aquifer system analysis model of the New Jersey Coastal Plain: U.S. Geological Survey Water-Resources Investigations Report 03–4268, 58 p. and CD-ROM. [Also available at https://pubs.usgs.gov/wri/wri03-4268/.]

Watt, M.K., Johnson, M.L., and Lacombe, P.J., 1994, Hydrology of the unconfined aquifer system, Toms River, Metedeconk River, and Kettle Creek basins, New Jersey, 1987–90: U.S. Geological Survey Water-Resources Investigations Report 93-4110, 5 pls. [Also available at https://pubs.er.usgs.gov/publication/wri934110.]

Wieben, C.M., and Chepiga, M.M., 2018, Hydrologic assessment of Edwin B. Forsythe National Wildlife Refuge, New Jersey: U.S. Geological Survey Scientific Investigations Report 2017–5088, 38 p., https://doi.org/10.3133/sir20175088.

Wilson, J.D., and Naff, R.L., 2004, The U.S. Geological Survey modular ground-water model—GMG linear solver package documentation: U.S. Geological Survey Open-File Report 2004–1261, 47 p., accessed March 9, 2018, at https://pubs.usgs.gov/of/2004/1261.

Woolman, Lewis, 1893, Artesian wells in southern New Jersey, *in* Geological Survey of New Jersey, Annual report of the State Geologist for the year 1892, p. 275–311, accessed September 2, 2016, at http://www.state.nj.us/dep/njgs/enviroed/oldpubs/SG-Annual-Report-1892.pdf.

Zapecza, O.S., 1989, Hydrogeologic framework of the New Jersey Coastal Plain, Regional Aquifer-System Analysis—Northern Atlantic Coastal Plain: U.S. Geological Survey Professional Paper 1404–B, 49 p., 24 pls. [Also available at https://pubs.er.usgs.gov/publication/pp1404B.]

For additional information, contact:
Director, New Jersey Water Science Center
U.S. Geological Survey
3450 Princeton Pike, Suite 110
Lawrenceville, NJ 08648

or visit our website at:
http://nj.usgs.gov/

Prepared by USGS West Trenton Publishing Service Center

ISSN 2328-0328 (online)
https://doi.org/10.3133/sir20175135